



Norwegian University  
of Life Sciences

**Master's Thesis 2021 30 + 30 ECTS**

Faculty of Science and Technology

# **Evaluation of the modulus of elasticity of timber beams using non-destructive methods**

Henrik Stokke-Bettum

Arne Henrik Granvoll Jørgensen

Structural Engineering and Architecture

## Acknowledgement

The authors appreciate the continuous support and moral help from our supervisor Ebenezer Ussher throughout the work with this thesis. Without him this thesis would not have been possible.

We would like to thank our co-supervisors Roberto Tomasi and Mauro Andreolli for guiding us through this thesis. We are thankful to Maruo Andreolli and Timbertech for giving us the opportunity to conduct tests with a new dynamic method.

We would also like to thank Roar Økseter for help and access to the laboratories and equipment needed for the thesis.

Inspiration and input from Xiaojun Gu were very helpful and helped us to progress with this thesis.

The moral support from family and friends throughout this thesis are also deeply appreciated.

Lastly, we would like to thank our friends Isak, Viktoria, Vilde and Giulia for helping us through the masters degree, these last two years.

Place, date

Oslo, 31.05.2021

*Arne Henrik Jørgensen*

---

Arne Henrik Granvoll Jørgensen

*Henrik Stokke-Bettum*

---

Henrik Stokke-Bettum

## Abstract

The traditional method to determine mechanical properties of timber is by conducting static tests, which are both time consuming and destroy the material. In addition, it is very challenging to perform static tests on timber structures in their operational state. With this thesis the authors aim to compare and evaluate various non-destructive methods to determine the modulus of elasticity of timber beams. The effects of damages and defects on the modulus of elasticity (MOE) of timber beams are also evaluated.

This study identifies various non-destructive methods, three of which are chosen as test methods: Timber Grader MTG by Brookhuis, Operational Modal method and Smartphone method by Timbertech. Various support conditions are evaluated for the different non-destructive methods. The Timber Grader MTG is observed to be consistent for all the tested support conditions. The Operational Modal and Smartphone methods are very sensitive to support conditions. A simply supported condition with steel rollers is selected for the MOE evaluations. Six timber beams each of spruce and impregnated pine were on tested both edgewise and flatwise scenarios.

Based on the selected support condition flatwise test setups produced more reliable results than the edgewise test setups for the Operational Modal method and the Smartphone method.

The results of the tests indicate a good correlation between modulus of elasticity obtained from the three non-destructive methods for the timber beams however, results from static test may be used to assess the accuracy of those obtained from the non-destructive tests.

Damages were induced in the beams by making holes at two different locations. The non-destructive methods correlates well when it comes to the modulus of elasticity in damaged beams, though the reliability of the different methods varies. The smartphone method appears to indicate the changes in dynamic modulus of elasticity due to damages, whereas the Operational Modal method only seems to indicate damages with changes in the higher modes of the beams. The Timber Grader MTG appears to indicate the existence of damages in beams but due to the nature of the test method it is suggested that the results be verified with static tests.

## Sammendrag

Den tradisjonelle måten å bestemme de mekaniske egenskapene til trevirke på er ved å gjennomføre statiske tester, noe som er både tidskrevende og det ødelegger materialet. I tillegg er det utfordrende å gjennomføre statiske tester på trekonstruksjoner i sin operative status. Forfatterens mål med denne oppgaven er å sammenligne og evaluere forskjellige ikke-destruktive metoder for å bestemme elastitetsmodul i trebjelker. Effekten av skader og feil på den statiske elastitetsmodulen i trebjelker blir også evaluert.

Denne studien identifiserer forskjellige ikke-destruktive metoder, hvor tre metoder ble valgt som test metoder: Timber Grader MTG av Brookhuis, Operativ Modal metode og Smarttelefon metode av Timbertech. Forskjellige opplagerbetingelser ble evaluert for de forskjellige ikke-destruktive metodene. Timber Grader MTG ble observert til å være konsistent for alle de testede opplagerbetingelsene. Den operative modal metoden og smarttelefon metoden var veldig sensitiv til opplagerbetingelsene. En fritt opplagt betingelse med stål gildere ble valgt for å evaluere elastisitetsmodul. Seks bjelker hver av gran og impregnert furu ble testet på både stående og liggende scenarioer.

Basert på den valgte opplagerbetingelsen, ga liggende testoppsett mer pålitelig resultater enn stående testoppsett med Operativ Modal metode og Smarttelefon metode.

Resultatene viser en god korrelasjon mellom elastitetsmodulen gitt fra de tre ikke-destruktive metodene på trebjelkene, men resultater fra statisk testing kan benyttes for å vurdere nøyaktigheten av de oppnådde resultatene fra ikke-destruktive tester.

Skader ble påført bjelkene ved å lage hull på to forskjellige plasser. De ikke-destruktive metodene korrelerer godt når det kommer til den elastitetsmodulen i skadete bjelker, men påliteligheten til de forskjellige metodene varierer.

Smarttelefonmetoden virker å indikere endringen i dynamisk elastitetsmodul på grunn av skader, mens den Operative Modal metoden ser ut til å bare indikere skader med endringer i de høyere modene av bjelkene. Timber Grader MTG virker å indikere at det finnes skader i bjelkene, men på grunn av måten testingen gjennomføres anbefales det at resultatene verifiseres med statisk testing.

## Table of contents

Acknowledgement.....	i
Abstract .....	ii
Sammendrag .....	iii
List of figures .....	4
List of tables .....	7
List of equations .....	9
List of abbreviations .....	10
List of symbols .....	11
1. Introduction .....	13
1.1 Research questions.....	14
1.2 Research objectives .....	14
1.3 Summary of contribution .....	15
1.4 Limitations .....	15
2. State-of-the-art .....	17
2.1 Estimation of modulus of elasticity with non-destructive methods .....	17
2.2 Detecting damages with non-destructive methods .....	17
3. Theory .....	21
3.1 Timber.....	21
3.2 Beam theory .....	21
3.3 Modulus of Elasticity .....	22
3.3.1 Dynamic modulus of elasticity .....	24
3.4 Non-destructive determination of modulus of elasticity .....	24
3.4.1 Sylvatest .....	25
3.4.2 Timber Grader MTG .....	26
3.4.3 Operational Modal method .....	27
3.4.4 Smartphone method.....	28
3.5 Continuous and discrete systems .....	29
3.5.1 Discrete system .....	30
3.5.2 Continuous system.....	31
3.6 Frequency .....	31
3.6.1 Natural frequency .....	32
3.6.2 Nyquist frequency.....	33

3.6.3 Mode shapes.....	33
3.7 Operational modal analysis .....	35
3.7.1 Ambient vibrational test.....	36
3.8 Response.....	37
3.9 Signal Processing.....	37
3.9.1 Frequency domain decomposition (FDD) .....	38
4. Method.....	39
4.1 Specimens.....	39
4.2 Measurement of specimen weight.....	41
4.3 Moisture content.....	43
4.4 Repetitive testing.....	47
4.5 Timber Grader MTG.....	47
4.5.1 Equipment.....	47
4.5.2 Software .....	49
4.5.3 Testing.....	52
4.6 Operational Modal method .....	53
4.6.1 Equipment.....	53
4.6.2 Software .....	56
4.6.3 Sampling rate and sampling time .....	63
4.6.4 Background "noise" .....	64
4.6.5 Placement of accelerometers .....	65
4.6.6 Deciding on support conditions .....	66
4.6.7 Chosen support conditions .....	73
4.6.8 Testing.....	74
4.7 Smartphone method .....	76
4.7.1 Equipment.....	76
4.7.2 Software .....	77
4.7.3 Testing.....	78
4.8 Damages .....	79
4.8.1 Holes.....	79
4.8.2 Knots .....	81
5. Results and discussion .....	83
5.1 Deciding on support conditions.....	83

5.2 Chosen support condition .....	93
5.3 Repetitive testing.....	95
5.4 Edgewise vs flatwise .....	97
5.5 Effects of accelerometer mass .....	107
5.6 Modulus of elasticity for all methods.....	110
5.7 Effect of moisture on the modulus of elasticity .....	113
5.8 Effect of density on the modulus of elasticity .....	117
5.9 Evaluation of the modulus of elasticity .....	120
5.10 Damages and defects .....	121
5.10.1 Operational Modal method .....	121
5.10.2 Timber Grader MTG .....	126
5.10.3 Smartphone Method.....	127
5.10.4 Knots in beams.....	130
5.11 Summary discussions.....	132
5.11.1 Undamaged beams .....	132
5.11.2 Damages and defects on beams .....	133
5.11.3 Non-destructive methods on structures in their operating state .....	135
6. Conclusion.....	137
6.1 Further work .....	138
References.....	139
Appendix.....	143
A1. Sensitivity of accelerometers .....	143
A2. FDD script for Matlab .....	144
A3. Excel-script for drawing mode shapes .....	147
A4. Strength properties of timber [46].....	148
A5. Mode shape script for Matlab.....	149
A6. Digital Appendix .....	150

## List of figures

Figure 3.1 - Bending stresses in a beam [14, page 266].....	22
Figure 3.2 - Modulus of elasticity [16].....	23
Figure 3.3 - Sylvatest setup [21].....	26
Figure 3.4 - How to use Timber Grader MTG.....	27
Figure 3.5 - Free-free support condition for Operational Modal method [24].....	28
Figure 3.6 – Smartphone test setup.....	28
Figure 3.7 - Dynamic modulus of elasticity app.....	29
Figure 3.8 - A model of an SDOF beam [19, page 490].....	30
Figure 3.9 - A model of an MDOF beam [19, page 490].....	31
Figure 3.10 - Mode shape 1 for a simply supported beam.....	34
Figure 3.11 - Mode shape 2 for a simply supported beam.....	34
Figure 3.12 - Mode shape 3 for a simply supported beam.....	35
Figure 3.13 - Mode shape 4 for a simply supported beam.....	35
Figure 4.1 - Edge marking of beams.....	39
Figure 4.2 - Brookhuis EAG 80 scale.....	41
Figure 4.3 - Weighing of accelerometers.....	42
Figure 4.4 - Weighing of specimens with Bergmann PB3002-S Delta range scale.....	43
Figure 4.5 - Termaks drying cabinet.....	44
Figure 4.6 - Brookhuis FMD6 Moisture Meter [31].....	45
Figure 4.7 - Brookhuis Timber Grader MTG [32].....	47
Figure 4.8 - Instruction of Timber Grader MTG [33].....	48
Figure 4.9 - Layout for Timber Grader Software.....	49
Figure 4.10 - Measure settings for Timber Grader MTG.....	50
Figure 4.11 - Calibration stick for Timber Grader MTG.....	50
Figure 4.12 - Batch settings for Timber Grader MTG.....	51
Figure 4.13 - Property settings for Timber Grader MTG.....	51
Figure 4.14 - Test setup for Timber Grader MTG.....	52
Figure 4.15 - PCB Piezotronics Sensor Signal Conditioner – Model 482C05 Series [36].....	53
Figure 4.16 - HBM Quantum X – MX1601B [37].....	53
Figure 4.17 - PCB Piezotronics ICP accelerometers – 393B12 [38].....	54
Figure 4.18 - Industrial twisted shielded cable, 50 Ft – 024R50 [39].....	54
Figure 4.19 - Two-branch signal cables with BNC connector.....	54
Figure 4.20 - TP-cable [40].....	55
Figure 4.21 - Connection plug bridge.....	56
Figure 4.22 - Layout for Catman Easy.....	57
Figure 4.23 - Sensor database.....	57
Figure 4.24 - IEPE sensor option.....	58
Figure 4.25 - Sensor sensitivity settings.....	58
Figure 4.26 - Visualization tab.....	59
Figure 4.27 - Axes options.....	60
Figure 4.28 - Calling script function in Matlab.....	61
Figure 4.29 - Picking peaks in FDD.....	61



Figure 4.30 - Natural frequencies and mode shapes from Matlab .....	62
Figure 4.31 - Excel script for drawing mode shapes .....	63
Figure 4.32 - Accelerometer on floor .....	64
Figure 4.33 - Interference frequencies.....	64
Figure 4.34 - Placement of accelerometers on beams .....	65
Figure 4.35 - Free-free support condition .....	66
Figure 4.36 - Elastic bands as supports .....	67
Figure 4.37 - Pinned-pinned support condition with screw .....	67
Figure 4.38 - Simply supported beam on timber supports .....	68
Figure 4.39 - Simply supported beam on rubber supports.....	69
Figure 4.40 - Simply supported beam on clamped rubber supports .....	69
Figure 4.41 - Simply supported beam on timber supports with clamping .....	70
Figure 4.42 - Simply supported beam with steel plate .....	70
Figure 4.43 - Simply supported beam with steel angles .....	71
Figure 4.44 - Simply supported beam on steel rollers flatwise .....	71
Figure 4.45 - Simply supported beam on steel rollers edgewise .....	72
Figure 4.46 - Simply supported beam on steel rollers with insulation beneath support .....	73
Figure 4.47 - Acceleration data for accelerometers .....	75
Figure 4.48 - Natural frequencies.....	75
Figure 4.49 - FDD .....	76
Figure 4.50 - Equipment for Smartphone method.....	76
Figure 4.51 - App for Smartphone method .....	77
Figure 4.52 - Test setup for smartphone.....	78
Figure 4.53 - Hole at mid-point of beam.....	79
Figure 4.54 - Holes at quarter-points of beam.....	80
Figure 4.55 - Placement of hole at the mid-point of beams .....	80
Figure 4.56 - Placement of holes at the quarter-points of beams.....	81
Figure 4.57 - Measurement of knot size .....	82
Figure 5.1 - Regression between flatwise and edgewise dynamic modulus of elasticity using Operational Modal method .....	99
Figure 5.2 - Regression between flatwise and edgewise dynamic modulus of elasticity using Smartphone method .....	99
Figure 5.3 - Edgewise mode shape 1 for beam 9 .....	101
Figure 5.4 - Edgewise mode shape 2 for beam 9 .....	102
Figure 5.5 - Edgewise mode shape 3 for beam 9 .....	102
Figure 5.6 - Edgewise mode shape 4 for beam 9 .....	102
Figure 5.7 - Flatwise mode shape 1 for beam 9 .....	103
Figure 5.8 - Flatwise mode shape 2 for beam 9 .....	103
Figure 5.9 - Flatwise mode shape 3 for beam 9 .....	103
Figure 5.10 - Flatwise mode shape 4 for beam 9 .....	104
Figure 5.11 - Edgewise FDD for beam 9 .....	105
Figure 5.12 - Flatwise FDD for beam 9 .....	105
Figure 5.13 - Regression for MOE between Timber Grader MTG and Operational Modal method .....	110

Figure 5.14 - Regression for MOE between Timber Grader MTG and Smartphone method	111
Figure 5.15 - Regression for DMOE between Smartphone method and Operational Modal method .....	111
Figure 5.16 - Regression between SMOE and moisture content for Timber Grader MTG ....	114
Figure 5.17 - Regression between DMOE and moisture content for Operational Modal method .....	115
Figure 5.18 - Regression between DMOE and moisture content for Smartphone method ..	116
Figure 5.19 - Regression between SMOE and density for Timber Grader MTG .....	117
Figure 5.20 - Regression between DMOE and density for Operational Modal method.....	118
Figure 5.21 - Regression between DMOE and density for Smartphone method .....	119
Figure 5.22 - Regression between modulus of elasticity from Timber Grader MTG and knots .....	131
Figure 5.23 - Regression between dynamic modulus of elasticity from Smartphone method and knots .....	131
Figure 5.24 - Regression between dynamic modulus of elasticity from Operational Modal method and knots .....	132
Figure 5.25 - Regression for damaged beams between Operational Modal method and Smartphone method .....	133
Figure 5.26 -Regression for damaged beams between Timber Grader MTG and Smartphone method .....	134
Figure 5.27 - Regression for damaged beams between Operational Modal method and Timber Grader MTG .....	134

## List of tables

Table 3.1 – Wavenumber $k_n$ for mode $n$ .....	24
Table 4.1 - Beam properties .....	40
Table 4.2 - Weight of beams for every test method .....	41
Table 4.3 - Moisture content of beams with dry oven .....	45
Table 4.4 - Moisture content of beams before every test.....	46
Table 4.5 - Timber Grader MTG boundary conditions .....	52
Table 4.6 - Calculation of dynamic modulus of elasticity from fundamental frequency.....	74
Table 4.7 - Discrepancy between theoretical and experimental frequencies .....	75
Table 4.8 - List of beams damaged and the placement of the holes.....	81
Table 5.1 - Discrepancy between Timber Grader MTG and Operational Modal method for free-free support.....	83
Table 5.2 - Discrepancy for natural frequencies for free-free support conditions.....	85
Table 5.3 - Discrepancy between Timber Grader MTG and Operational Modal method for screw pinned-pinned support .....	85
Table 5.4 - Discrepancy for natural frequencies for screw pinned-pinned support.....	86
Table 5.5 - Discrepancy between Timber Grader MTG and Operational Modal method for simply supported timber supports.....	86
Table 5.6 - Discrepancy for natural frequencies for simply supported timber support .....	87
Table 5.7 - Discrepancy between Timber Grader MTG and Operational Modal method for taped simply supported timber supports .....	88
Table 5.8 - Discrepancies for natural frequencies for taped simply supported timber support .....	88
Table 5.9 - Discrepancy between Timber Grader MTG and Operational Modal method for simply supported rubber support .....	89
Table 5.10 - Discrepancy for natural frequencies for simply supported rubber support.....	89
Table 5.11 - Discrepancy between Timber Grader MTG and Operational Modal method for clamped simply supported timber supports .....	89
Table 5.12 - Discrepancy for natural frequencies for clamped simply supported timber support .....	90
Table 5.13 - Discrepancy between Timber Grader MTG and Operational Modal method for simply supported steel plate supports.....	90
Table 5.14 - Discrepancy for natural frequencies for simply supported steel plate support ..	91
Table 5.15 - Discrepancy between Timber Grader MTG and Operational Modal method for simply supported and steel angle stabilization.....	91
Table 5.16 - Discrepancy for natural frequencies for simply supported and steel angle stabilized.....	92
Table 5.17 - Discrepancy between Timber Grader MTG and Operational Modal method for taped simply supported steel rollers support.....	92
Table 5.18 - Discrepancy for natural frequencies for taped simply supported steel rollers support .....	93
Table 5.19 - Discrepancy for natural frequencies for taped simply supported steel rollers support with insulation .....	94

Table 5.20 - Timber Grader MTG tests, static modulus of elasticity.....	95
Table 5.21 - Timber Grader MTG tests, natural frequencies .....	95
Table 5.22 - Discrepancy in repetitive testing with Operational Modal method .....	96
Table 5.23 - Discrepancy in mode 2 with repetitive testing with Operational Modal method.....	96
Table 5.24 - Discrepancy in mode 3 with repetitive testing with Operational Modal method.....	96
Table 5.25 - Discrepancy in mode 4 with repetitive testing with Operational Modal method.....	96
Table 5.26 - Discrepancy in repetitive testing with Smartphone method.....	97
Table 5.27 - Discrepancy between edgewise and flatwise with Operational Modal method.....	98
Table 5.28 - Discrepancy between edgewise and flatwise with Smartphone method .....	98
Table 5.29 - Discrepancy between edgewise theoretical and experimental natural frequencies for beam 9 using Operational Modal method .....	100
Table 5.30 - Discrepancy between flatwise theoretical and experimental natural frequencies for beam 9 using Operational Modal method .....	101
Table 5.31 - Table of accelerometer mass to beam mass.....	108
Table 5.32 - Discrepancy between dynamic modulus of elasticity for beam with and without accelerometer mass .....	109
Table 5.33 - Modulus of elasticity for all test methods .....	110
Table 5.34 - Table of moisture content and MOE for Timber Grader MTG.....	113
Table 5.35 - Table of moisture content and DMOE for Operational Modal method .....	115
Table 5.36 - Table of moisture content and DMOE for Smartphone method .....	116
Table 5.37 - Table of SMOE and density for Timber Grader MTG .....	117
Table 5.38 - Table of DMOE and density for Operational Modal method.....	118
Table 5.39 - Table of DMOE and density for Smartphone method .....	119
Table 5.40 - Change of the fundamental frequency between undamaged and damaged flatwise beams using Operational Modal method.....	121
Table 5.41 - Change of the dynamic modulus of elasticity between undamaged and damaged flatwise beams using Operational Modal method.....	123
Table 5.42 - Change of the second natural frequency between undamaged and damaged flatwise beams.....	124
Table 5.43 - Change of the third natural frequency between undamaged and damaged flatwise beams.....	125
Table 5.44 - Change of the fourth natural frequency between undamaged and damaged flatwise beams.....	126
Table 5.45 - Change of the static modulus of elasticity between undamaged and damaged flatwise beams using the Timber Grader MTG .....	127
Table 5.46 - Change of the fundamental frequency between undamaged and damaged flatwise beams using Smartphone method .....	128
Table 5.47 - Change of the dynamic modulus of elasticity between undamaged and damaged flatwise beams using Smartphone method .....	129
Table 5.48 - Number of knots vs modulus of elasticity.....	130

List of equations

Equation 1 - Equation of dynamic modulus of elasticity with natural frequency [19] ..... 24  
Equation 2 - Equation of dynamic modulus of elasticity for ultrasonic waves [21] ..... 25  
Equation 3 - Velocity of sonic wave [21] ..... 25  
Equation 4 - Equation of frequency [26] ..... 31  
Equation 5 - Equation of angular frequency [26] ..... 32  
Equation 6 - Equation of angular frequency for a SDOF system ..... 32  
Equation 7 - Equation of Natural frequency with relation to dynamic modulus of elasticity  
[19, page 400] ..... 32  
Equation 8 - Equation of moisture content ..... 44

## List of abbreviations

CLT – Cross laminated timber

MOE – Modulus of elasticity

OMA – Operational modal analysis

DMOE – Dynamic modulus of elasticity

SMOE – Static modulus of elasticity

DAQ – Data acquisition

PSD – Power spectral density

FDD – Frequency domain decomposition

FFT – Fast Fourier Transform

EWP – Engineered wood products

MC – Moisture content

## List of symbols

$\sigma$  - Stress (N/mm<sup>2</sup>)

$\sigma_c$  – Compression stress (N/mm<sup>2</sup>)

$\sigma_T$  – Tensile stress (N/mm<sup>2</sup>)

$\varepsilon$  - Strain (Unitless)

E – Modulus of elasticity (N/mm<sup>2</sup>)

I – Moment of inertia (mm<sup>4</sup>)

$E_d$  – Dynamic modulus of elasticity (N/mm<sup>2</sup>)

w – Line mass (kg/m)

L – Length (m)

$f_n$  – Natural frequency of mode n (Hz)

$k_n$  - Wavenumber correlating to mode n (Unitless)

n – number

$\pi$  - Pi (Unitless)

$\rho$  - Density (kg/m<sup>3</sup>)

c - Velocity of sonic wave (m/s)

t – time (s)

k – stiffness (N/m)

c – damping (kg/s)

m – modal mass/mass (kg)

f – Frequency (Hz)

T – Period (s)

$\omega$  - Angular frequency (Hz)

$b$  – Width (mm)

$h$  – Height (mm)

$f_{nT}$  – Theoretical natural frequency of mode  $n$

$f_{nE}$  – Experimental natural frequency of mode  $n$

$R^2$  – Regression (%)



## 1. Introduction

Timber has been used in construction for centuries and for construction of both small and large structures but has become more and more popular in the recent years. The benefits of building with timber are the high strength to self-weight ratio of the material, which can make construction both cheaper and easier. There is also the possibility for a range of different designs with timber. The breathing properties of the timber also contributes to better indoor climate. The fact that timber stores CO<sub>2</sub> and is a natural product, makes the construction material more climate and environmentally friendly. With the use of pre-cut cross laminated timber (CLT) elements and timber beams it is possible to have a fast, clean, and silent production on the construction site [1].

However, there are some disadvantages with timber. Timber is an anisotropic material and thus have different material properties in different directions. Timber is also a variable material, which means the density in timber varies along the length, and knots and cracks may influence the mechanical properties of the structure. Timber also deteriorates and weakens through its lifespan [2, page 1].

The standard way of determining the mechanical properties of timber usually involves static testing, which is time consuming, and destroys the specimen. It is also not possible to evaluate the mechanical properties and damages in timber structures in its operating state, with static testing. This has led to extensive research in developing other methods to find the mechanical properties of timber structures. One way of determining the mechanical properties of timber is by evaluating the dynamic response of a timber structure. Dynamic methods can be conducted on the timber structures in their operating state and the methods are non-destructive [3, page 1].

By conducting dynamic tests on timber periodically, it is possible to monitor the mechanical properties of timber structures throughout their life span, to detect deterioration and damages.

## 1.1 Research questions

Based on the availability of various non-destructive methods, the following research questions arise, which the authors attempt to answer:

- *What are some of the available non-destructive methods in evaluating modulus of elasticity of structures and how effective are they?*
- *How do non-destructive methods compare in evaluating the modulus of elasticity of timber beams?*
- *How do support conditions contribute to evaluating the modulus of elasticity of timber structures, when applying operational modal analysis techniques?*
- *How do non-destructive methods compare in evaluating the effects of damages and defects on structural timber beams?*

## 1.2 Research objectives

The main goal of this thesis is to assess the effectiveness of non-destructive methods and service-condition methods in evaluating the mechanical properties of timber structures.

Specifically, this may be broken down into the following:

- Identifying various non-destructive methods applicable for the evaluation of the modulus of elasticity (MOE) for structural systems.
- Understanding how operational modal analysis (OMA) is used as a non-destructive method in evaluating modulus of elasticity of timber structures.
- Identifying suitable boundary conditions for OMA as a non-destructive method for the evaluation of modulus of elasticity of structural systems.
- Comparing modulus of elasticity evaluated from OMA with results from other non-destructive methods.
- Evaluating the effect of defects and damages on the modulus of elasticity of timber structures using non-destructive methods.

### 1.3 Summary of contribution

A summary of the authors contribution in this field of study is provided as follows:

- When conducting tests with Operational Modal method, it is important to consider the percentage of weight of equipment such as accelerometers that are likely to influence the modal properties of the system.
- The Timber Grader MTG made by Brookhuis, appears to be correctly measuring the modulus of elasticity of both natural and impregnated timber based on the excellent correlation with the other non-destructive methods. The Timber Grader literature reports on the equipment only being used on plain timber.
- Operational Modal tests conducted with a smartphone have good correlation in dynamic modulus of elasticity (DMOE) with other more sophisticated Operational Modal methods. The authors are privileged to be part in pioneering the use of the smartphones in this field.
- Just as reported in previous research for steel structures, the differences in natural frequencies due to damages appear to be dependent on the location of the damages, in timber beams as well.
- A comprehensive method has been developed for the three non-destructive methods listed in this thesis, to make further work easier for researchers.

### 1.4 Limitations

Here the limitations of the thesis are listed:

- Static tests on timber beams were not conducted due to machine malfunction. The machine could not be fixed due to COVID-19 restrictions.
- The COVID-19 restrictions also affected accessibility to the laboratory, thereby limiting the number of tests.
- The effects of shear forces on bending in beams are not considered in this thesis.
- The effects of damping in beams are not considered in this thesis.
- There were conducted three repetitive tests for two of the beams for Operational Modal method and Smartphone method, as a verification to do one test for the remaining beams.
- The beams that were tested, were not dried to 12 % moisture content before testing. This led to beams being tested at different moisture content with different tests.

- The equations and formulas the Timber Grader MTG use to calculate the static modulus of elasticity (SMOE) from obtained frequencies in testing, are not published publicly. This did not allow the authors to explore its efficiency by comparing with other dynamic analytical formulations.

## 2. State-of-the-art

### 2.1 Estimation of modulus of elasticity with non-destructive methods

For some decades researchers have been trying to determine the modulus of elasticity of a structure based on the natural frequencies with the help of operational modal analysis. The frequency of a structure is based on the stiffness and the mass; hence the modulus of elasticity should be possible to determine based on the natural frequencies [4, page 10-11].

According to the authors in [5], two glulam beams were tested using operational modal analysis. The different modes on the beams were excited by rubbing the beams gently with a wooden stick and the motion was captured by accelerometers. The two glulam beams were also tested with static tests in order to compare the two methods. The dynamic tests were in good accordance with the static tests according to the authors in [5].

Another team of researchers have determined the dynamic modulus of elasticity in clear wood samples of tropic hardwood, with three different methods: longitudinal vibrations, flexural vibration, and ultrasonic method. The longitudinal and flexural vibration tests were performed with a hammer and a microphone that captured the resonance frequency. The team concluded that even though the dynamic modulus of elasticity was higher than the static modulus of elasticity for all the species of hardwood, there was still a good linear regression between them. The team also concluded that the dynamic modulus of elasticity can effectively be used to determine SMOE if a useful regression model is developed with enough testing [6].

Udaya B. Halabe, Gangadhar M. Bidigalu, Hota V.S. GangaRao, and Robert J. Ross [3] performed flatwise vibration tests for southern pine and compared the results to static bending tests. The authors obtained a regression of  $R^2$  82 % between the DMOE and SMOE in the green state and a regression of  $R^2$  70 % in the dry state. The results also showed that the values for the SMOE were higher than the DMOE [3].

### 2.2 Detecting damages with non-destructive methods

In the past years there has been an extensive work to use non-destructive methods to assess damages to structures [7, page 210]. The monitoring of civil engineering structures is important to secure the safety and the integrity of the structure itself and the people that are around or using it. Because of this, many methods have been developed to not only

monitor, but also discover possible damages, the location of these and the extent of the damage [8, page 1].

Some of the methods and research that have been done were focusing on the dynamic properties of structures and the modal responses in terms of the natural frequencies and mode shapes of the structure. The studies have been looking into changes in natural frequencies and related these to changes in the properties of the beam. There have also been studies that investigated locations of defects in a beam due to changes in the natural frequencies [7, page 1].

The methods mentioned in the section above are called vibrational methods. The theory behind this method is that a damage or damages to a structure will affect the stiffness of the structure or the mass, which will result in a change in the vibrational properties of the structures, for example natural frequencies or mode shapes of the structure. It has been concluded that a damage has to be of a certain size so that the natural frequencies are capable of discovering it [8, page 1 and 2].

There are also methods that depend on using changes in the mode shapes to identify damage. Some of these methods rely on changes in the mode shape curvature to detect and localize the damage [8, 9]. It is important to remember that natural frequencies of a structure reflect the whole structure, but a damage can be just a local phenomenon, hence the use of natural frequencies are not appropriate to identify and localize the damage [8, 10]. It is also reported that the shift in frequencies between undamaged and damaged structure are small. Because of this it is important to measure responses with a high precision in order to detect the changes [9, page 1 and 2]. However, there have been several studies trying to use the natural frequencies of a structure to both identify and localize damage to a structure. One of these studies have been looking at a fixed- fixed beam using relative natural frequency change curves to determine and detect damage, where they are localized, and their significance [8, 10].

Methods using changes in the natural frequencies to detect and localize damages and their significance often involves finite element models to model changes in the stiffness in different locations in the beam to simulate damage and then check the changes in the natural frequencies. The localization of the damage and the severity of it is based on

recognizing certain pattern changes between the undamaged structure and the damaged structure [9, 10].

The reliability of using finite element model can be questioned because changes in the natural frequencies due to damage can be smaller than the changes between the finite element model and the undamaged structure. It is therefore important that the finite element model is as exact as possible. This raises questions on how to model the structure to be as close to the real structure itself, it is important that the changes in the natural frequencies or mode shapes between the model and the real structure are significantly smaller than the changes due to damage. Modelling of damage can be done by reducing the stiffness at a local point in the model. In addition to this, the natural frequencies changes with temperature and the loads applied, so these factors are also important to take into consideration [9, page 2].

Previous research has found a connection between critical points on a beam and the natural frequencies. There are points along the beam where the strain-energy is zero and there are points along the beam where strain-energy is at the maximum. For the different mode shapes the strain energy will be zero where the mode shape curvature is zero and maximum where the mode shape curvature is at the maximum. This is because there is no bending where the mode shape curvature is zero, only rotation. The maximum curvature of the mode shape will occur where the maximum bending occurs. Furthermore, if there is a damage at an inflection point where the curvature of the mode shape is zero, the total energy of the beam will not change [9, 11].

This means that if a damage is located at the inflection points of a certain mode, the damage will not affect the total strain energy of the beam, because of this a change in the natural frequency of the actual mode will not occur. If the damage is located at one of the points where the maximum curvature of a certain mode is located, there will be a loss in the total energy of the beam, resulting in a change in the natural frequency of the actual mode [9, 11].

In figure 2.1 it is seen that the changes in frequencies for the first 4 modes in a simply supported steel beam depend on the location of the damage. For example, it is observed that for the first mode a damage in the middle gives the biggest frequency change. However,

for the second mode a damage in the mid-span of the beam will not give any change in frequency for this particular mode [9].

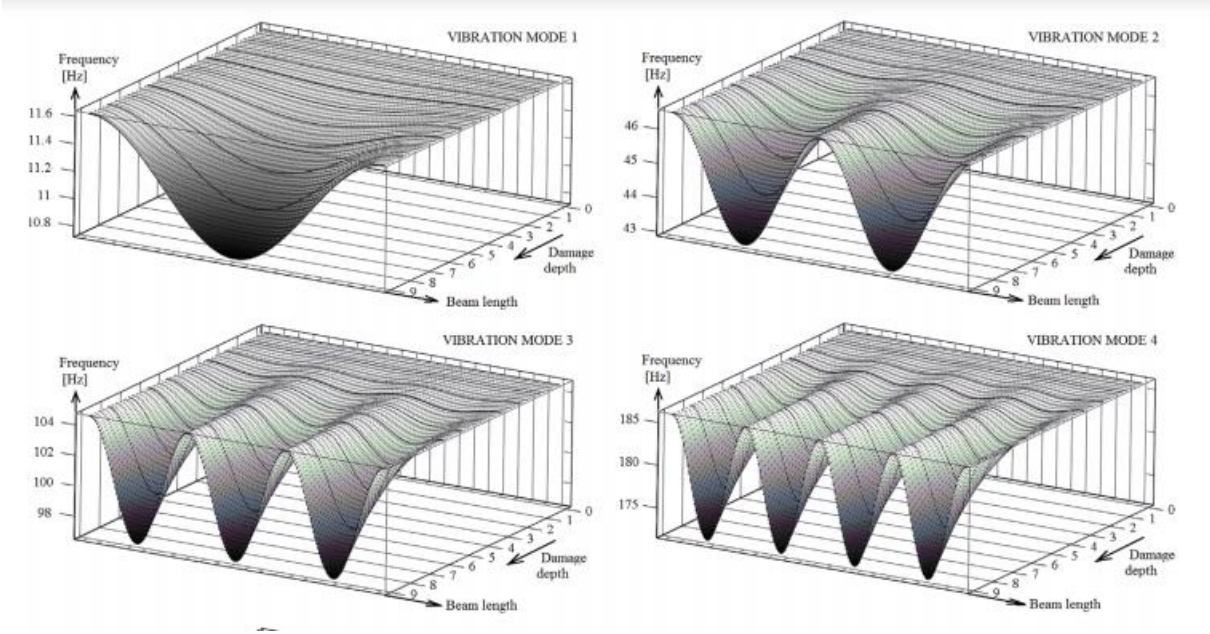


Figure 2.1 – Changes in the mode shapes natural frequency depending on location and depth of damage [9]



## 3. Theory

### 3.1 Timber

Timber is an anisotropic material, which means it has different mechanical properties in different directions in the material [12]. This reflects that strength and stiffness vary through the material based on load direction. The reason for differences in mechanical properties in timber is the fiber grain angle, growth rings and knots. The fiber goes in the longitudinal direction which is the direction the tree is growing. Timber has best mechanical properties in the direction of the fibers. The fiber angle is disturbed by knots growing from the stem of the tree. When a knot appears, the fiber must grow around it. Since the strength and stiffness is higher in the direction of the fiber, the knots result in reduction of strength and stiffness in timber. The strength and stiffness of timber is also affected by the moisture content in the material. High moisture content reduces the strength and stiffness of the material. The growth rings in trees also affect the mechanical properties of timber. Bigger growth rings lead to less density in the material, and strength of the material is reduced [2].

The most common species to build with in Norway are Norwegian Spruce and Pine. Spruce is usually not impregnated while the pine is usually impregnated to resist moisture.

### 3.2 Beam theory

Beams are horizontal structural elements that transfer loads that are applied laterally to the element's axis, to supports such as walls or columns. Beams transfer the loads to supports by shear forces and bending moments. Stress and strain occur in a beam when a bending moment is induced. The capability of a beam to transfer loads and withstand deformations depend on its strength and stiffness respectively which in turn depend on the modulus of elasticity [13].

A beam influenced by a force laterally to its axis, obtain deformation. The deformation in the beam leads to compression-strain in one part of the beams cross-section and extension-strain in the other part. This in turn leads to compression stresses in one part of the cross-section and tensile stresses in the other part. In the neutral axis of a beam the strain and stress are zero. The stress and strain then gradually increase towards the top and the bottom of the cross-section as seen in figure 3.2. For a rectangular beam with even mass

distribution across the cross-section, the neutral axis is in the middle of the cross-section [14, page 260-266].

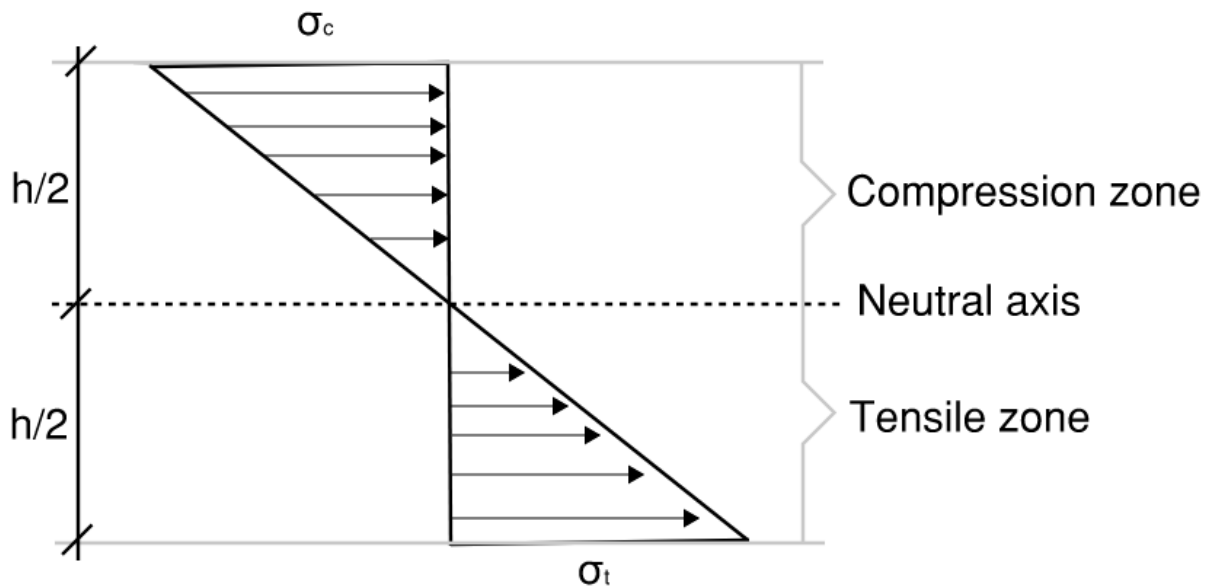


Figure 3.1 - Bending stresses in a beam [14, page 266]

Where  $\sigma_c$  is compression stress,  $\sigma_t$  is tensile stress and  $h$  is the height of the beam.

### 3.3 Modulus of Elasticity

Modulus of Elasticity is the measurement of the elasticity of a material, which means it measures a material's ability to resist deformation. When a force is applied to a material, the material will experience stress that will deform the material, but when the force is removed, the material will return to its original state. If the material returns to its original state, the stress is said to be in the elastic range. If the material is stressed beyond the elastic range the material reaches its yield strength and the material goes into the plastic range where the deformations are permanent, even when the stress is removed [15].

Figure 3.1 shows the stress-strain relationship of a material. The modulus of elasticity is defined as the slope in the elastic range of the material.

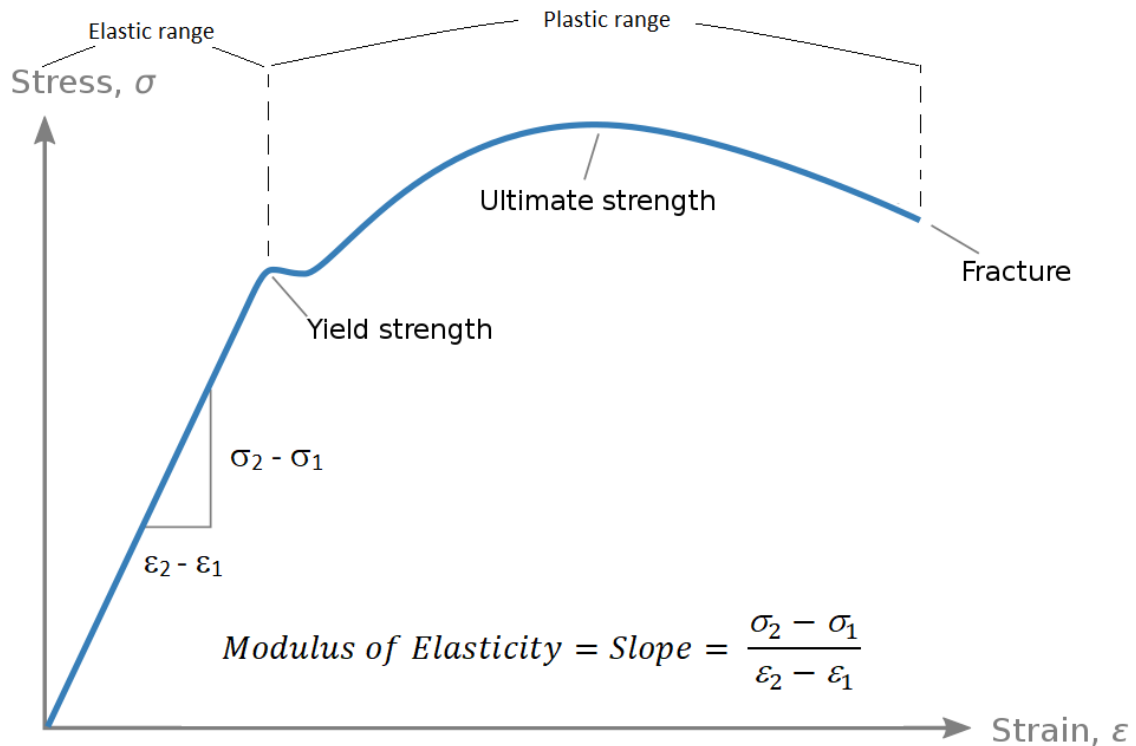


Figure 3.2 - Modulus of elasticity [16]

Where stress  $\sigma$  is defined as force divided by the cross-section area of the specimen and the strain  $\epsilon$  is the elastically deformed length of the material divided by the original length of the material [15].

Traditionally, modulus of elasticity is determined by a flexural bending test. The test is executed by placing the specimen across a span and pressing down along the span until the material fails. The specimen is placed on two supports and the specimen is pressed by either a point in the middle of the span or two points slightly to each side of the middle. The deflection and force are measured at the mid-span and the modulus of elasticity can be determined [17].

A combination of the modulus of elasticity (E) of a material and the specimens' moment of inertia (I) yields the specimens stiffness.

### 3.3.1 Dynamic modulus of elasticity

Dynamic modulus of elasticity is the relation between stress and strain when there are vibratory conditions. The dynamic modulus of elasticity is determined by exciting a specimen, which will give it an oscillatory stress and observing the strain in the specimen [18]. The dynamic modulus of elasticity can also be determined by observing the natural frequencies in a specimen.

The dynamic modulus of elasticity can be calculated from equation 1 [19, page 399].

$$E_d = \frac{f_n^2 4\pi^2 w L^4}{k_n^2 I}$$

*Equation 1 - Equation of dynamic modulus of elasticity with natural frequency [19]*

$E_d$  is the beams dynamic modulus of elasticity [N/mm<sup>2</sup>] and  $I$  is the moment of inertia [mm<sup>4</sup>].

$w$  is the line mass of the beam [kg/m] and  $L$  is the length of the beam [L].

$k_n$  is a factor relating to the  $n$ -th mode of the beam and dependent on the beams support conditions as seen in table 3.1. Referred to as wavenumber.

$f_n$  is the natural frequency of mode  $n$  [Hz]

*Table 3.1 – Wavenumber  $k_n$  for mode  $n$*

Support conditions	$k_n$ for mode $n$			
	Mode 1	Mode 2	Mode 3	Mode 4
Simply supported [19, page 400]	$\pi^2$	$4\pi^2$	$9\pi^2$	$16\pi^2$

### 3.4 Non-destructive determination of modulus of elasticity

Some non-destructive methods to evaluate timber today are based on computer programs which transfer vibrations into frequencies and stress waves where the propagation time is measured. In the general term these methods are known as dynamic testing. The two basic methods that are commonly used are based on stress waves and ultrasound.

The dynamic methods are affected by the moisture content, growth ring orientation and cracks/deterioration of the beam. The reason for this is that the propagation time is a way to measure the condition of the wood in terms of stiffness or strength [20, page 10].

### 3.4.1 Sylvatest

One way of testing the longitudinal dynamic modulus of elasticity in timber beams is the ultrasonic method, also referred to as a Sylvatest [20]. Wood has good acoustic properties, which means the transmission of sonic waves works well in the material. The quality of the wood is evaluated by the time it takes for the sonic stress wave to transfer through the wood. The test device consists of a transmitting and a receiving transducer, a control box, and a humidity measurement probe. The transducers are installed directly into the wood and the transmitting transducer emits a sonic wave from an oscillating piezoelectric core [21]. The sonic waves travel directly from the transmitting transducer to the receiving transducer and the device measures the time it takes. By determining the in-situ density  $\rho$  and the moisture content of timber, the dynamic modulus of elasticity  $E_d$  of the timber beam can be calculated by equation 2 [21].

$$E_d = \rho c^2$$

*Equation 2 - Equation of dynamic modulus of elasticity for ultrasonic waves [21]*

Where  $\rho$  is the in-situ density of the beam and  $c$  is the velocity of the sonic wave from transmitter to receiver. The velocity  $c$  of the sonic wave is calculated as shown in equation 3 [21].

$$c = \frac{L}{t}$$

*Equation 3 - Velocity of sonic wave [21]*

$L$  is the distance between the transmitting and receiving transducers and  $t$  is the time it takes for the sonic wave to travel between them.

Hana Hasníková and Petr Kuklík in [21] reports that the modulus of elasticity measured from static tests are in the order of 85 – 90 % of the obtained the dynamic modulus of elasticity obtained from the ultrasonic method [21]. This must be kept in mind when evaluating the dynamic modulus of elasticity of a timber beam.

According to Hana Hasníková and Petr Kuklík in [21] there have been experiments to evaluate how cracks influence the Sylvatest regarding the dynamic modulus of elasticity. Figure 3.3 shows a typical experimental set up of a Sylvatest with cracks in the beam.

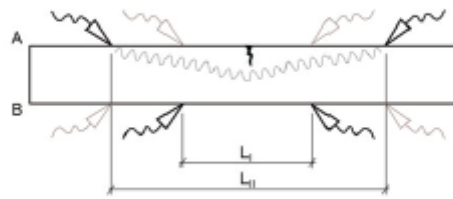


Figure 3.3 - Sylvatest setup [21]

The transducers were set up on both sides and a crack was inflicted on only one of the sides. After measuring the velocity of the wave on both sides they increased the crack [21].

The experiment showed that if the transducers were mounted at the same side where the crack was present in the timber, the time for the sonic wave to travel from transmitter to receiver was prolonged, because the sonic wave had to travel around the crack. This in turn reduced the calculated dynamic modulus of elasticity. When the transducers were mounted on the opposite side of where the crack was, there was no effect on the travel time between the transducers. This showed that the measured velocity of the sonic wave in timber would vary based on where the transducers were mounted and if there were any cracks, defects, or damages in the timber [21].

#### 3.4.2 Timber Grader MTG

The Timber Grader MTG is a handheld device made by Brookhuis that can determine the static modulus of elasticity, strength class and natural frequency of timber.

The device uses ultrasonic stress waves to determine the properties of the timber. The device is placed at the end of a timber beam and using a "Stress Wave Activator", the device sends a stress wave in the longitudinal direction. The stress wave is then reflected and sent back at the other end of the timber beam. A stress wave detector in the device receives the stress wave that was sent back, and it registers the natural frequency of the timber beam [22, 23]. The device then uses the natural frequency and parameters such as density, cross-section dimensions, and moisture content of the beam to calculate the dynamic modulus of elasticity. The Timber Grader then outputs the static modulus of elasticity to the user, by multiplying the DMOE with a factor [23].

The Timber Grader MTG is only intended for solid timber and not timber which is laminated (Glulam), finger-jointed, modified or treated with flame retardants [22].

Figure 3.4 shows the Timber Grader MTG and how it is used on the timber [22].



*Figure 3.4 - How to use Timber Grader MTG*

### 3.4.3 Operational Modal method

Operational Modal method is one of the non-destructive methods that may be used to find the dynamic modulus of elasticity for a given beam. By using ambient vibrational tests, it is possible to determine the mode shapes and the natural frequencies of a beam [24].

The test is conducted with accelerometers placed on suitable locations on a beam. The beam is then set in motion by ambient excitations and the accelerations are captured and processed to determine the natural frequencies and mode shapes. The fundamental frequency/first natural frequency can then be used to calculate the dynamic modulus of elasticity. The procedure of the dynamic modulus of elasticity is dependent on the support conditions of the beam. Support conditions might affect the measured natural frequencies and create some uncertainties [24].

One way to eliminate the uncertainties from the supports is to have the beam supported freely as seen in figure 3.5.

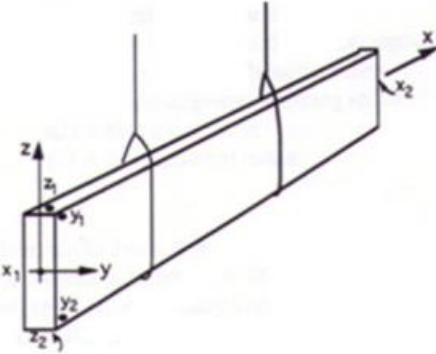


Figure 3.5 - Free-free support condition for Operational Modal method [24]

From previous work with Operational Modal method, it has been established that there is a correlation between the dynamic modulus of elasticity and the static modulus of elasticity [24].

### 3.4.4 Smartphone method

A smartphone modified by Timbertech, a timber engineering company, is the instrument used in this method. The accelerometer that already existed in the smartphone was replaced with one calibrated for dynamic testing. The smartphone is then placed and tied at the midspan of a simply supported beam as shown in figure 3.6.



Figure 3.6 – Smartphone test setup



Timbertech has developed an app where the dimensions and density are input as shown in figure 3.7.

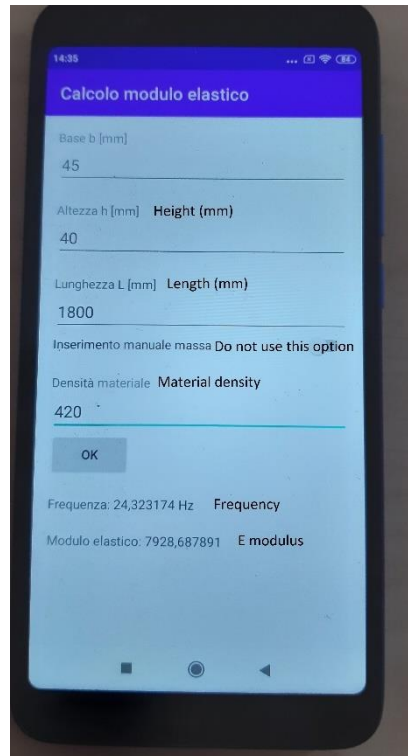


Figure 3.7 - Dynamic modulus of elasticity app

The app is then started, and the beam can be excited with an impact. The accelerometer in the smartphone then registers the motion and the app converts the accelerations to the fundamental/first natural frequency of the beam. Using the same theory as the Operational Modal method and equation 1 the smartphone calculates the dynamic modulus of elasticity for the fundamental frequency. The principle of this method is the same as if only one accelerometer in the mid-span was used for the Operational Modal Method.

### 3.5 Continuous and discrete systems

A system can often be described as discrete but also at the same time as continuous. It is often easier to solve a discrete system than a continuous one. If a system is described as discrete, the information obtained may not be as accurate as when it is described as a continuous system. Whether to describe a system as a discrete or continuous, is often a question about accuracy and expediency. Discrete and continuous systems are closely related. If a discrete model is made finer by increasing the degrees of freedom and the number of masses, it eventually leads to a continuous system [25, page 127].

### 3.5.1 Discrete system

A discrete system is characterized by the fact that the masses involved are separated from each other, but it could be coupled together with springs that have stiffness. In addition to this, a discrete system might also have damping. A discrete system can either be a single degree of freedom system or a multiple degree of freedom system with possibly infinite degrees of freedom. A multiple degree of freedom system is a system that has two or more degrees of freedom. A single degree of freedom system may be modeled with one concentrated mass and its stiffness represented with a spring and damping represented with dashpot. For a multiple degree of freedom system, two or more concentrated masses that can be coupled together with springs and dashpots may be used to simulate the system. The number of degree of freedom in a system is what decides how many natural frequencies a system may have. This means that a single degree of freedom system will have one natural frequency while a multiple degree of freedom will have a finite number of natural frequencies [19, page xvi and 254].

A single degree of freedom system consists of only one mass and a spring and possibly dampers. An example of a single degree of freedom system can be a simply supported beam illustrated as a lumped mass model with the mass concentrated in the middle. The damping of the system will be cracking or friction in the system when the system vibrates [19, page xvi and 254].

In figure 3.8 an idealized model of the single degree of system of a simply supported beam is seen. The beam is illustrated as a lumped mass model. The model contains damper (C), spring (K), and modal mass (m). In figure 3.8 the model assumes all the mass is in the middle and that there is no mass in the spring K. The energy loss that may occur in the system is taken care of by the damping C [19, page xvi and 254].

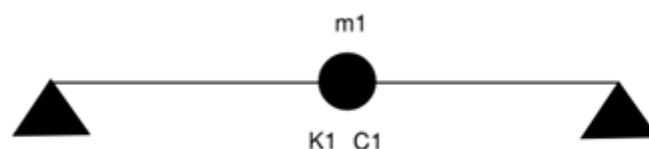


Figure 3.8 - A model of an SDOF beam [19, page 490]

An illustration of a multiple degree of freedom system can be a lumped mass model of a simply supported beam where the masses are concentrated and located at three points along the beam and the springs, and the stiffnesses are connecting the three masses. The damping is also connected between the masses and can be friction or cracking in the materials when the system is vibrating. In figure 3.9 a lumped mass model of a multiple degree of freedom system beam is seen [19, page xvi and 254].

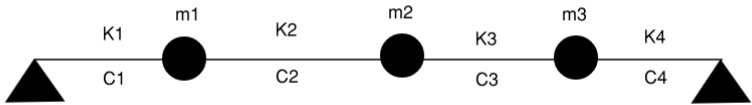


Figure 3.9 - A model of an MDOF beam [19, page 490]

3.5.2 Continuous system

In a continuous system the masses are not independent of each other but directly linked together. Such systems have distributed mass and stiffness properties. An example of a continuous system can be a beam. In theory a beam can be discretized into very small pieces of masses. A continuous system will because of that reason have an infinite number of degrees of freedom. Because of infinite number of degrees of freedom, a continuous system will have infinite natural frequencies and corresponding mode shapes [19, page xvi and 375].

3.6 Frequency

Frequency is a measurement of how many times a periodic occurrence repeats itself per unit of time. The unit for frequency is Hz (1/s) and the symbol is  $f$  [26].

Frequency is dependent of a systems turnaround time or its period. The period is the time for an oscillated system to return to its original state. The frequency is determined by equation 4, where  $T$  is the systems period [26]:

$$f = \frac{1}{T}$$

Equation 4 - Equation of frequency [26]

Angular frequency is another term used for waves and oscillation instead of regular frequency. Angular frequency indicates the number of radians traversed per unit of time. The period for an angular frequency is a circle or  $2\pi$  radians. The relation between the angular frequency  $\omega$  and frequency  $f$  is governed by equation 5 [26]:

$$\omega = 2\pi f$$

*Equation 5 - Equation of angular frequency [26]*

For a SDOF system the angular frequency is defined by equation 6.

$$\omega = \sqrt{\frac{k}{m}}$$

*Equation 6 - Equation of angular frequency for a SDOF system*

Where  $k$  is the stiffness of the system (N/m) and  $m$  is the mass of the system (kg).

### 3.6.1 Natural frequency

Natural frequency is the frequency at which a system oscillates when it has been set in motion by an impulse force and left to oscillate freely [27]. A system can have multiple natural frequencies and each of the frequencies correlates to a given mode shape as explained in "3.5.3 Mode shapes".

The natural frequency in a mechanical system is determined by its mass, as the oscillating system will try to return the mass to equilibrium. The natural frequency is therefore the frequency the system is vibrating at to return the mass to equilibrium [27].

The natural frequency for a beam in its  $n$ -th mode is given by equation 7 [19, page 400]:

$$f_n = \frac{k_n}{2\pi} \sqrt{\frac{E_d I}{w L^4}}$$

*Equation 7 - Equation of Natural frequency with relation to dynamic modulus of elasticity [19, page 400]*

$k_n$  is found in table 3.1.

### 3.6.2 Nyquist frequency

The Nyquist theorem states that if you want to record a frequency, the sampling frequency needs to be at least two times the frequency you wish to record. The Nyquist frequency is therefore the sampling frequency incorporated for data recording in order to achieve the expected frequencies of interest [28].

### 3.6.3 Mode shapes

Natural frequency and mode shapes are coupled together. Each natural frequency is linked to a specific mode shape. A beam is described as a continuous system, and it can have infinite number of degrees of freedoms along the axis. A beam will therefore have multiple natural frequencies and multiple mode shapes [25].

A beam will usually vibrate in an arbitrary form, but when the vibration matches one of the natural frequencies of the beam it will start to vibrate in a certain form, this form is called mode shape. Depending on the different mode shapes there will be some points along the beam where the displacement is zero. These points are called nodes. The peaks of the mode shapes are called anti-nodes [25, page 148]. The cause of vibration can be induced by different dynamic forces like, walking, wind, earthquakes, cars, removing and applying forces, etc.

The first mode shape has the lowest natural frequency, this is referred to as the fundamental natural frequency. The next natural frequencies will gradually increase in size. The number of natural frequencies and mode shapes in a beam are dependent on the number of degrees of freedom.

For a pinned-pinned beam which is a continuous system, the first four mode shapes are as represented in figure 3.10 to 3.13. The mode shapes for a pinned-pinned beam will always be zero at both the ends of the beam. For the first mode there will be an anti-node at the midspan of the beam [25, page 148].

The second mode has an additional node where the beam does not move, and this point is in the middle of the beam. The second mode will have anti-nodes  $L/4$  from each end, where  $L$  is the length of the span [25, page 148].

The third mode have 4 nodes, two at both ends and two additional nodes located at  $L/3$  from each end. The anti-nodes for the third mode will appear in the middle of the beam and  $L/6$  from each end [25, page 148].

The fourth mode will have five nodes, one at both ends, one located  $L/4$  from each end and one in the middle. The anti-nodes will be between the nodes as seen in figure 3.12 [25, page 148].

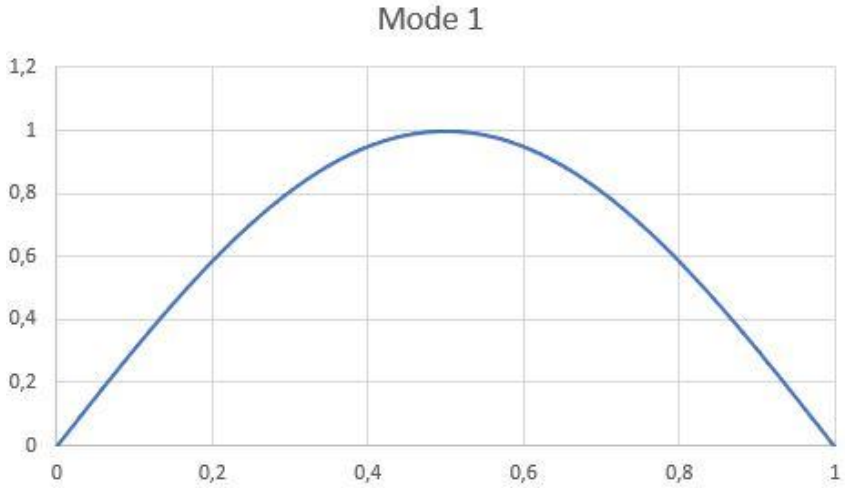


Figure 3.10 - Mode shape 1 for a simply supported beam

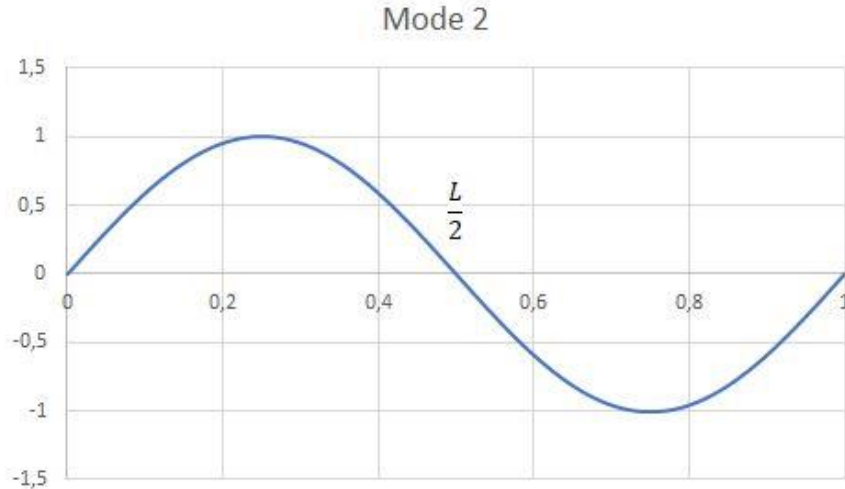


Figure 3.11 - Mode shape 2 for a simply supported beam

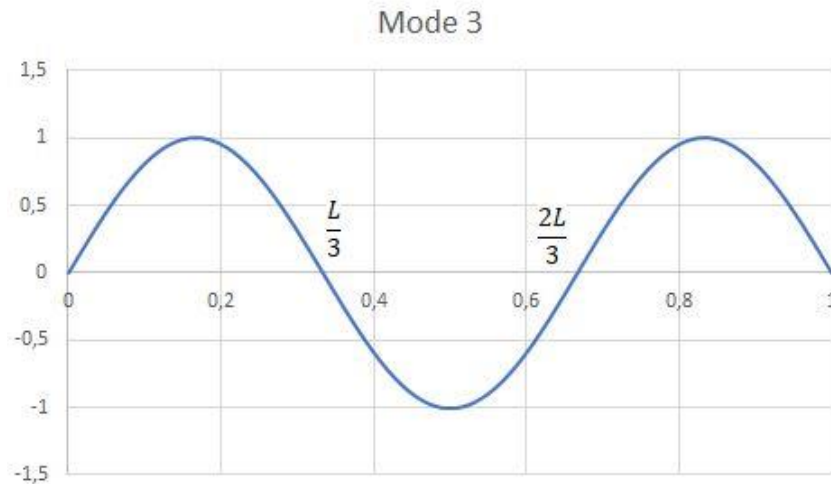


Figure 3.12 - Mode shape 3 for a simply supported beam

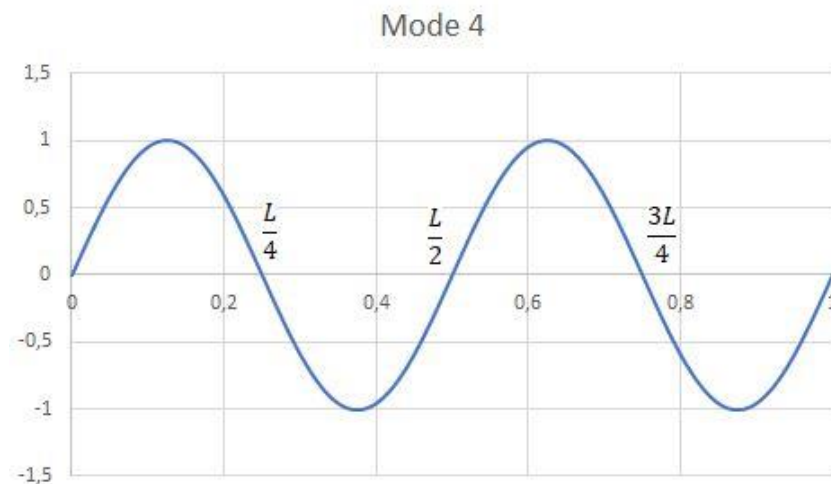


Figure 3.13 - Mode shape 4 for a simply supported beam

### 3.7 Operational modal analysis

Operational modal analysis uses vibrational response measurements to determine the modal properties of a structure. The modal properties are natural frequencies, damping ratios and mode shapes and the response of a structure is determined under ambient loading. OMA makes it possible to determine the modal properties without knowing the input forces [4, page vii and 3].

When performing a modal analysis on a structure, the "in-situ" modal properties are determined. The modal properties that are determined can vary from the predicted/theoretical modal properties. According to Siu-Kui Au in [4] the difference between the natural frequencies determined through OMA and the theoretical natural

frequencies can be 30 %. The discrepancies can be due to variations along the structure in both mass and stiffness and boundary conditions which could also be complicated to model mathematically. The natural frequencies in a structure can also vary based on the temperature, humidity, and the age of the structure. The damping mechanism in a structure is also hard to predict and it is therefore hard to calculate theoretical natural frequencies [4, page 4].

### 3.7.1 Ambient vibrational test

The term operational modal Analysis has its origin in the ambient vibrational test. In an ambient vibrational test, the structure is subjected to a variety of different excitations that are not measured, whilst the response of the system is measured. It can be complicated to determine the modal properties with an ambient vibrational test, because the output of the test is a combination of the dynamic properties and the excitation [4, page 8]. One can assume that the excitations induce multiple frequencies in the structure, so that there will be resonance at the natural frequencies, which will give good results for the modal properties. The upside with the ambient vibrational test is that the tests can be performed under the structures "operating condition" on site and in-situ and it is easy to conduct. That is why the method is called operational modal analysis [4, page 8].

Some disadvantages with the ambient vibrational test are presented below [4, page 8 and 9]:

- The modal properties are determined by ambient vibration which usually gives a lower level than the serviceability- and design-levels, an example being the modulus of elasticity.
- The method is also less reliable than the tests where the excitations are measured, because the vibration response can be so small that the measurement noise cannot be ignored. This means the ambient vibrational test might give variability between two sets of tests, which might give some uncertainty in the identification of the modal properties.
- Some sources of uncertainty for the identification of modal properties might come from the sampling rate and the duration of the test, or measurement error from either the hardware or the software.



In spite of the limitations ambient vibrational tests have proven to be quite useful in evaluating structures operational status, such as the modulus of elasticity of structural elements [5].

### 3.8 Response

A system that is submitted to a variety of ambient excitations will have a response, in the form of displacements and its derivatives (velocities and accelerations). The damping in the system will affect the magnitude of the responses. The damping in the system will reduce the displacements and in situations with minimum damping resonance may occur to increase the displacements. Damping is defined as loss of energy in a system that is oscillating. The loss of energy comes from friction or other resistance in the system and may differ based on the material type. Resonance is a phenomenon where the applied force that excites the system induces the same frequencies as the system's natural frequencies. This will in turn increase the oscillation/acceleration of the system with time [29, page 125-164].

### 3.9 Signal Processing

When conducting an ambient vibrational test, the data is analyzed on a computer. The vibrational signal is picked up mechanically with for example accelerometers and sent electrically to be converted to a digital signal. The digital signals contain information about the motion of the specimen. The data and the real motion are never exactly alike. Differences in data and real motion are called "noise". To be able to read the signals as close to reality as possible, the data should be processed in a data acquisition (DAQ) device to reduce the "noise" and digitalize the signal, before being sent to the computer [4, page 223].

The ambient excitation on structure has a broadband power spectral density (PSD). The peaks of the PSD are near the natural frequencies of the structure. This is because of resonance in the structure from the ambient excitation. At higher frequencies, the peaks will not appear because the dynamic amplification of the structure approaches a constant. The PSD data signals are then sent to the DAQ hardware. The DAQ hardware filters out the frequencies in the data that are near or beyond the Nyquist frequency and reduces the "noise". The DAQ hardware then digitizes the data signals and sends it to the computer as measured data [4, page 223].

### 3.9.1 Frequency domain decomposition (FDD)

The computer receiving the data needs a software to read the digital signals and record it. Software like Catman Easy from HBM can process signals from accelerometers. To be able to determine the natural frequencies the data must be transformed to frequency domain spectrum through Fast Fourier Transform (FFT) and then converted into Frequency domain decomposition (FDD).

The FDD estimates the PSD of the data signals and identifies the peaks. The FDD then uses these peaks to obtain the natural frequencies and damping by isolating the peaks in a frequency domain spectrum [30, page 4].

## 4. Method

For determining the modulus of elasticity in a non-destructive way, three methods were chosen:

1. Timber Grader MTG, by Brookhuis, which measures the static modulus of elasticity through longitudinal ultrasonic waves.
2. Operational Modal method, with accelerometers, which measures the dynamic modulus of elasticity through dynamic flexural vibration.
3. Smartphone method, by Timbertech, which also measures the dynamic modulus of elasticity through dynamic flexural vibration.

### 4.1 Specimens

When deciding on specimens it is important that the specimens can be tested by the three methods that were chosen. In the case of these three methods, it is the Timber Grader MTG that sets the limitations.

The Timber Grader MTG cannot perform tests on engineered wood products (EWP) like glulam or CLT, so it is decided to choose specimens of solid timber. The Timber Grader MTG also sets the limitation for the dimensions of the specimens. The thickness, width and length cannot exceed 115x250x8000 mm.

The wooden species chosen for the tests are Norwegian spruce and impregnated pine. The species are chosen because they are the two most normal species to use for construction in Norway. Timber beams with dimensions of 48 x 148 mm and 48 x 198 mm are chosen to not exceed the requirements from the Timber Grader MTG. The beams are cut to a length of 4000 mm so that all the beams have the same length. Each side is then marked with side A and side B as seen in figure 4.1.

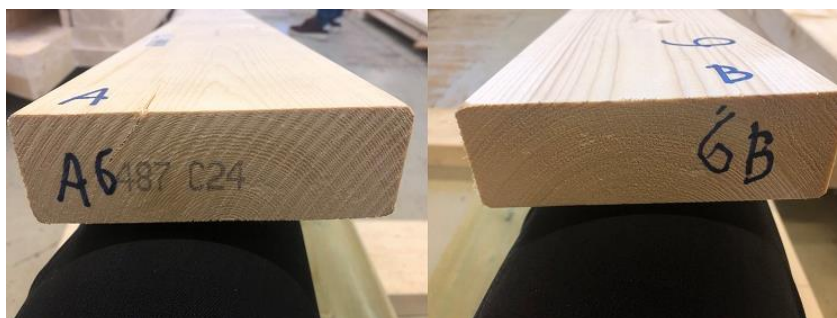


Figure 4.1 - Edge marking of beams

The beams are given a number, so they are identifiable. Table 4.1 shows the beams with their species, original length (from manufacturer), cut length, dimensions, and strength classification from the manufacturer.

*Table 4.1 - Beam properties*

Specimen	Species	Original length (mm)	Length (mm)	Width x Thickness (mm)	Strength classification (N/mm <sup>2</sup> )
1	Spruce	4530	4000	48 x 198	C24
2	Spruce	4530	4000	48 x 198	C24
3	Spruce	4540	4000	48 x 198	C24
4	Spruce	4870	4000	48 x 148	C24
5	Spruce	4860	4000	48 x 148	C24
6	Spruce	4870	4000	48 x 148	C24
7	Pine	5140	4000	48 x 198	C24
8	Pine	4630	4000	48 x 198	C24
9	Pine	4500	4000	48 x 198	C24
10	Pine	4840	4000	48 x 148	C24
11	Pine	4850	4000	48 x 148	C24
12	Pine	4860	4000	48 x 148	C24

## 4.2 Measurement of specimen weight

Before conducting each of the three tests, the specimens were weighed and registered in an excel-file. The instrument used is a Brookhuis EAG 80. It consists of a weight reader and two scales with rubber cladding as seen in figure 4.2.



Figure 4.2 - Brookhuis EAG 80 scale

The weight of the beams when testing the beams with the different methods are reported in table 4.2.

Table 4.2 - Weight of beams for every test method

Specimen	Weight (kg) Timber Grader MTG	Weight (kg) Operational Modal method	Weight (kg) Smartphone method
1	14,1	13,75	13,75
2	15,25	14,95	14,95
3	15,45	14,7	14,35
4	12,95	12,85	12,85
5	14,05	13,7	13,7
6	11,95	11,55	11,55
7	18,25	17,6	17,6
8	20,8	19,35	19,35
9	25,8	24,15	24,15
10	14,9	14,35	14,35
11	22,75	17,5	17,5
12	14,85	14,15	14,15

The reason for weight difference as shown in table 4.2 is the loss of moisture in the timber. The specimens were stored outside under roof at winter when they were retrieved. The Timber Grader MTG test was conducted shortly after retrieving the specimens. The beams were then stored inside a lab with a moisture and temperature regulator that aims to obtain 12 % moisture content and 20 degrees Celsius in the timber. The other measurements were conducted sometime later, which means some moisture had been lost.

The accelerometers were also weighed to see if their weight would affect the results in the Operational Modal tests. The accelerometers were weighed by putting a piece of plywood on the rubber scales as seen in figure 4.3, the scale was zeroed, and the accelerometers taped to the plywood. The weight of all 10 accelerometers combined is 2,75 kg.



*Figure 4.3 - Weighing of accelerometers*

### 4.3 Moisture content

When the beams were cut to adjust the lengths, 5 cm of each beam of the leftovers were taken aside to measure the moisture content. All the specimens were weighed on a Bergmann PB3002-S Delta range scale as seen in figure 4.4.



Figure 4.4 - Weighing of specimens with Bergmann PB3002-S Delta range scale



The specimens were then put in a Termaks drying cabinet, as seen in figure 4.5, at a temperature of 103 degree Celsius for 2 days until the specimens were completely dry.



Figure 4.5 - Termaks drying cabinet

On the second day one specimen was taken out, weighed, and put back into the drying cabinet for a couple of hours. The same specimen was weighed again to see if the weight had changed. When it was registered that the weight was the same, all specimens were taken out and weighed. The moisture content was then calculated by equation 8.

$$MC\% = \frac{Wet\ weighth\ (g) - Dry\ weight\ (g)}{Dry\ Weight\ (g)} * 100$$

Equation 8 - Equation of moisture content



The moisture content of all the specimens were registered before doing the Timber Grader MTG test and is presented in table 4.3.

Table 4.3 - Moisture content of beams with dry oven

Beam	Weight - Wet (g)	Weight - Dry (g)	Moisture content (%)
1	188,11	162,57	16 %
2	172,23	148,20	16 %
3	182,36	158,47	15 %
4	156,40	139,30	12 %
5	173,10	148,89	16 %
6	138,60	120,81	15 %
7	238,25	201,89	18 %
8	263,15	219,43	20 %
9	332,13	276,76	20 %
10	177,62	142,18	25 %
11	280,46	170,25	65 %
12	169,28	142,10	19 %

Using a dry oven before conducting testing with each method was both time consuming and not possible with only a small number of specimens. Therefore, the moisture content was also determined for every beam before every test-method with a Brookhuis FMD6 Moisture Meter as seen in figure 4.6.



Figure 4.6 - Brookhuis FMD6 Moisture Meter [31]

The species and temperature of the timber are chosen on the panel. The species chosen for the tests are Spruce Nordic and Pine Scots. Next the needles on the "hammer" are pressed into the middle of the specimen's thickness. The two needles should be parallel to the grains of the specimen. The moisture meter then shows the moisture content of the specimen on the display. For these beams, the moisture content is measured at a length 750 mm from the end at each side and at the mid-span. The measurements are done in the middle of the width. The three measurements are then averaged as the specimen's moisture content. The moisture content is measured before every set of method testing. The moisture content for all the specimens and the three methods are provided in table 4.4.

*Table 4.4 - Moisture content of beams before every test*

Beam	Moisture content (%) Timber Grader MTG	Moisture content (%) Operational Modal method	Moisture content (%) Smartphone method
1	16 %	13,9 %	13,9 %
2	18 %	14,4 %	14,4 %
3	17 %	11,7 %	11,7 %
4	17 %	15,6 %	15,6 %
5	19 %	15,8 %	15,8 %
6	17 %	12,6 %	12,6 %
7	20 %	16,1 %	16,1 %
8	22 %	15,8 %	15,8 %
9	23 %	14,0 %	14,0 %
10	20 %	14,4 %	14,4 %
11	-	21,7 %	21,7 %
12	18 %	11,5 %	11,5 %

The reason for no data for beam 11 on the Timber Grader is that the specimen was extremely moist when retrieved and the moisture meter could not read such high moisture contents. Table 4.3 shows that the real moisture content of beam 11 was 65 %, which is too high for the moisture meter.

#### 4.4 Repetitive testing

When testing with the Timber Grader MTG, 12 tests are conducted per beam, which means the repetitive testing gives safety in the credibility of the results.

For the Operational Modal method and the Smartphone method, two beams were tested three times with each method. When the results were observed to be approximately equal for each set of three tests, it was decided it was not necessary to do repetitive tests for the rest of the beams. The beams that have been tested repetitively are beam 3 and beam 6. The rest of the beams have been tested once edgewise and once flatwise.

#### 4.5 Timber Grader MTG

##### 4.5.1 Equipment

The Timber Grader MTG is a handheld ultrasonic device developed by Brookhuis that measures the longitudinal static modulus of elasticity and can be seen in figure 4.7.



Figure 4.7 - Brookhuis Timber Grader MTG [32]

The device is calibrated using a calibration stick that comes with the device. The species, dimensions, weight, and moisture content of the specimen are input in the device by a software on the computer and the device is ready to be operated [22].

The Timber Grader is used by placing it at the end of a beam and pressing the device lightly against the wood and pressing the yellow button as seen in figure 4.8.



*Figure 4.8 - Instruction of Timber Grader MTG [33]*

The Timber Grader then indicate the output on the device in terms of both the frequency and the static modulus of elasticity. The device measures the dynamic modulus of elasticity but through a factor unbeknown to the authors, calculate and outputs the static modulus of elasticity to the user. The dynamic modulus of elasticity is not possible to take out of the device.

The supports of the wood must be wooden or plastic girders, so that there is vibration free support of the wood. The girders are not to be placed on the ends of the wood when measuring with the Timber Grader MTG. The Timber Grader MTG must be held still when measuring the wood. The Timber Grader MTG has not been tested on impregnated timber before.

## 4.5.2 Software

The software used is the Timber Grader Software, which is an application that can be downloaded. The layout of the software is seen in figure 4.9.

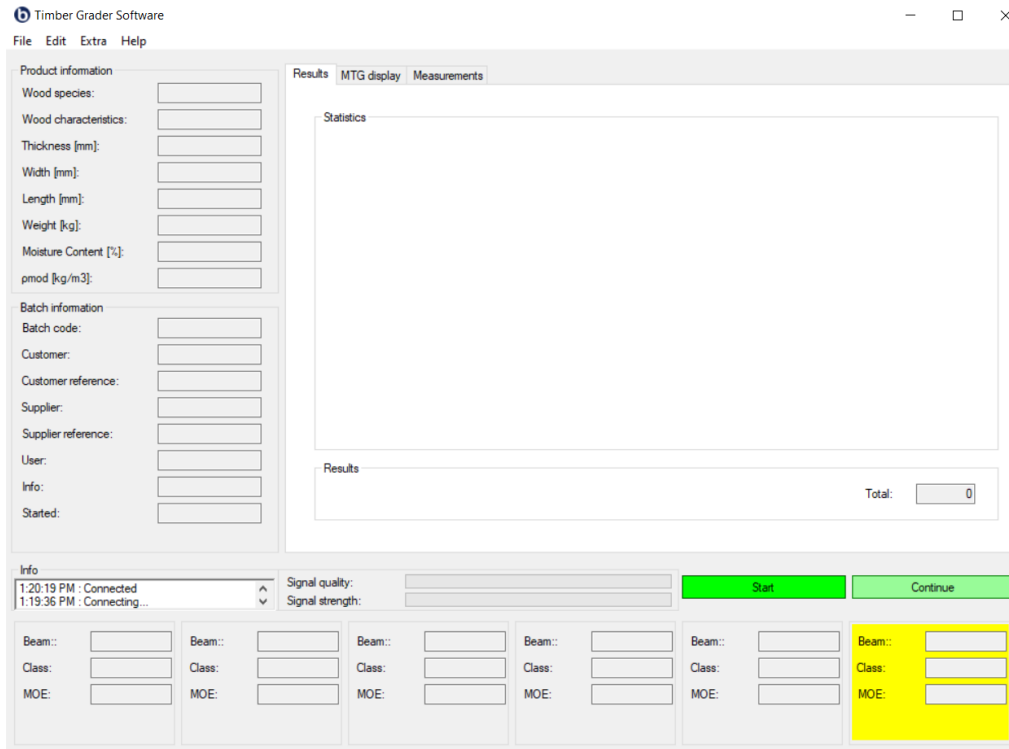


Figure 4.9 - Layout for Timber Grader Software

The first thing that needs to be done is to set the measure settings by going into edit and clicking on "Measure Settings" and clicking on new. Figure 4.10 shows the measure settings. A name is given to the setting. Then natural frequency is chosen for the settings, and wood type is set to softwood, and the density is set to calculate. The other options are set to pc.

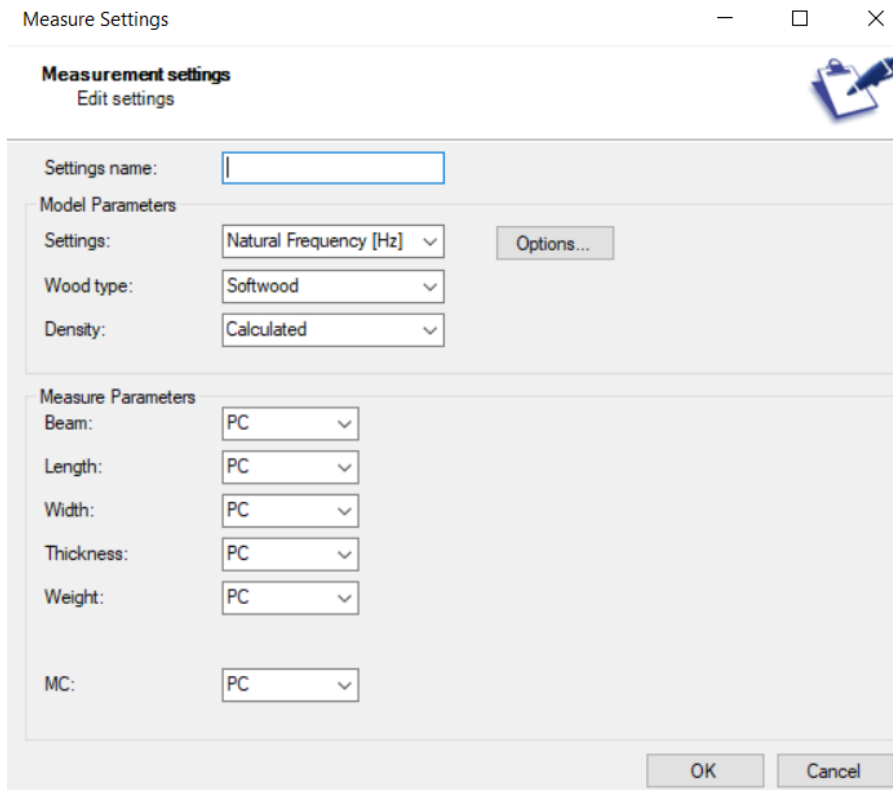


Figure 4.10 - Measure settings for Timber Grader MTG

Next the calibrate option is pressed under the extra tab. The software then needs the reference value for the calibration stick, which is printed on the stick as seen in figure 4.11.

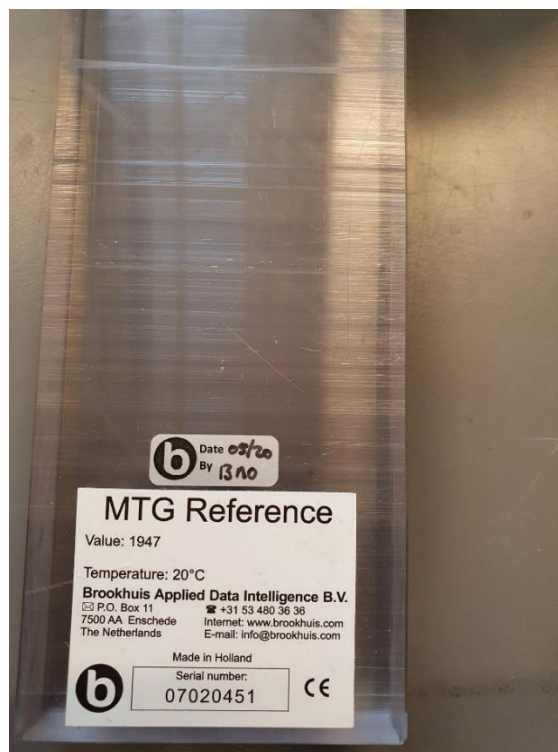


Figure 4.11 - Calibration stick for Timber Grader MTG

The start button is pressed and the Timber Grader MTG is calibrated by placing it at the end of the calibration stick and pressing the yellow button. The Timber Grader MTG is then calibrated.

Next the start button seen in figure 4.9 is pressed. Under settings the Natural Frequency setting is chosen as seen in figure 4.12.

Untitled - Batch

**Batch**  
Edit new Batch

Batch No: MTG0378000079

Customer: My First Customer ... Customer ref.:

Supplier: My First Supplier ... Supplier ref.:

User: Henrik og Ane ... Info:

Setting: Naturlig frekvens ...

OK Cancel

Figure 4.12 - Batch settings for Timber Grader MTG

Next the species is chosen. Pinus sylvestris for pine and Picea abies for spruce. Next the dimension, weight and moisture content for the specimen are chosen as seen in figure 4.13.

Products

**Product**  
Edit product

Thickness [mm]: 48

Width [mm]: 148

Length [mm]: 4000

Weight [kg]: 17.00

MC [%]: 21.7

Batch characteristic: Planned ...

Beam: 1

OK Cancel

Figure 4.13 - Property settings for Timber Grader MTG

When ok is pressed, then the Timber Grader MTG is ready for testing. When a specimen is tested the results are saved in the software, both the natural frequency and the modulus of elasticity.

### 4.5.3 Testing

All twelve beams were tested with the Timber Grader MTG. The scales with rubber-cladding as seen in figure 4.2 were used as supports for the beams. Three distances on the supports were tested to see if it affected the static modulus of elasticity. Distances of 3,5 meters, 2,5 meters and 1,5 meters were tested. Setup of the beam is seen in figure 4.14.



Figure 4.14 - Test setup for Timber Grader MTG

Twelve tests were conducted per beam. The beams were tested edgewise, flatwise and at each end at every support distance as seen in table 4.5.

Table 4.5 - Timber Grader MTG boundary conditions

Side A						Side B					
Flatwise			Edgewise			Flatwise			Edgewise		
3,5 m	2,5 m	1,5 m	3,5 m	2,5 m	1,5 m	3,5 m	2,5 m	1,5 m	3,5 m	2,5 m	1,5 m

The resulting static modulus of elasticity was registered in an excel-file.



## 4.6 Operational Modal method

### 4.6.1 Equipment

The equipment needed in the Operational Modal method [34, 35]:

- 3 PCB Piezotronics Sensor Signal Conditioner – Model 482C05 Series (Figure 4.15)
- 1 HBM Quantum X – MX1601B (Figure 4.16)
- 10 PCB Piezotronics ICP accelerometers – 393B12 (Figure 4.17)
- 10 Industrial twisted shielded cable, 50 Ft – 024R50 (Figure 4.18)
- 10 Two-branch signal cables with BNC connector (Figure 4.19)
- 1 TP-cable (Figure 4.20)
- Computer
- Double sided tape
- An excitation device that simulates operational conditions



Figure 4.15 - PCB Piezotronics Sensor Signal Conditioner – Model 482C05 Series [36]



Figure 4.16 - HBM Quantum X – MX1601B [37]



Figure 4.17 - PCB Piezotronics ICP accelerometers – 393B12 [38]



Figure 4.18 - Industrial twisted shielded cable, 50 Ft – 024R50 [39]

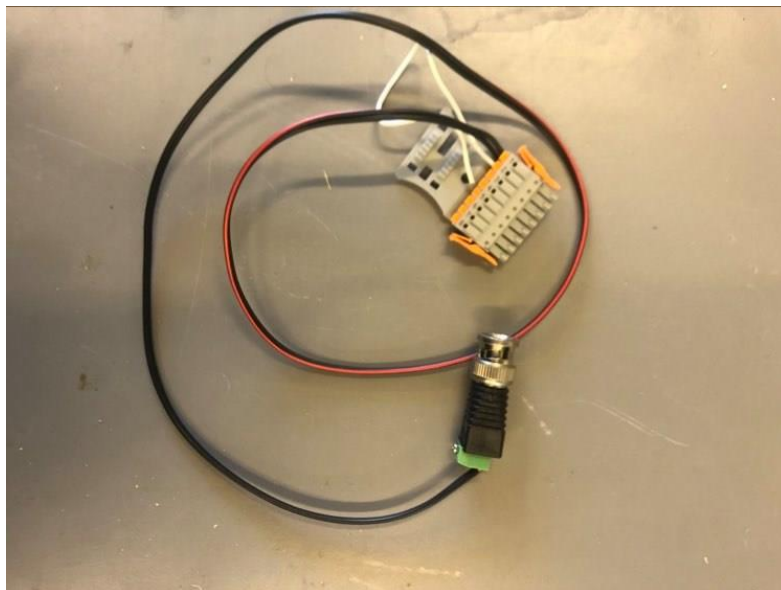
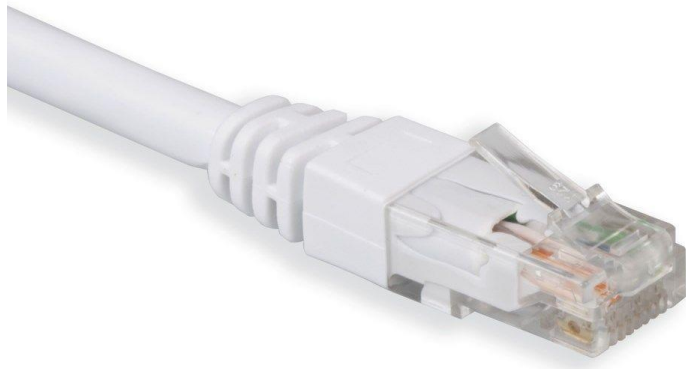


Figure 4.19 - Two-branch signal cables with BNC connector



*Figure 4.20 - TP-cable [40]*

The Piezotronics accelerometers are connected to a beam with double sided tape. When the beam is excited, the accelerometers register the motion and send data signals to the signal conditioners through the industrial twisted cables. The accelerometers are easily overflowed when set in motion. The signal conditioners both receive data signals from the sensors, and power the sensors [41, page 6]. The signal conditioners have 4 available input ports each, so 3 signal conditioners are needed to support 10 accelerometers. The signal conditioner then sends the data signal to the Quantum X through a two-branch signal cable, with BNC connector, inserted into the number 1 spot of the connection plug, see figure 4.21. The connection plug needs to be bridged as seen in figure 4.21 to be able to register any measurements [34, page 112].

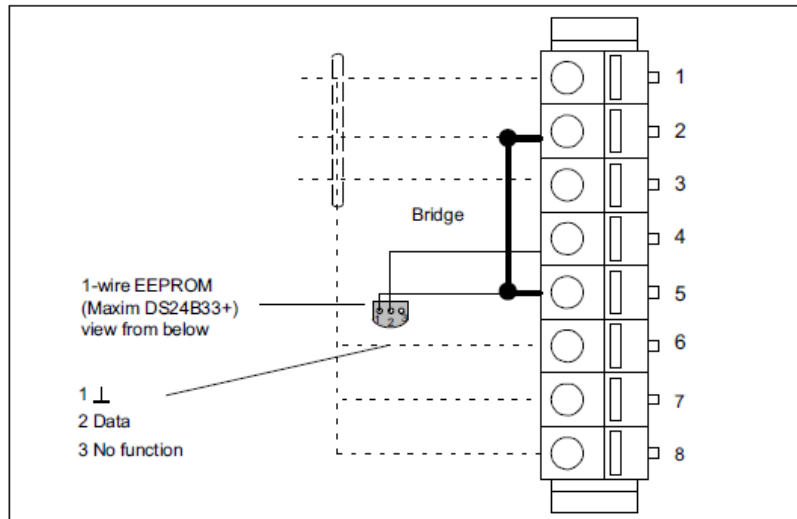


Figure 4.21 - Connection plug bridge

The Quantum X filters the incoming frequencies and reduces "noise" from the signals. The data signals are also digitized and sent to the computer through a TP-cable.

#### 4.6.2 Software

Catman Easy is the software used to process the data signals. Catman Easy is a data acquisition software that makes it easy to acquire, visualize, and analyze measuring data [42].

When Catman Easy is opened, the new DAQ project (QuantumX/SomatXR) is chosen, and in the next window the MX1601B is connected. The layout as seen in figure 4.22 will then be opened.

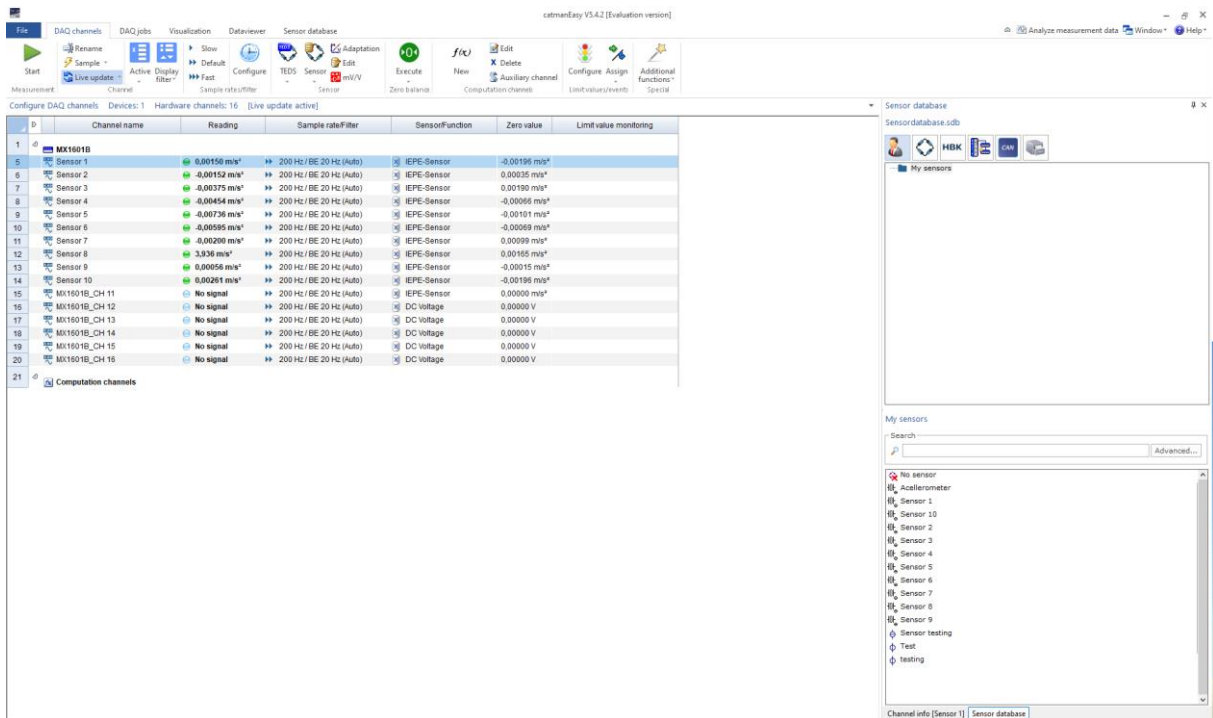


Figure 4.22 - Layout for Catman Easy

The first thing that needs to be done, is to create and configure the sensors. This is done in the Liveupdate tab and right clicking My sensors as seen in figure 4.23 and clicking on New sensor.

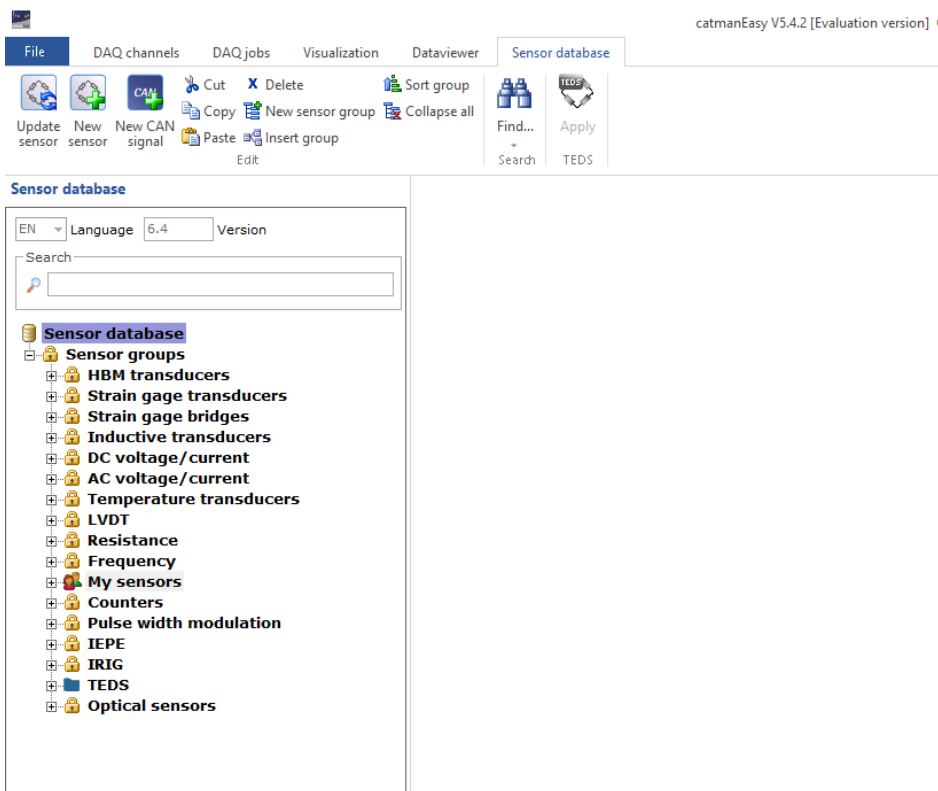


Figure 4.23 - Sensor database

The accelerometers are IEPE-sensors and are chosen in the window seen in figure 4.24.

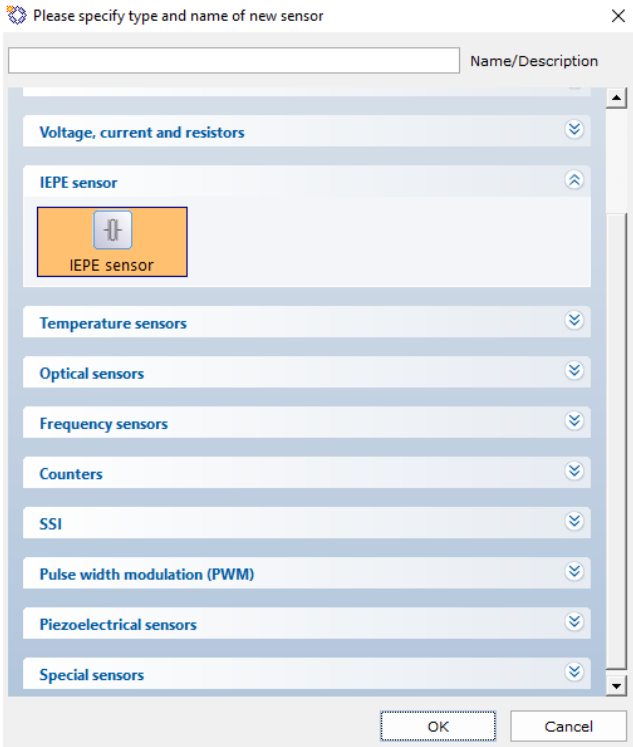


Figure 4.24 - IEPE sensor option

Next the sensitivity for the accelerometers is input in the Transducer characteristic tab as seen in figure 4.25.

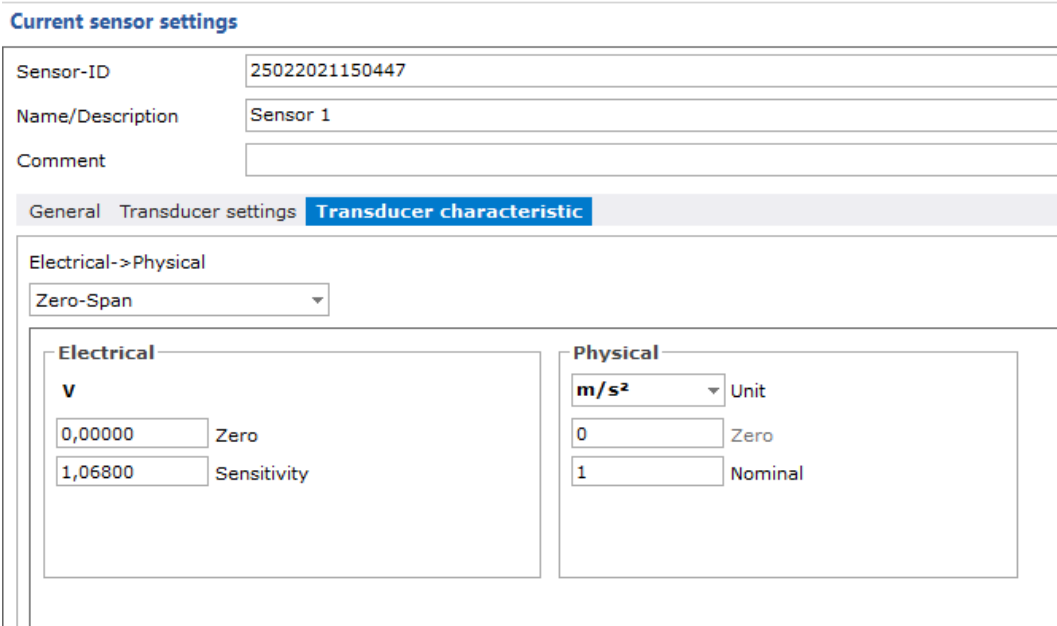


Figure 4.25 - Sensor sensitivity settings

On the physical tab the unit needs to be changed to  $m/s^2$  and put nominally to 1. The sensitivity for all 10 accelerometers is found in Appendix-A1.

When all 10 accelerometers have been created and configured in Catman Easy they become visible in the down-right corner of figure 4.22. Next the sensors are dragged from the down-right corner to the correct channels in the middle of figure 4.22. It is important that the correct sensors are dragged to the correct channel based on the connected accelerometer.

Next the sampling rate is input by marking all accelerometers and pressing the configure button in figure 4.22. When the accelerometers have been in standing for a time without any influences the zero-point for the accelerometers are set by pressing the execute button seen in figure 4.22.

Next the visualization tab is pressed, and scope panel is chosen from the New button as seen in figure 4.26 and the Live FFT button is pressed. The sensors are then checked off in order from 1 to 10 in the Channels tab. Three sensors can also be chosen in the Live FFT tab.

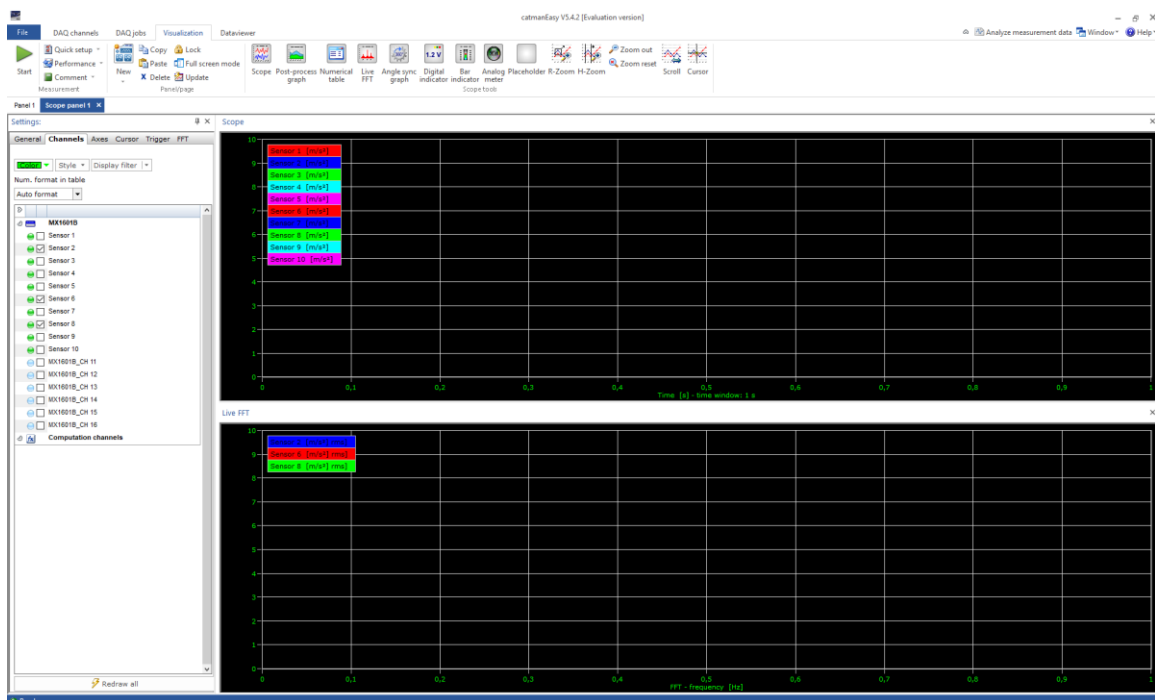


Figure 4.26 - Visualization tab

Next the Axes tab is chosen, and the sampling time is set in the time window as seen in figure 4.27.

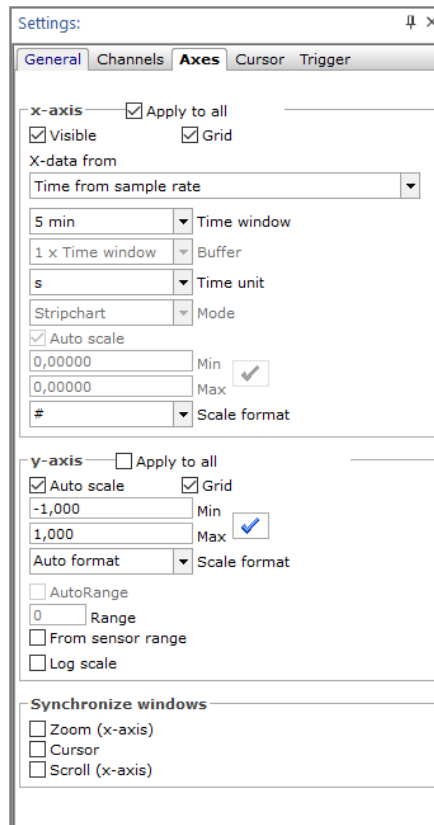


Figure 4.27 - Axes options

Lastly the start button in the top left corner seen in figure 4.26 is pressed to start the test. The same button is pressed to stop the test.

The accelerations from the test are exported into a text file by right clicking the Scope screen seen in figure 4.26 and clicking the Export/print graph and choosing a save location.

Next the accelerations are copied from the text-file and copied into an Excel-file, where the time columns are removed for all the accelerations.

A Matlab script is used to process the data from Catman Easy. The script is called FDD and is written by Mohammad Farshchin, Ph.D candidate at The University of Michigan [43]

The script can be seen in Appendix-A2. The script gives the FDD for the beam by processing the acceleration data. The script is called by the name of the Excel-file with the accelerations and the sampling rate. When the script has processed the data the FDD graph will appear, and the script will ask how many peak accelerations that wants to be examined as seen in figure 4.28.



```
>> [Frq,phi]=FDD('Accelerations.xlsx',500);  
FDD is in progress, please wait ...  
Enter the number of desired peaks:4
```

Figure 4.28 - Calling script function in Matlab

When the number of peaks has been written, the peaks can be chosen from the graph as seen in figure 4.29.

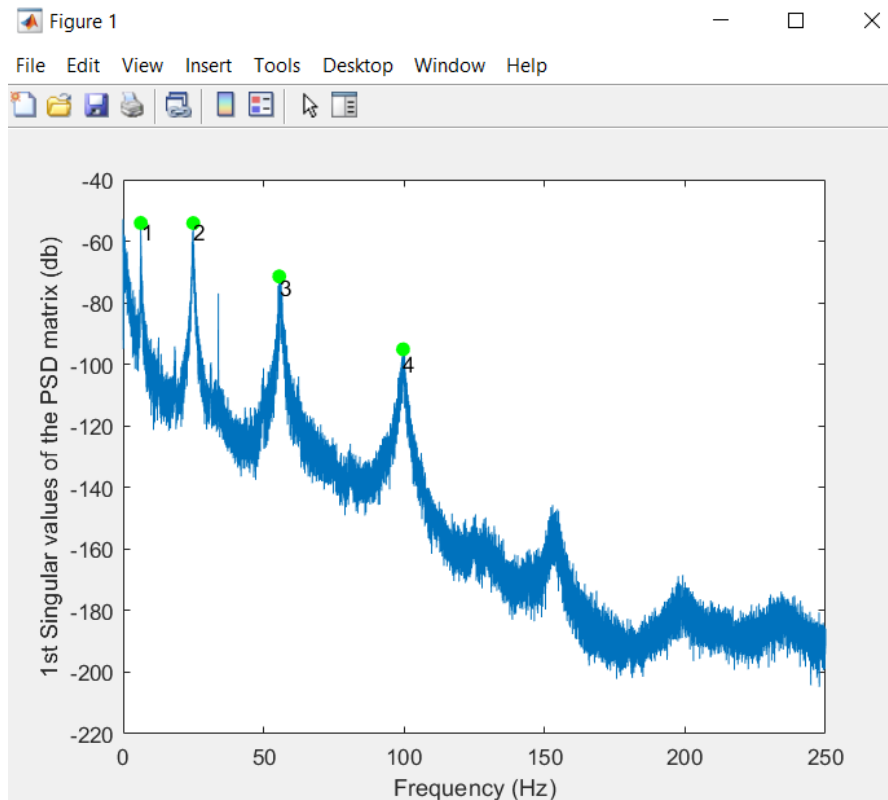


Figure 4.29 - Picking peaks in FDD

When the peaks have been chosen the script will give the natural frequencies and mode shapes for the chosen peaks as seen in figure 4.30.

```

-----
                          Identification Results
-----

Identified frequencies
Mode: 1; Modal Frequency: 6.287 (Hz)
Mode: 2; Modal Frequency: 24.96 (Hz)
Mode: 3; Modal Frequency: 55.56 (Hz)
Mode: 4; Modal Frequency: 99.64 (Hz)
Related mode shapes
Mode shape # 1:

-0.0648 - 0.0000i
-0.1880 - 0.0427i
-0.2351 - 0.0545i
-0.3364 - 0.0858i
-0.4208 - 0.1050i
-0.4728 - 0.1137i
-0.4110 - 0.1106i
-0.3183 - 0.0857i
-0.2424 - 0.0403i
-0.0707 + 0.0062i

Mode shape # 2:

-0.0614 - 0.0000i
-0.3459 + 0.0112i
-0.4005 + 0.0122i
-0.4380 + 0.0149i
-0.2825 + 0.0019i
0.0143 + 0.0007i
0.2996 - 0.0024i
0.4374 - 0.0162i
0.3913 - 0.0315i
0.0900 - 0.0179i

```

Figure 4.30 - Natural frequencies and mode shapes from Matlab

The mode shapes are given in complex numbers. An Excel script has been developed by the authors of the thesis with inspiration from a Matlab script made by Mohammad Farshchin, Ph.D candidate at The University of Michigan (see Appendix-A5) [44]. The Excel script transforms the complex mode shapes to real mode shapes. This is done by taking the modulus of the complex numbers and normalizing them. The sign of the normalized modulus is determined by the phase angle of the complex numbers. The Excel-script then draws the mode shape as seen in figure 4.31. The Excel-script with formatting can be seen in Appendix-A3.

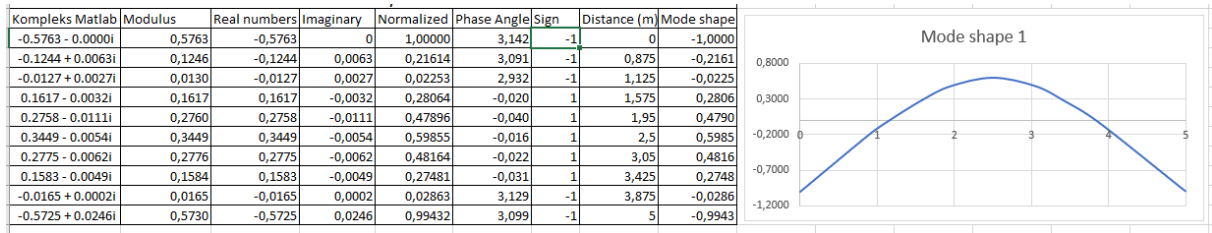


Figure 4.31 - Excel script for drawing mode shapes

#### 4.6.3 Sampling rate and sampling time

A sampling rate needs to be set in Catman Easy before starting a test. The target for these tests is to find the first four natural frequencies. Using the formula for natural frequency, the theoretical fourth natural frequency is found using the static modulus of elasticity obtained from the Timber Grader MTG testing. The Nyquist theorem is then applied to the fourth natural frequency to decide the sampling rate. The sampling rate is then two times the fourth natural frequency and rounded up.

The sampling rates for all the beams flatwise are 500 Hz and for the edgewise 1000 Hz.

The more data points collected by the accelerometers the better the results for the natural frequencies and the modes shapes will be. The sampling time is therefore set to 5 minutes/300 seconds. This means that 150 000 data points are collected per accelerometer for the 500 Hz sampling rate, 300 000 data points for the 1000 Hz, and 750 000 data points for the 2500 Hz.

#### 4.6.4 Background "noise"

With an ambient vibrational test all background "noise" will be included in the outputted results. To be able to ignore these background "noises", two accelerometers were placed on the laboratories floor as seen in figure 4.32.



Figure 4.32 - Accelerometer on floor

The resulting FFT is shown in figure 4.33 and shows which background frequencies there are in the room.

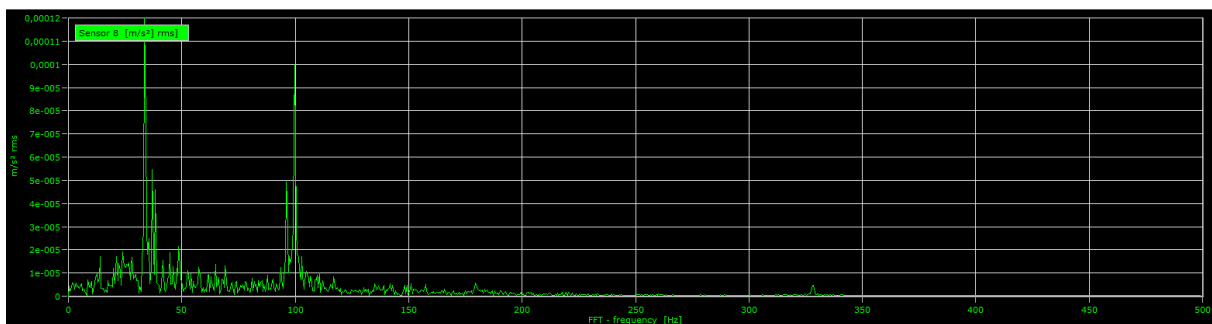


Figure 4.33 - Interference frequencies

The background frequencies in the laboratory are at 33,94 Hz and 99,98 Hz. These frequencies may interfere with the natural frequencies and the mode shapes.

4.6.5 Placement of accelerometers

The placement of the accelerometers is determined by the mode shapes of the beams. To capture the most resonance, which in turn makes it easier to read the natural frequencies from the FDD, the accelerometers should be placed at the anti-nodes of each mode shape. That means the placement of the accelerometers will be different for a simply supported beam and a free-free beam. For both support conditions an accelerometer is placed at each end of the beam to read the end of the mode shapes. There are a total of 10 accelerometers to be placed.

For a simply supported beam the anti-node of mode 1 is at the middle of the beam as seen in figure 3.9. That means an accelerometer is placed at this point. For mode 2 the anti-nodes are at the quarter points of the beam as seen in figure 3.10. An accelerometer is placed at each of these points. For mode 3 the anti-nodes are at  $L/6$ ,  $L/2$ , and  $5L/6$  as seen in figure 3.11. There is already an accelerometer in  $L/2$  from mode 1, so two additional accelerometers are placed at  $L/6$ , and  $5L/6$ . For mode 4 the anti-nodes are at  $L/8$ ,  $3L/8$ ,  $5L/8$ , and  $7L/8$  as seen in figure 3.12. There are only three accelerometers left, so there are placed an accelerometer at  $L/8$ ,  $3L/8$ , and at  $5L/8$ . The reason for excluding one of the anti-nodes of the fourth mode, is that there are already three other anti-nodes being captured for the fourth mode. The placement of the accelerometers for the beams with the length 4 meters and that is simply supported are seen in figure 4.34.

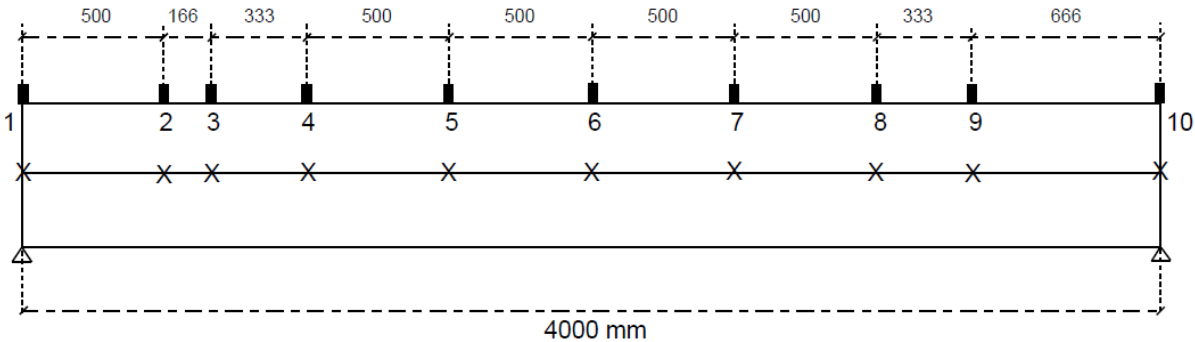


Figure 4.34 - Placement of accelerometers on beams

The rectangles at the top of the beam are the placements of the accelerometers when the beams are edgewise and the X's are the placements when the beams are flatwise. The accelerometers are placed in the middle of the width of the beam when flatwise.

#### 4.6.6 Deciding on support conditions

To be able to know if the results of the tests were correct, the theoretical natural frequencies up to the fourth mode were calculated. Tests were conducted and the results compared to the theoretical natural frequencies. Many different support conditions were tried out before finding a support condition that gave approximately the right results. In this section all the support conditions that were tried but did not give the right results are listed.

The first support condition that was tested was a self-developed free-free configuration. For this configuration two frames were constructed with a top beam connecting them. The test beams were then hung edgewise with elastic bands from the top beam. The elastic bands were placed at the nodes of the free-free mode 1 and striped close to the test beam to stabilize it. The beam was then excited with a light tap of a stick. This configuration did not give results that were comparable to the theoretical calculations. The configuration can be seen in figure 4.35 and 4.36.



*Figure 4.35 - Free-free support condition*



*Figure 4.36 - Elastic bands as supports*

The second support condition that was tested was a pinned-pinned configuration. Two supports consisting of three pieces of timber were constructed. A screw was drilled through the supports and through the test beam and each end. The beam was then excited with a light tap of a stick. This configuration did not give results that were comparable to the theoretical calculations. The configuration can be seen in figure 4.37.



*Figure 4.37 - Pinned-pinned support condition with screw*

The third support condition that was tested was a simply supported configuration. Two frames with some heavy timber at the bottom were constructed to get stiff supports. The test beam was then placed on top of each support at the ends, without any restraints. This configuration gave better results closer to the theoretical calculations, but still a little off. The configuration can be seen in figure 4.38.



*Figure 4.38 - Simply supported beam on timber supports*

The fourth configuration is identical of the third, but the test beam was taped to the support with a double-sided tape. This configuration gave slightly better results than the third configuration, but the results were still a little bit off.

With the fifth configuration a different material was used as supports to see if the natural frequencies were sensitive to different support materials. With this configuration rubber clad scales were clamped to the top of the supports and the test beam was placed on top of the rubber without any restraints. This configuration gave worse results than the third and fourth configuration. The configuration can be seen in figure 4.39.





*Figure 4.39 - Simply supported beam on rubber supports*

The sixth configuration was identical to the fifth, with one exception; the beam was clamped to the rubber. This configuration also gave the wrong results. The configuration can be seen in figure 4.40.

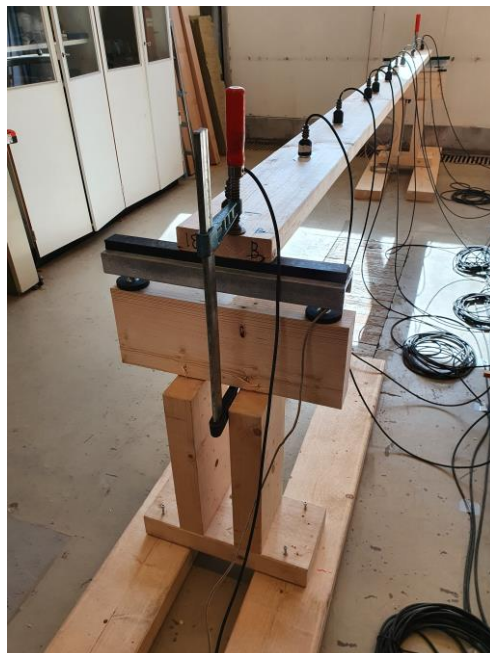


*Figure 4.40 - Simply supported beam on clamped rubber supports*

The seventh configuration was identical to the third with one exception; the beam was clamped to the supports. This configuration also gave the wrong results. The configuration can be seen in figure 4.41.



*Figure 4.41 - Simply supported beam on timber supports with clamping*

With the eighth configuration a steel plate was taped to the supports to again see if the natural frequencies were sensitive to different support materials. This gave almost as good results as the third configuration, but still a little off. The configuration can be seen in figure 4.42.



*Figure 4.42 - Simply supported beam with steel plate*

The ninth configuration was similar to the third, but the test beam was set edgewise and supported by steel angles to stabilize the beam. This configuration gave the wrong results. The configuration can be seen in figure 4.43.

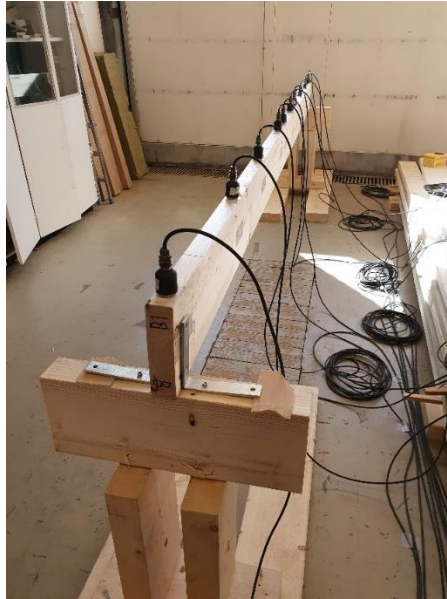


*Figure 4.43 - Simply supported beam with steel angles*

With the tenth configuration steel rollers were clamped to the supports to get as thin supports as possible for the test beam. The test beam was taped to the rollers. This gave the best results out of all the configurations. One more adjustment was needed to be the configuration of choice, which is seen in chapter "4.7.7 Chosen support conditions". The tenth configuration can be seen in figure 4.44 and 4.45.



*Figure 4.44 - Simply supported beam on steel rollers flatwise*



*Figure 4.45 - Simply supported beam on steel rollers edgewise*



#### 4.6.7 Chosen support conditions

The support condition that gave the best results were steel rollers that were clamped to a heavy constructed frame with insulation beneath as seen in figure 4.46. The beams were also taped to the steel rollers.



*Figure 4.46 - Simply supported beam on steel rollers with insulation beneath support*

This configuration gave both a heavy and stiff support for the beams and close to no ambient interference from the floor due to the insulation between the floor and the supports. This is the support condition used for testing all 12 beams with the Operational Modal method.

#### 4.6.8 Testing

All twelve beams were tested with the simply supported condition explained in "4.5.6 Chosen support conditions" both edgewise and flatwise. The accelerometers were placed in the locations given in "4.5.5 Placement of accelerometers". The sampling rate and sampling time were set to the values given in "4.5.3 Sampling rate and sampling time" in Catman Easy. The test was then started on Catman Easy.

The beams were excited with a stick. The beams were tapped lightly, at random intervals and nearby each of the anti-nodes of the first four mode shapes. The taps must be light to prevent the accelerometers from overflowing. After 5 minutes the test was ended, and the accelerations were exported from Catman Easy into the FDD Matlab script. The FDD script was run, and the natural frequencies and complex mode shapes were obtained.

Next the complex mode shapes were run through the authors Mode Shape script in Excel to obtain the real mode shapes.

The fundamental frequency is then put into another Excel script to calculate the dynamic modulus of elasticity for the beams as seen in table 4.6.

Table 4.6 - Calculation of dynamic modulus of elasticity from fundamental frequency

<b>Test 1 - Flatwise</b>	<b>Without accelerometer mass</b>		
Wavnumber 1	k1	9,870	
Natural frequency 1st mode	fn	6,142	Hz
Width	b	0,195	m
Height	h	0,047	m
Moment of Inertia	I	1,68712E-06	m <sup>4</sup>
Line mass	m	3,438	kg/m
Moisture content		13,9 %	
Dynamic Modulus of Elasticity	E	7974722932	N/m <sup>2</sup>

The other natural frequencies are also put into the Excel script to compare them against the theoretical natural frequencies. The theoretical frequencies are calculated using the dynamic modulus of elasticity given by the experimental fundamental frequency of the tested beam as seen in table 4.7.

Table 4.7 - Discrepancy between theoretical and experimental frequencies

DMOE from Operational Modal test	E	7974722932 N/m <sup>2</sup>			
		Mode 1	Mode 2	Mode 3	Mode 4
Wavnenumber n	kn	9,870	39,478	88,826	157,914
Theoretical Natural Frequency	fn <sub>T</sub>	6,142 Hz	24,568 Hz	55,278 Hz	98,272 Hz
Experimental Natural Frequency	fn <sub>E</sub>	6,142 Hz	24,11 Hz	54,85 Hz	97,08 Hz
Discrepancy			1,86 %	0,77 %	1,21 %

The accelerations, the natural frequencies and FDD graph as seen in figures 4.47, 4.48, and 4.49 respectively were then saved in an online saving cloud for every beam edgewise and flatwise.

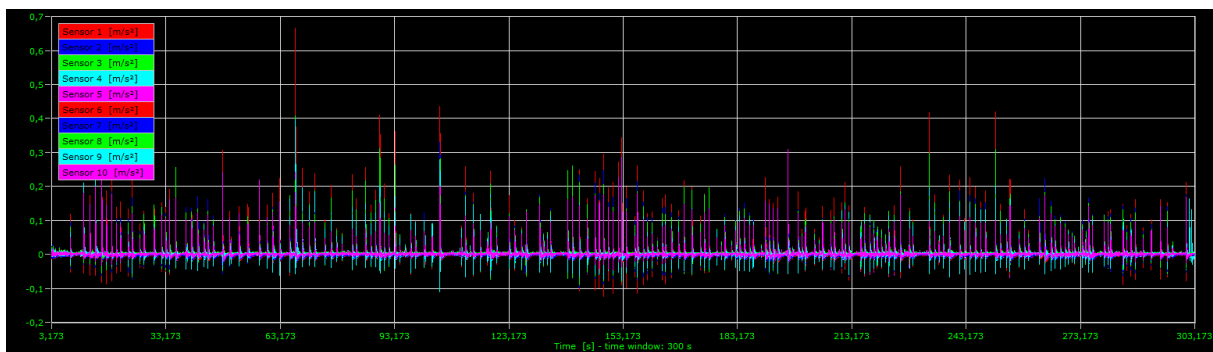


Figure 4.47 - Acceleration data for accelerometers

```

Identified frequencies
Mode: 1; Modal Frequency: 21.68 (Hz)
Mode: 2; Modal Frequency: 84.75 (Hz)
Mode: 3; Modal Frequency: 130.7 (Hz)
Mode: 4; Modal Frequency: 217.8 (Hz)
    
```

Figure 4.48 - Natural frequencies

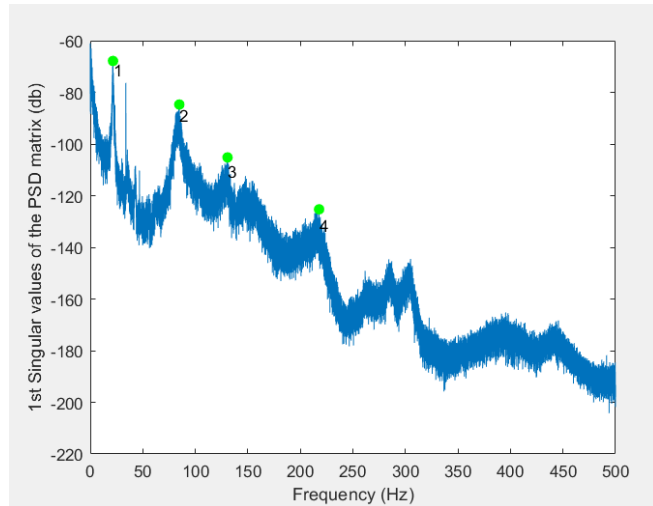


Figure 4.49 - FDD

## 4.7 Smartphone method

### 4.7.1 Equipment

The equipment needed for this method is a modified smartphone by Timbertech and an adjustable strap as seen in figure 4.50.



Figure 4.50 - Equipment for Smartphone method

The already existing accelerometer in the smartphone has been replaced with a more precise accelerometer suitable for vibration tests.



#### 4.7.2 Software

Timbertech has developed an app to coincide with replaced accelerometer in the smartphone as seen in figure 4.51.



Figure 4.51 - App for Smartphone method

The app is called "*Calcolo modula elastico*" and is not downloadable from the internet. It is only locally on this modified smartphone. In the app the layout is as seen in figure 3.6. The dimensions and density of the beam are plotted in the app. The app will obtain the fundamental frequency when a beam is tested and calculate the dynamic modulus of elasticity using the formula presented in equation 1.

### 4.7.3 Testing

The smartphone is strapped to the mid-point of a beam as seen in figure 4.52.



*Figure 4.52 - Test setup for smartphone*

The dimensions and density of the tested beam are input into the app and the start button in the app is pressed. The beam is then excited with a stick with a random force at any location of the beam. For these testing, the excitation was close to the middle of the beam. The app then outputs the fundamental frequency and the dynamic modulus of elasticity. The outputs are then saved in an Excel-file online.

## 4.8 Damages

### 4.8.1 Holes

In order to assess the effect of damages on the MOE two of each beam "class" were tested. Two spruce 48 x 198 mm, two spruce 48 x 148 mm, two pine 48 x 198 mm, and two pine 48 x 148 mm. One of the beams in each class are damaged by cutting out a hole of 80 mm in diameter at 80 mm from the middle of the beam as seen in figure 4.53.



*Figure 4.53 - Hole at mid-point of beam*

The other beam in the class is damaged by cutting two holes of 80 mm in diameter at 80 mm from the quarter points and towards the ends as seen in figure 4.54.



Figure 4.54 - Holes at quarter-points of beam

See figure 4.55 for placement of the hole at the mid-span and figure 4.56 for the placement of the holes at the quarter-points. The holes are placed in the middle of the width.

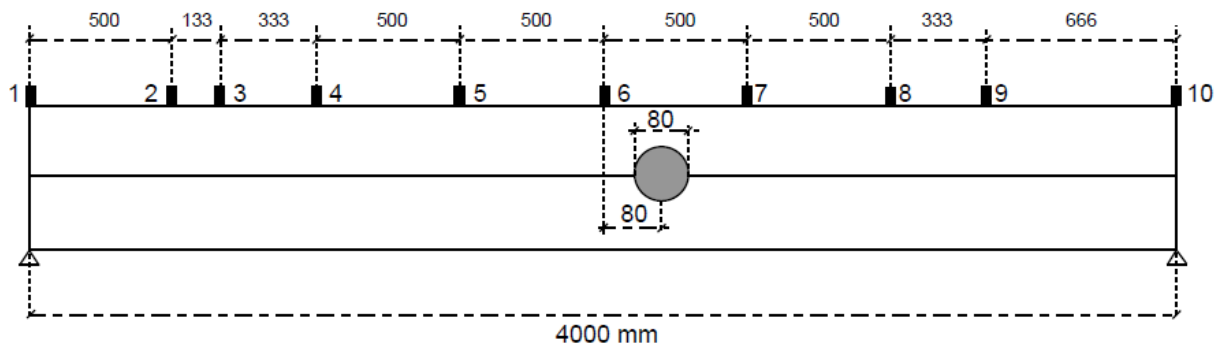


Figure 4.55 - Placement of hole at the mid-point of beams

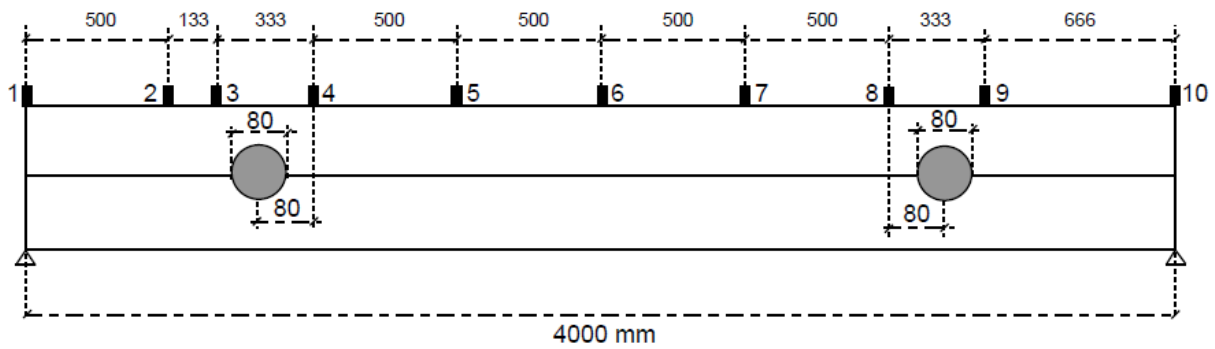


Figure 4.56 - Placement of holes at the quarter-points of beams

Table 4.8 shows which beams that are damaged, and at which location the damages are.

Table 4.8 - List of beams damaged and the placement of the holes

Beam	Placement
1	Middle
2	Quarters
4	Middle
5	Quarters
8	Quarters
9	Middle
10	Quarters
11	Middle

The placement of the hole in the middle is based on the anti-node of Mode 1 and Mode 3, to see if it will affect the mode shapes and the natural frequencies. The placement of the holes at the quarter points are based on the anti-nodes of Mode 2. The reason that the holes are placed a little to the side of the half-point and quarter-points is because the accelerometers must be placed exactly at those points when flatwise.

After the holes are taken, all 8 damaged beams are tested with all three non-destructive methods.

#### 4.8.2 Knots

To evaluate and compare the modulus of elasticity between different specimens, the knots on every specimen are investigated. According to NS-INSTA 142 knots are measured in the width of the beam, not the length. Knots with measurements less than 5 mm are not registered. Knots are only counted on the sapwood side and the edge sides, not on the heartwood side [45].

For all specimens, all knots over 5 mm were counted on the sapwood side and edge sides and registered in an Excel-file. The measurements were done with a digital caliper as seen in figure 4.57.



*Figure 4.57 - Measurement of knot size*

## 5. Results and discussion

To evaluate if the results from the Operational Modal method are correct, the first four modes are observed even though the fundamental frequency is only needed to calculate the dynamic modulus of elasticity. This is to evaluate the higher-order natural frequencies and modes shapes and see how they compare with the theoretical modal properties of the beams.

All the test results for this thesis like natural frequencies, MOE, FDD, mode shapes and regressions for all the beams with the three non-destructive methods are indicated in the digital Appendix-A6.

### 5.1 Deciding on support conditions

In this chapter all the resulting natural frequencies for the tested support conditions and their discrepancies with the higher modes are listed. Beam 1 was tested for all the support configurations.

The first support condition that was tested was the free-free configuration. The beam was tested edgewise. Based on the test on beam 1 the Timber Grader MTG gave a static modulus of elasticity of 9219 N/mm<sup>2</sup>. Using equation 7 the natural frequencies for the first three modes were calculated, with the static modulus of elasticity obtained from the Timber Grader MTG and compared to the first four modes from the Operational Modal test. Table 5.1 indicates the discrepancy between the theoretical values given from the Timber Grader MTG SMOE and the test values.

Table 5.1 - Discrepancy between Timber Grader MTG and Operational Modal method for free-free support

Timber Grader MTG MOE	E	9219 N/mm <sup>2</sup>					
		Mode 1		Mode 2		Mode 3	
Wavnumber n	kn	22,373		61,673		120,903	
Theoretical Natural Frequency	fn <sub>T</sub>	62,109 Hz		171,208 Hz		335,636 Hz	
Experimental Natural Frequency	fn <sub>E</sub>	50,35 Hz		138,2 Hz		256,5 Hz	
Discrepancy		18,93 %		19,28 %		23,58 %	

The variations were considered to be too large for the experimental natural frequencies to be correct. If the experimental frequencies are to be trusted, a fundamental frequency of 50,35 Hz only results in a dynamic modulus of elasticity of 6059 N/mm<sup>2</sup>. According to earlier

work with operational modal analysis the dynamic modulus of elasticity is usually lower than the design modulus of elasticity, though no range of magnitude is suggested. This could be the reason the tests are producing a low dynamic modulus of elasticity but considering that the design modulus of elasticity for a C24 beam is usually around 11 000 N/mm<sup>2</sup> (as seen in Appendix A4.) makes the tests results unconvincing. It seemed unlikely at the time of testing that these huge variations in modulus of elasticity could be correct. For this reason, the free-free support configuration was not pursued further.

For the later tests with the other support configurations as described in chapter "4.6.6 *Deciding on support conditions*", it was observed that the dynamic modulus of elasticity was always smaller than the static modulus of elasticity obtained from the Timber Grader MTG, and the design MOE levels. The discrepancies between the experimental and theoretical modes were also always significant. Considering the purpose of this thesis was to test and compare different non-destructive methods, it was decided that the MOE obtained from the various methods should first be evaluated separately and then compared later, in case some of the methods provides wrong results. The possibility that the Operational Modal test provided the correct DMOE, even though it was low, had to be taken into consideration.

It was therefore decided that the fundamental frequency obtained from the Operational Modal testing would be used to calculate the dynamic modulus of elasticity using equation 1. The calculated DMOE was then used to calculate the first three to four natural frequencies of the beams with equation 7. The discrepancies between the theoretical and experimental modes were then calculated and evaluated.

As explained earlier, this was decided after the free-free configuration was abandoned. In the later stages of working with this thesis, it was decided to use the fundamental frequency obtained from the free-free test and calculate the first three natural frequencies. Table 5.2 indicates the experimental and theoretical frequencies and their discrepancy for the free-free configuration.



Table 5.2 - Discrepancy for natural frequencies for free-free support conditions

**Test - Edgewise**

Wavnumber 1	k1	22,373	
Natural frequency 1st mode	fn	50,35	Hz
Width	b	0,047	m
Height	h	0,195	m
Moment of Inertia	I	2,9042E-05	m <sup>4</sup>
Line mass	m	3,438	kg/m
Moisture content		13,9	%

DMOE from Operational Modal testing	E	6059	N/mm <sup>2</sup>
-------------------------------------	---	------	-------------------

		Mode 1	Mode 2	Mode 3
Wavnumber n	kn	22,373	61,673	120,903
Theoretical Natural Frequency	fn <sub>T</sub>	50,350 Hz	138,794 Hz	272,092 Hz
Experimental Natural Frequency	fn <sub>E</sub>	50,350 Hz	138,2 Hz	256,5 Hz
Discrepancy			0,43 %	5,73 %

As seen in table 5.2 the correlation between the theoretical and experimental natural frequencies are in fact decent. If the fundamental frequency and in turn the low DMOE can be trusted, it would mean in hindsight that the Operational Modal method is suitable for the free-free support configuration that was constructed. Unfortunately, this was discovered too late in the process of working with the thesis, so tests could not be conducted with the free-free configuration.

The second support configuration tested was the pinned-pinned connection with a screw through each end of the beam. The beam was tested edgewise. The results were not decent compared to the SMOE obtained from the Timber Grader MTG as seen in table 5.3.

Table 5.3 - Discrepancy between Timber Grader MTG and Operational Modal method for screw pinned-pinned support

Timber Grader MTG MOE	E	9219	N/mm <sup>2</sup>
-----------------------	---	------	-------------------

		Mode 1	Mode 2	Mode 3
Wavnumber n	kn	9,870	39,478	88,826
Theoretical Natural Frequency	fn <sub>T</sub>	27,40 Hz	109,59 Hz	246,59 Hz
Experimental Natural Frequency	fn <sub>E</sub>	24,87 Hz	127,2 Hz	306,5 Hz
Discrepancy		9,23 %	16,06 %	24,30 %

The discrepancy between the natural frequencies were considered too significant to be correct. Calculations with the DMOE obtained from the Operational Modal method were also done for this configuration as seen in table 5.4.

Table 5.4 - Discrepancy for natural frequencies for screw pinned-pinned support

**Test - Edgewise**

Wavnenumber 1	k1	9,870	
Natural frequency 1st mode	fn	24,87	Hz
Width	b	0,047	m
Height	h	0,195	m
Moment of Inertia	I	2,9042E-05	m <sup>4</sup>
Line mass	m	3,438	kg/m
Moisture content		13,9	%

DMOE from Operational Modal testing	E	7595	N/mm <sup>2</sup>
-------------------------------------	---	------	-------------------

		Mode 1	Mode 2	Mode 3
Wavnenumber n	kn	9,870	39,478	88,826
Theoretical Natural Frequency	fn <sub>T</sub>	24,870 Hz	99,476 Hz	223,821 Hz
Experimental Natural Frequency	fn <sub>E</sub>	24,870 Hz	127,2 Hz	306,5 Hz
Discrepancy			27,87 %	36,94 %

The variations were even higher for this calculation. The reason for these variations could be that the screws restrained the beams at the supports, in a manner that the beam was no longer considered as pinned-pinned supported. It could also be due to the supports not being stable enough, and that ambient vibrations from the floor were influencing the results.

The third configuration was a simply supported configuration with timber frames as supports. It was decided to test the beams flatwise, as the edgewise tests were not providing any decent results. The comparison between the SMOE obtained from the Timber Grader MTG and the theoretical natural frequencies can be seen in table 5.5.

Table 5.5 - Discrepancy between Timber Grader MTG and Operational Modal method for simply supported timber supports

Timber Grader MTG MOE	E	9219	N/mm <sup>2</sup>
-----------------------	---	------	-------------------

		Mode 1	Mode 2	Mode 3
Wavnenumber n	kn	9,870	39,478	88,826
Theoretical Natural Frequency	fn <sub>T</sub>	6,60 Hz	26,42 Hz	59,43 Hz
Experimental Natural Frequency	fn <sub>E</sub>	6,348 Hz	24,41 Hz	51,76 Hz
Discrepancy		3,87 %	7,59 %	12,91 %

The discrepancies are lower than the previously tested support conditions. Table 5.6 indicates the discrepancies when the natural frequencies are calculated with the obtained DMOE from the Operational Modal test.

Table 5.6 - Discrepancy for natural frequencies for simply supported timber support

**Test - Flatwise**

Wavnenumber 1	k1	9,870	
Natural frequency 1st mode	fn	6,348	Hz
Width	b	0,195	m
Height	h	0,047	m
Moment of Inertia	I	1,6871E-06	m <sup>4</sup>
Line mass	m	3,438	kg/m
Moisture content		13,9	%

DMOE from Operational Modal testing	E	8518	N/mm <sup>2</sup>
-------------------------------------	---	------	-------------------

		Mode 1	Mode 2	Mode 3
Wavnenumber n	kn	9,870	39,478	88,826
Theoretical Natural Frequency	fn <sub>T</sub>	6,348 Hz	25,391 Hz	57,130 Hz
Experimental Natural Frequency	fn <sub>E</sub>	6,348 Hz	24,41 Hz	51,76 Hz
Discrepancy			3,86 %	9,40 %

It is observed in table 5.6 that the discrepancy is lower for this support configuration, but the variations could be relatively better. The reason for the discrepancies could be due to the thickness of the supports. The supports had a thickness of 150 mm, and the beam was resting over the total thickness. This means the length of the beam is in reality reduced by 300 mm. Another reason might be that the beam has no restraints at the supports, which might lead to the beam being in motion at the supports when excited.

The fourth support configuration was chosen to prevent the beam from being in motion at the supports. The beam was tested flatwise. The support was identical to the third configuration, but the beam was taped to the supports. This would restrain the beam slightly, but hopefully not so much that the beam was not considered simply supported. This slight improvement of the supports gave better results both for the comparison with the natural frequencies obtained from the Timber Grader MTG as seen in table 5.7. The results were also improved when the natural frequencies were calculated with the DMOE obtained from the Operational Modal method as seen in table 5.8.

Table 5.7 - Discrepancy between Timber Grader MTG and Operational Modal method for taped simply supported timber supports

Timber Grader MTG MOE	E	9219	N/mm <sup>2</sup>	
		Mode 1	Mode 2	Mode 3
Wavnenumber n	kn	9,870	39,478	88,826
Theoretical Natural Frequency	fn <sub>T</sub>	6,60 Hz	26,42 Hz	59,43 Hz
Experimental Natural Frequency	fn <sub>E</sub>	6,378 Hz	25,12 Hz	54,57 Hz
Discrepancy		3,42 %	4,90 %	8,18 %

Table 5.8 - Discrepancies for natural frequencies for taped simply supported timber support

**Test - Flatwise**

Wavnenumber 1	k1	9,870	
Natural frequency 1st mode	fn	6,378	Hz
Width	b	0,195	m
Height	h	0,047	m
Moment of Inertia	I	1,6871E-06	m <sup>4</sup>
Line mass	m	3,438	kg/m
Moisture content		13,9 %	

DMOE from Operational Modal testing	E	8599	N/mm <sup>2</sup>
-------------------------------------	---	------	-------------------

		Mode 1	Mode 2	Mode 3
Wavnenumber n	kn	9,870	39,478	88,826
Theoretical Natural Frequency	fn <sub>T</sub>	6,378 Hz	25,511 Hz	57,400 Hz
Experimental Natural Frequency	fn <sub>E</sub>	6,378 Hz	25,12 Hz	54,57 Hz
Discrepancy			1,53 %	4,93 %

The discrepancies seen in table 5.8 are relatively satisfactory, but other support configurations were tested to see if it were possible to get even better results.

The fifth configuration was tested to see if the support material would have any effect on the results. Rubber-clad scales were used as supports, and the beam was not restrained to the rubber. The beam was tested flatwise. The results for the comparison with the Timber Grader MTG and calculation with the DMOE obtained from Operational Modal Method can be seen in table 5.9 and 5.10.

Table 5.9 - Discrepancy between Timber Grader MTG and Operational Modal method for simply supported rubber support

Timber Grader MTG MOE	E	9219	N/mm <sup>2</sup>
		Mode 1	Mode 2
Wavnenumber n	kn	9,870	39,478
Theoretical Natural Frequency	fn <sub>T</sub>	6,60 Hz	26,42 Hz
Experimental Natural Frequency	fn <sub>E</sub>	6,165 Hz	26,98 Hz
Discrepancy		6,64 %	2,14 %

Table 5.10 - Discrepancy for natural frequencies for simply supported rubber support

**Test - Flatwise**

Wavnenumber 1	k1	9,870	
Natural frequency 1st mode	fn	6,165	Hz
Width	b	0,195	m
Height	h	0,047	m
Moment of Inertia	I	1,6871E-06	m <sup>4</sup>
Line mass	m	3,438	kg/m
Moisture content		13,9 %	

DMOE from Operational Modal testing	E	8034	N/mm <sup>2</sup>
-------------------------------------	---	------	-------------------

		Mode 1	Mode 2
Wavnenumber n	kn	9,870	39,478
Theoretical Natural Frequency	fn <sub>T</sub>	6,165 Hz	24,659 Hz
Experimental Natural Frequency	fn <sub>E</sub>	6,165 Hz	26,98 Hz
Discrepancy			9,41 %

The results for the rubber supports are not satisfactory. The elastic nature of the rubber supports is probably contributing to motion of the beam at the supports.

The sixth support condition was similar to the third. The motion effect was removed by clamping the beam to the timber supports. The beam was tested flatwise. Table 5.11 and 5.12 indicates the results for comparison with Timber Grader MTG and calculation of the natural frequencies with the DMOE obtained from the Operational Modal method.

Table 5.11 - Discrepancy between Timber Grader MTG and Operational Modal method for clamped simply supported timber supports

Timber Grader MTG MOE	E	9219	N/mm <sup>2</sup>
		Mode 1	Mode 2
Wavnenumber n	kn	9,870	39,478
Theoretical Natural Frequency	fn <sub>T</sub>	6,60 Hz	26,42 Hz
Experimental Natural Frequency	fn <sub>E</sub>	7,019 Hz	25,85 Hz
Discrepancy		6,29 %	2,14 %

Table 5.12 - Discrepancy for natural frequencies for clamped simply supported timber support

**Test - Flatwise**

Wavnumber 1	k1	9,870	
Natural frequency 1st mode	fn	7,019	Hz
Width	b	0,195	m
Height	h	0,047	m
Moment of Inertia	I	1,6871E-06	m <sup>4</sup>
Line mass	m	3,438	kg/m
Moisture content		13,9	%

DMOE from Operational Modal testing	E	10414	N/mm <sup>2</sup>
-------------------------------------	---	-------	-------------------

		Mode 1	Mode 2	Mode 3
Wavnumber n	kn	9,870	39,478	88,826
Theoretical Natural Frequency	fn <sub>T</sub>	7,019 Hz	28,075 Hz	63,168 Hz
Experimental Natural Frequency	fn <sub>E</sub>	7,019 Hz	25,85 Hz	54,32 Hz
Discrepancy			7,92 %	14,01 %

The fundamental frequency was increased because of the clamping. The reason for this is probably that the beam is restrained at the supports, in such a manner that the beam is no longer simply supported. This in turn will increase the discrepancies on the higher modes due to the calculations being based on simply supported boundary conditions.

The seventh support configuration is similar to the third, however a steel plate has been placed between the beam and the support to see if the material of the support affects the natural frequencies. The beam is also taped to the steel plate. The beam was tested flatwise. Table 5.13 and 5.14 indicates the results for comparison with Timber Grader MTG and calculation of the natural frequencies with the DMOE obtained from the Operational Modal method.

Table 5.13 - Discrepancy between Timber Grader MTG and Operational Modal method for simply supported steel plate supports

Timber Grader MTG MOE	E	9219	N/mm <sup>2</sup>
-----------------------	---	------	-------------------

		Mode 1	Mode 2	Mode 3
Wavnumber n	kn	9,870	39,478	88,826
Theoretical Natural Frequency	fn <sub>T</sub>	6,60 Hz	26,42 Hz	59,43 Hz
Experimental Natural Frequency	fn <sub>E</sub>	6,805 Hz	26,28 Hz	54,96 Hz
Discrepancy		3,05 %	0,51 %	7,53 %

Table 5.14 - Discrepancy for natural frequencies for simply supported steel plate support

**Test - Flatwise**

Wavnenumber 1	k1	9,870	
Natural frequency 1st mode	fn	6,805	Hz
Width	b	0,195	m
Height	h	0,047	m
Moment of Inertia	I	1,6871E-06	m <sup>4</sup>
Line mass	m	3,438	kg/m
Moisture content		13,9	%

DMOE from Operational Modal testing	E	9789	N/mm <sup>2</sup>
-------------------------------------	---	------	-------------------

		Mode 1	Mode 2	Mode 3
Wavnenumber n	kn	9,870	39,478	88,826
Theoretical Natural Frequency	fn <sub>T</sub>	6,805 Hz	27,219 Hz	61,243 Hz
Experimental Natural Frequency	fn <sub>E</sub>	6,805 Hz	26,28 Hz	54,96 Hz
Discrepancy			3,45 %	10,26 %

The discrepancy between the Timber Grader MTG and the experimental natural frequencies from the Operational Modal test is decent, except on the third mode. The same can be seen in table 5.14. The reason for the discrepancies might yet again be due to the beam laying across the entire thickness of the support, which in reality reduces the length of the beam.

With the eighth support condition the beam was tested edgewise again with steel angles as stabilizers at the supports. Table 5.15 and 5.16 indicates the results for comparison with Timber Grader MTG and calculation of the natural frequencies with the DMOE obtained from the Operational Modal method.

Table 5.15 - Discrepancy between Timber Grader MTG and Operational Modal method for simply supported and steel angle stabilization

Timber Grader MTG MOE	E	9219	N/mm <sup>2</sup>
-----------------------	---	------	-------------------

		Mode 1	Mode 2	Mode 3
Wavnenumber n	kn	9,870	39,478	88,826
Theoretical Natural Frequency	fn <sub>T</sub>	27,40 Hz	109,59 Hz	246,59 Hz
Experimental Natural Frequency	fn <sub>E</sub>	26,02 Hz	96,21 Hz	178,6 Hz
Discrepancy		5,03 %	12,21 %	27,57 %

Table 5.16 - Discrepancy for natural frequencies for simply supported and steel angle stabilized

Wavnumber 1	k1	9,870	
Natural frequency 1st mode	fn	26,02	Hz
Width	b	0,047	m
Height	h	0,195	m
Moment of Inertia	I	2,9042E-05	m <sup>4</sup>
Line mass	m	3,438	kg/m
Moisture content		13,9 %	

DMOE from Operational Modal testing	E	8314	N/mm <sup>2</sup>
-------------------------------------	---	------	-------------------

		Mode 1	Mode 2	Mode 3
Wavnumber n	kn	9,870	39,478	88,826
Theoretical Natural Frequency	fn <sub>T</sub>	26,020 Hz	104,076 Hz	234,171 Hz
Experimental Natural Frequency	fn <sub>E</sub>	26,020 Hz	96,21 Hz	178,6 Hz
Discrepancy			7,56 %	23,73 %

The discrepancies are not decent for any of the comparisons. It has been a repeating problem through testing in this thesis that the edgewise tests did not provide decent discrepancy between the experimental and theoretical results. The reason for this is discussed in section "5.4 Edgewise vs flatwise".

The ninth support condition tested was the taped steel rollers on the timber supports. The beam was tested flatwise. Table 5.17 and 5.18 indicates the results for comparison with Timber Grader MTG and calculation of the natural frequencies with the DMOE obtained from the Operational Modal method.

Table 5.17 - Discrepancy between Timber Grader MTG and Operational Modal method for taped simply supported steel rollers support

Timber Grader MTG MOE	E	9219	N/mm <sup>2</sup>
-----------------------	---	------	-------------------

		Mode 1	Mode 2	Mode 3
Wavnumber n	kn	9,870	39,478	88,826
Theoretical Natural Frequency	fn <sub>T</sub>	6,60 Hz	26,42 Hz	59,43 Hz
Experimental Natural Frequency	fn <sub>E</sub>	6,264 Hz	24,7 Hz	53,76 Hz
Discrepancy		5,15 %	6,49 %	9,55 %



Table 5.18 - Discrepancy for natural frequencies for taped simply supported steel rollers support

**Test - Flatwise**

Wavnumber 1	k1	9,870	
Natural frequency 1st mode	fn	6,264	Hz
Width	b	0,195	m
Height	h	0,047	m
Moment of Inertia	I	1,6871E-06	m <sup>4</sup>
Line mass	m	3,438	kg/m
Moisture content		13,9	%

DMOE from Operational Modal testing	E	8294	N/mm <sup>2</sup>
-------------------------------------	---	------	-------------------

		Mode 1	Mode 2	Mode 3
Wavnumber n	kn	9,870	39,478	88,826
Theoretical Natural Frequency	fn <sub>T</sub>	6,264 Hz	25,055 Hz	56,374 Hz
Experimental Natural Frequency	fn <sub>E</sub>	6,264 Hz	24,7 Hz	53,76 Hz
Discrepancy			1,42 %	4,64 %

As seen in table 5.17 the discrepancies are relatively significant on the higher modes. Table 5.18 indicates the lowest discrepancies on the higher modes, out of all the support conditions tested. This may be due to the fact that the support is both heavy and stiff. The curvature of the steel rollers provides a seamless connection between the beam and the supports, which enables the full length of the beam to be utilized.

Chapter "5.2 Chosen support condition" shows the results for the chosen support condition.

## 5.2 Chosen support condition

As discovered in chapter "5.1 Deciding on support condition" the support condition that gave the best results on all modes was the taped steel roller on top of timber frames. The results were almost satisfactory. The only issue with this support condition was that the FDD given from testing with the Operational Modal method had a lot of interference. That means it was challenging to pick the peaks in the FDD that correlated to the first four modes. As explained in chapter "4.7.4 Background "noise"", there are some vibrational interferences in the laboratory where the tests were conducted. There were background interferences recorded at 33,94 Hz and 99,98 Hz. These peaks were visible in the FDD for the beams tested with the steel rollers on top of the timber frames. These interferences can affect the natural frequencies and mode shapes of a beam due to them being significant. This might explain the discrepancies in the higher modes.

To address the interference frequencies, insulation was put between the timber frames and the floor. This measure completely removed the interference at 99,98 Hz and effectively reduced the interference at 33,94 Hz. The discrepancies on the higher modes were also reduced, but it resulted in a lower dynamic modulus of elasticity as seen in table 5.19 where the natural frequencies have been calculated with the DMOE obtained from the Operational Modal test.

Table 5.19 - Discrepancy for natural frequencies for taped simply supported steel rollers support with insulation

Test 1 - Flatwise							
Wavnumber 1	k1	9,870					
Natural frequency 1st mode	fn	6,142	Hz				
Width	b	0,195	m				
Height	h	0,047	m				
Moment of Inertia	I	1,68712E-06	m <sup>4</sup>				
Line mass	m	3,438	kg/m				
Moisture content		13,9	%				
DMOE from Operational Modal test	E	7974722932	N/m <sup>2</sup>				

		Mode 1	Mode 2	Mode 3	Mode 4
Wavnumber n	k1	9,870	39,478	88,826	157,914
Theoretical Natural Frequency	fn <sub>T</sub>	6,142 Hz	24,568 Hz	55,278 Hz	98,272 Hz
Experimental Natural Frequency	fn <sub>E</sub>	6,142 Hz	24,11 Hz	54,85 Hz	97,08 Hz
Discrepancy			1,86 %	0,77 %	1,21 %

The difference in DMOE from the support without insulation and with insulation is only around 300 N/mm<sup>2</sup> and only 0,122 Hz for the fundamental frequencies. From the theory it is known that operational modal analysis will not provide the same frequencies for every test conducted, even though the boundary conditions are identical. This is because the test is based on ambient unknown input. This means that the 0,122 Hz difference in the fundamental frequencies might be due to differences in the ambient vibrational test and not the support conditions.

Considering the discrepancies on the modes for this support condition are so low, this support condition is chosen to test all 12 beams.

### 5.3 Repetitive testing

Repetitive testing was conducted for all the test methods to ensure that the frequencies and modulus of elasticity are approximately the same between tests. If the repetitive testing provides approximately the same results for a couple of beams it would only be necessary to conduct one test with each method for the rest of the beams.

The beams were tested extensively with the Timber Grader MTG. The beams were tested flatwise, edgewise, at each end, and at different support lengths. Table 5.20 and 5.21 indicates the static modulus of elasticity and the frequencies obtained for beam 1.

Table 5.20 - Timber Grader MTG tests, static modulus of elasticity

Side A						Side B					
Flatwise Beam			Edgewise Beam			Flatwise Beam			Edgewise Beam		
Support: 3,5 m	Support 2,5 m	Support: 1,5 m	Support: 3,5 m	Support 2,5 m	Support: 1,5 m	Support: 3,5 m	Support 2,5 m	Support: 1,5 m	Support: 3,5 m	Support 2,5 m	Support: 1,5 m
9219	9219	9219	9219	9219	9219	9219	9219	9219	9219	9219	9103

Table 5.21 - Timber Grader MTG tests, natural frequencies

Side A						Side B					
Horizontal Beam			Standing Beam			Horizontal Beam			Standing Beam		
Support: 3,5 m	Support 2,5 m	Support: 1,5 m	Support: 3,5 m	Support 2,5 m	Support: 1,5 m	Support: 3,5 m	Support 2,5 m	Support: 1,5 m	Support: 3,5 m	Support 2,5 m	Support: 1,5 m
634	634	634	634	634	634	634	634	634	634	634	630

As the tables suggest, the modulus of elasticity is the same for any given condition when using the Timber Grader MTG. It is therefore reasonable to assume that the Timber Grader MTG is consistent with its results for the modulus of elasticity.

For the Operational Modal method, two beams were tested three times. The beams tested were beam 3 and 6, and they were tested flatwise. Table 5.22 shows the discrepancy between the two tests that were furthest apart of the three, on the natural frequency and dynamic modulus of elasticity.

Table 5.22 - Discrepancy in repetitive testing with Operational Modal method

Mode 1	Test 1	Test 2	Discrepancy
Beam 3 DMOE (N/mm <sup>2</sup> )	8 085	8 147	0,77 %
Beam 3 Fundamental frequency (Hz)	5,981	6,004	0,38 %
Beam 6 DMOE (N/mm <sup>2</sup> )	9 950	10 259	3,11 %
Beam 6 Fundamental frequency (Hz)	6,477	6,577	1,54 %

Table 5.23, 5.24, and 5.25 indicates the discrepancy between the two tests that were furthest apart of the three, on the natural frequencies of the higher modes.

Table 5.23 - Discrepancy in mode 2 with repetitive testing with Operational Modal method

Mode 2	Test 1	Test 2	Discrepancy
Beam 3 Natural frequency (Hz)	22,62	22,71	0,40 %
Beam 6 Natural frequency (Hz)	25,59	25,87	1,08 %

Table 5.24 - Discrepancy in mode 3 with repetitive testing with Operational Modal method

Mode 3	Test 1	Test 2	Discrepancy
Beam 3 Natural frequency (Hz)	52,83	53,29	0,87 %
Beam 6 Natural frequency (Hz)	58,83	59,08	0,42 %

Table 5.25 - Discrepancy in mode 4 with repetitive testing with Operational Modal method

Mode 4	Test 1	Test 2	Discrepancy
Beam 3 Natural frequency (Hz)	93,24	95,5	2,42 %
Beam 6 Natural frequency (Hz)	103,3	103,5	0,19 %

The conducted tests indicates that the obtained values will not always match, even though the tests are conducted in the same manner and with equal boundary conditions. The reason for this is that the tests are conducted with an ambient vibrational test. As stated in the theory ambient vibrational test provide variability between various tests on the same test setup. This is because all interferences are included in the measured data. The tests are also not conducted identically since a human is exciting the beams with a stick. Furthermore, it is impossible to achieve similar operational excitations between different tests.

The remaining test for both beams had a DMOE and a fundamental frequency between test 1 and 2. The authors found the discrepancies acceptable and satisfactory enough, that it was

decided only one test would be conducted for each of the remaining beams, edgewise and flatwise.

The repetitive testing with the Smartphone method was also conducted in the same manner as the Operational Modal method. Beams 3 and 10 were tested three times each, flatwise. Table 5.26 indicates the discrepancy between the two tests that were furthest apart of the three, on the natural frequency and the dynamic modulus of elasticity.

*Table 5.26 - Discrepancy in repetitive testing with Smartphone method*

Mode 1	Test 1	Test 2	Discrepancy
Beam 3 DMOE (N/mm <sup>2</sup> )	8 653	8 659	0,07 %
Beam 3 Fundamental frequency (Hz)	6,266	6,268	0,03 %
Beam 10 DMOE (N/mm <sup>2</sup> )	11 806	11 812	0,06 %
Beam 10 Fundamental frequency (Hz)	6,558	6,560	0,03 %

As can be observed in table 5.26 the differences between the tests are minimal. That means the Smartphone method is consequential in its results and it was decided only one test was necessary for each of the remaining beams, edgewise and flatwise.

#### 5.4 Edgewise vs flatwise

The most practical way to test the beams would have been edgewise, since that is how beams are used in construction. There was no problem to test the beams edgewise with the Timber Grader MTG as the device gave the same values for the beams both edgewise and flatwise as seen in table 5.20.

Problems ensued testing started with the Operational Modal method and the Smartphone method. It was quickly noticed that the DMOE obtained from flatwise testing was not the same as the ones obtained from edgewise testing. Table 5.27 and 5.28 indicates the difference in the DMOE between the beams when edgewise and flatwise, using the Operational Modal method and Smartphone method.

Table 5.27 - Discrepancy between edgewise and flatwise with Operational Modal method

Operational Modal method Dynamic modulus of elasticity (N/mm <sup>2</sup> )			
Beam	Flatwise	Edgewise	Discrepancy
1	7 975	6 440	23,8 %
2	7 730	5 272	46,6 %
3	8 025	6 120	31,1 %
4	8 660	7 471	15,9 %
5	9 868	9 070	8,8 %
6	10 259	8 966	14,4 %
7	9 387	7 567	24,1 %
8	11 699	8 123	44,0 %
9	15 545	10 361	50,0 %
10	10 201	10 542	3,2 %
11	13 961	12 123	15,2 %
12	9 422	9 836	4,2 %

Table 5.28 - Discrepancy between edgewise and flatwise with Smartphone method

Smartphone method Dynamic modulus of elasticity (N/mm <sup>2</sup> )			
Beam	Flatwise	Edgewise	Discrepancy
1	9 642	6 838	29 %
2	8 434	6 222	26 %
3	8 659	5 834	33 %
4	9 908	8 432	15 %
5	11 679	9 586	18 %
6	12 115	10 004	17 %
7	10 583	7 929	25 %
8	13 200	9 165	31 %
9	17 229	10 849	37 %
10	11 806	11 446	3 %
11	16 104	13 580	16 %
12	11 341	10 765	5 %

As seen in table 5.27 and 5.28 the discrepancy varies among the beams. When performing a regression, between the flatwise and edgewise DMOE, there is a R<sup>2</sup> of 60 % for Operational Modal test and R<sup>2</sup> of 66 % for the Smartphone test. Figure 5.1 and 5.2 indicates the regression between flatwise and edgewise DMOE for Operational Modal method and Smartphone method.

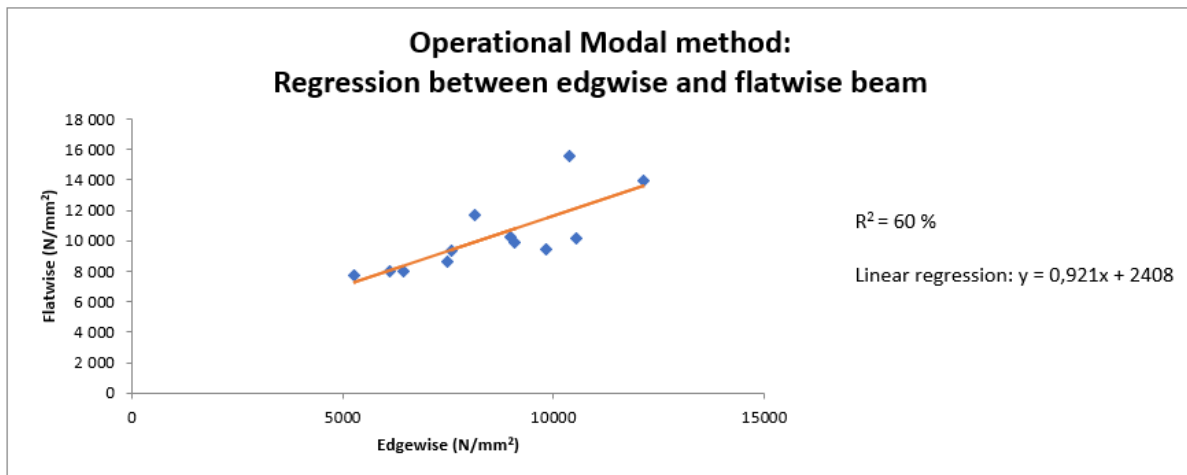


Figure 5.1 - Regression between flatwise and edgewise dynamic modulus of elasticity using Operational Modal method

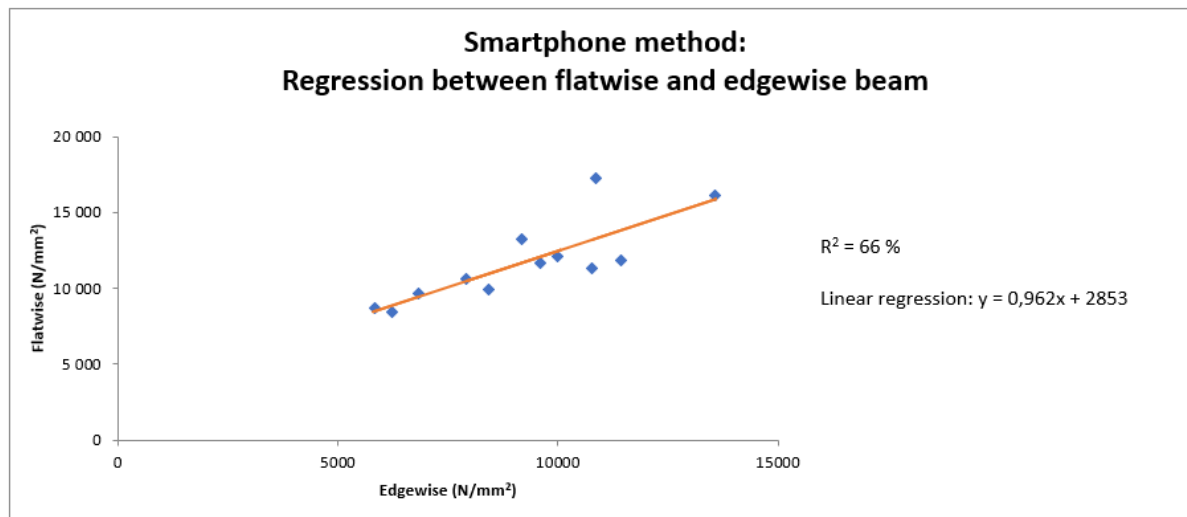


Figure 5.2 - Regression between flatwise and edgewise dynamic modulus of elasticity using Smartphone method

The low  $R^2$  and the regression lines indicates little coherence between the discrepancies of the flatwise and edgewise DMOE.

What is interesting to observe is that the slenderer the beams are the more discrepancy it is between the flatwise and edgewise results. Beams 1-3 and 7-9 have a height of 198 mm, while beams 4-6 and 10-12 have a height of 148 mm. The thickness of all the beams is 48 mm. When performing a regression between the beams with a height of 198 mm the  $R^2$  is 94 % for Operational Modal method and 96 % for the Smartphone method. The  $R^2$  for the beams with a height of 148 mm is 75 % for Operational Modal method and 82 % for the Smartphone method. This illustrates clearly that the discrepancies are due to the slenderness of the beams. The slenderer the beams are the higher discrepancy between flatwise and edgewise DMOE seems to be repeating.

The modulus of elasticity in timber is equal for edgewise and flatwise since the fibers are along the same direction. The results for both edgewise and flatwise should therefore be identical. This is not the case with Operational Modal test and Smartphone test. The question is, what result should be trusted and what could be the issue with the dynamic tests?

As can be seen in table 5.27 and 5.28 the DMOE obtained from the edgewise tests are most often lower than the flatwise tests. The values of the DMOE for the flatwise beams are already low compared to the standard modulus of elasticity for C24 beams, which is 11 000 N/mm<sup>2</sup> (see Appendix-A4). Since static tests were not conducted (due to constraints beyond the authors) it is hard to determine if the Operational Modal tests are providing correct results.

Another way to evaluate the results for the edgewise test, is to examine the natural frequencies and mode shapes for the higher modes. Table 5.29 indicates the discrepancy between the experimental natural frequencies and theoretical natural frequencies for beam 9, which has the worst discrepancy between flatwise and edgewise DMOE.

Table 5.29 - Discrepancy between edgewise theoretical and experimental natural frequencies for beam 9 using Operational Modal method

Mode 1			Mode 2			Mode 3			Mode 4		
kn	9,870		39,478		88,826		157,914				
fn <sub>T</sub>	21,350	Hz	85,400	Hz	192,150	Hz	341,600	Hz			
fn <sub>E</sub>	21,350	Hz	85,36	Hz	129,1	Hz	209,8	Hz			
			0,05 %		32,81 %		38,58 %				



As can be seen in table 5.29 the discrepancy between the natural frequencies increases drastically for mode 3 and 4. If these discrepancies are compared to the discrepancies for the flatwise test as seen in table 5.30 it can be recognized that there some uncertainties with the edgewise test.

Table 5.30 - Discrepancy between flatwise theoretical and experimental natural frequencies for beam 9 using Operational Modal method

Mode 1		Mode 2		Mode 3		Mode 4	
kn	9,870	39,478	88,826	157,914			
fn <sub>T</sub>	6,233 Hz	24,932 Hz	56,097 Hz	99,728 Hz			
fn <sub>E</sub>	6,233 Hz	23,7 Hz	56,37 Hz	96,74 Hz			
		4,94 %	-0,49 %	3,00 %			

Figure 5.3 to 5.6 indicates the mode shapes for beam 9 edgewise.

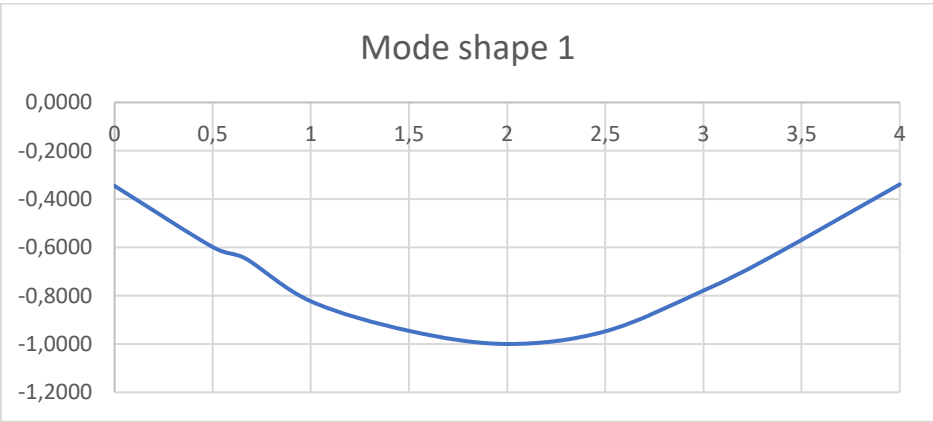


Figure 5.3 - Edgewise mode shape 1 for beam 9

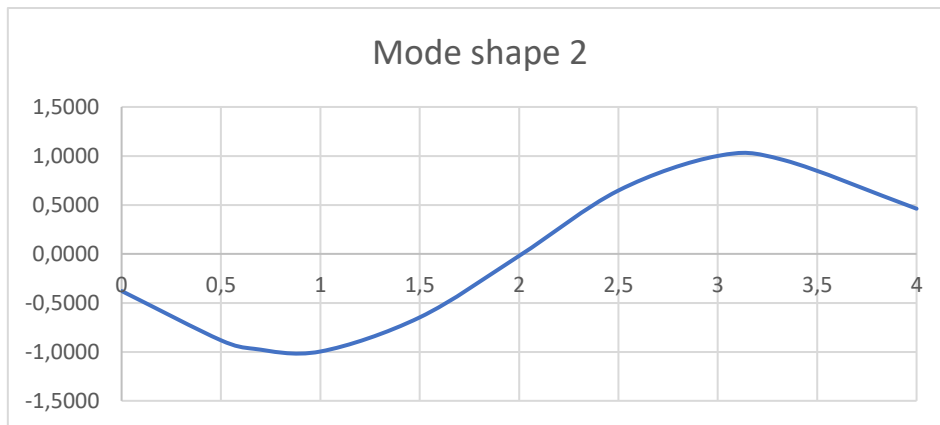


Figure 5.4 - Edgewise mode shape 2 for beam 9

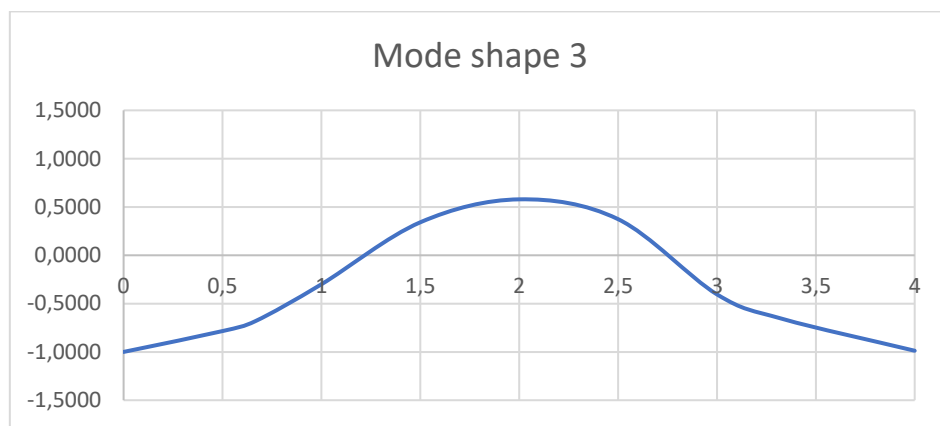


Figure 5.5 - Edgewise mode shape 3 for beam 9

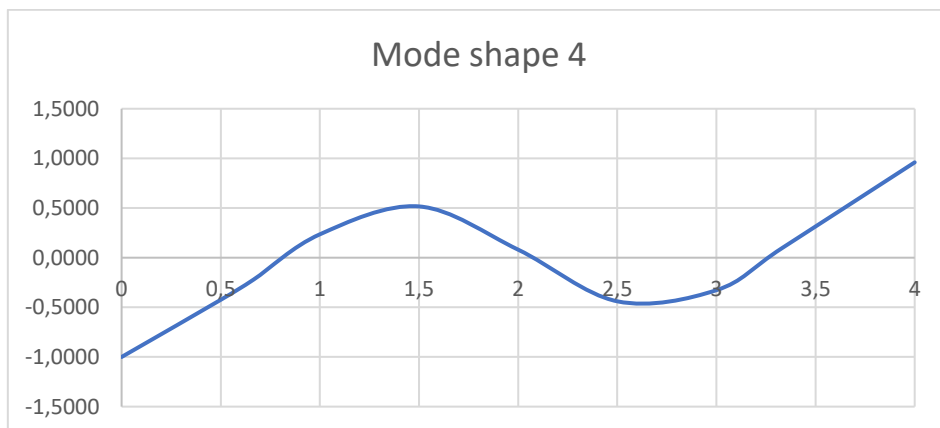


Figure 5.6 - Edgewise mode shape 4 for beam 9

If these mode shapes are compared to the theoretical mode shapes indicated in chapter "2.5.2 Mode shapes" it can be observed that the mode shapes are not very reliable. Mode shape 1 and 2 are acceptable but are not terminating at 0 at the ends, as expected. The curvature of mode shapes 3 and 4 are not even angling towards 0 at the ends.

The mode shapes for beam 9 flatwise can be seen in figure 5.7 to 5.10.

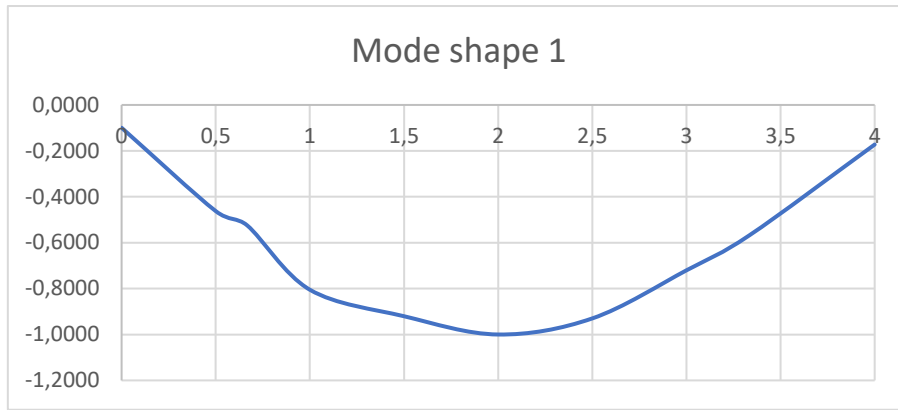


Figure 5.7 - Flatwise mode shape 1 for beam 9

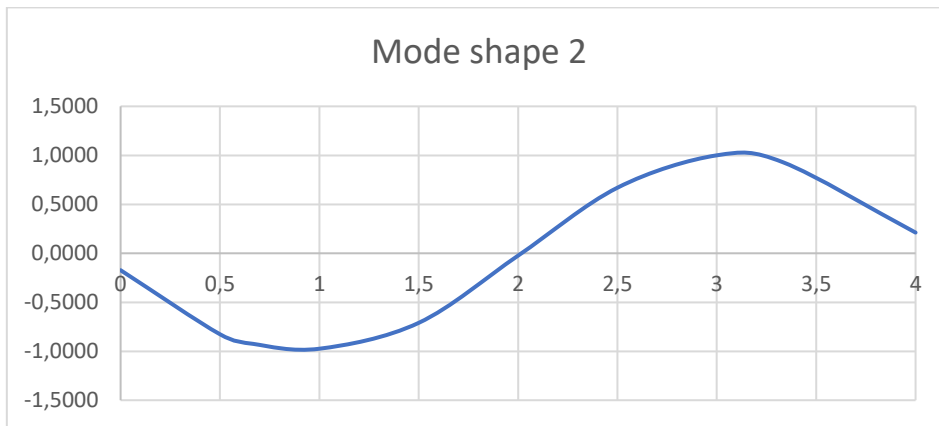


Figure 5.8 - Flatwise mode shape 2 for beam 9

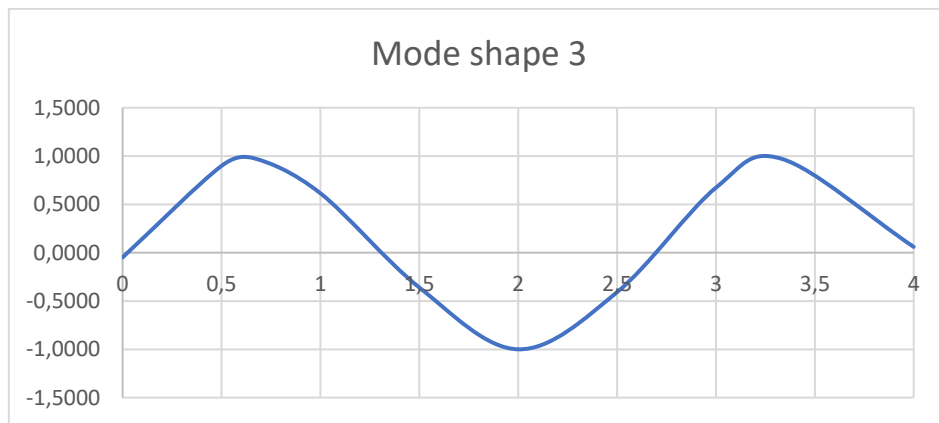


Figure 5.9 - Flatwise mode shape 3 for beam 9

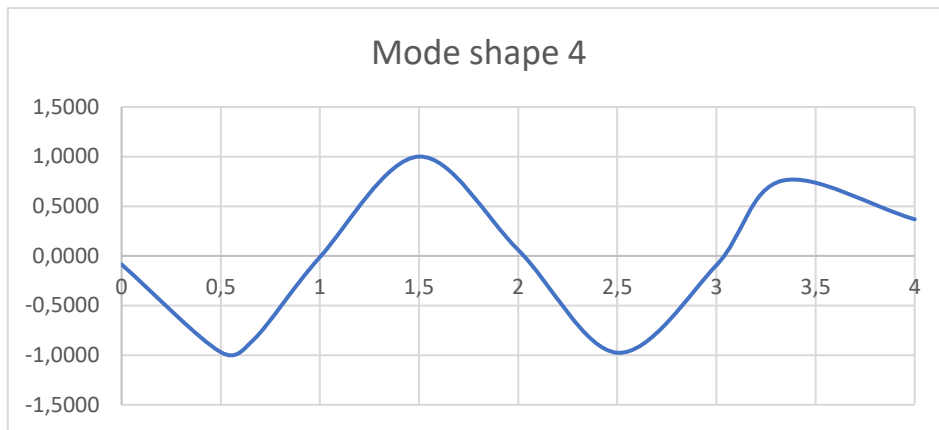


Figure 5.10 - Flatwise mode shape 4 for beam 9

The mode shapes for the flatwise test are considerably closer to the theoretical mode shapes and are therefore more reliable.

The mode shapes for edgewise tests are always not reliable for mode 3 and 4 (see Appendix-A6).

The FDD of the beams are also a way to compare the reliability of the edgewise and flatwise testing. Figure 5.11 indicates the FDD for beam 9 edgewise, while figure 5.12 indicates the FDD for beam 9 flatwise.

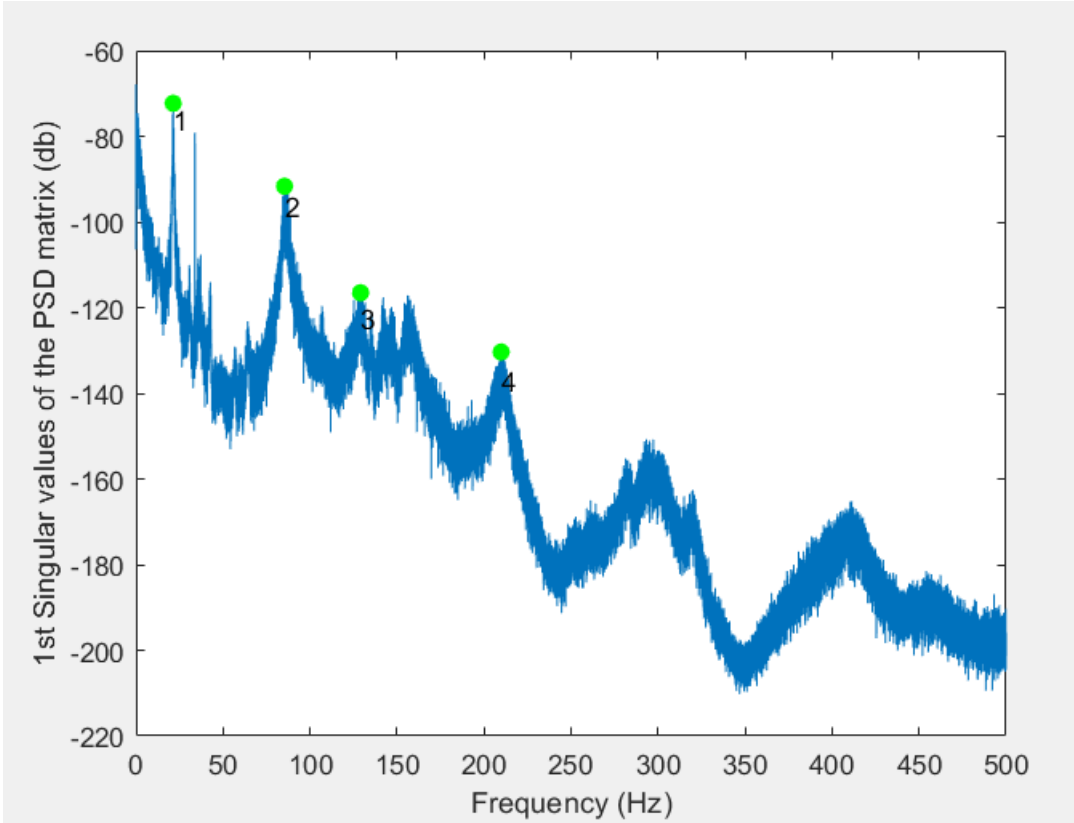


Figure 5.11 - Edgewise FDD for beam 9

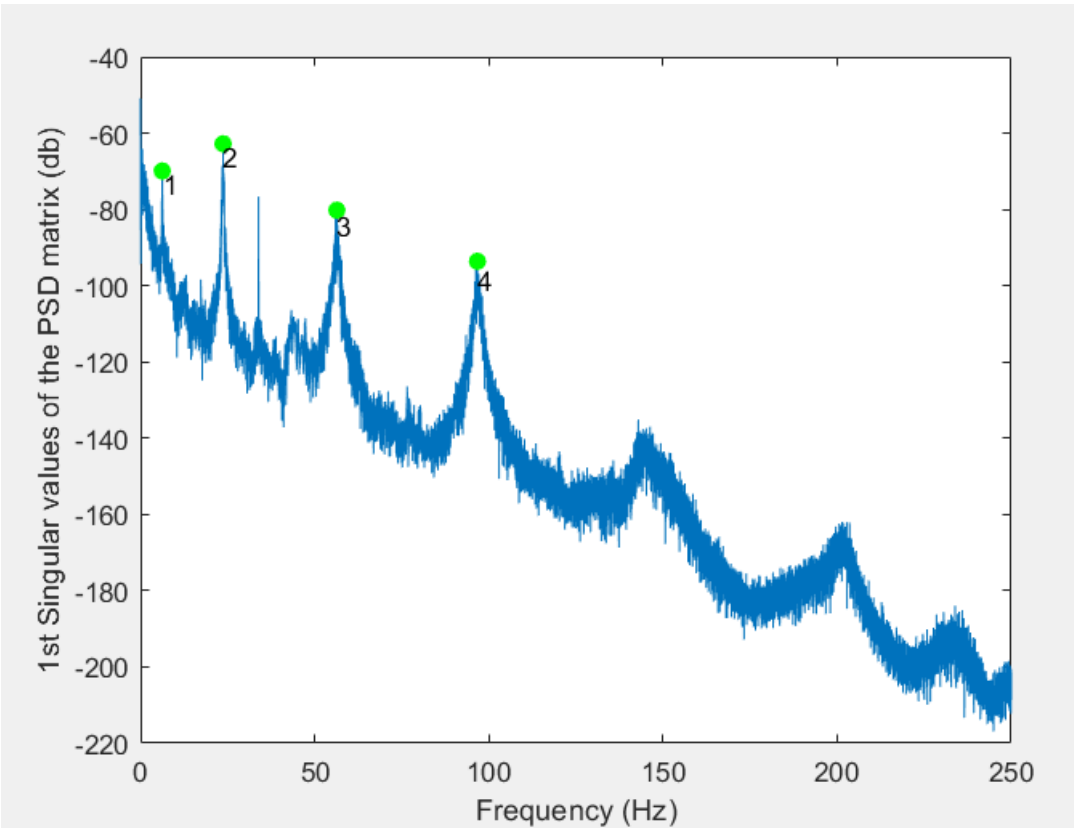


Figure 5.12 - Flatwise FDD for beam 9

The peaks of the natural frequencies are easily identifiable for beam 9 flatwise. There is only an interference at around 33 Hz, which the authors know is ambient interference. This FDD made it simple to pick the natural frequencies for the first four modes. Looking at the FDD for the edgewise test, the peaks are not as easily identified, and there are lots of interferences. The peaks in all the FDDs for all edgewise beams are hard to identify (see Appendix-A6). This makes it hard to select the natural frequencies and it tells us that the results from the edgewise testing might not be reliable.

So why are the results for natural frequencies and mode shapes for edgewise testing so inadequate? One reason the authors suggest is that the slenderness of the beams is causing horizontal motion and instability. This motion might excite out-of-plane mode shapes. If this is the case, in-plane and out-of-plane mode shapes might be interfering with each other and effecting the results.

The depth to thickness ratio of the beams when edgewise probably contributes through thickness shear deformations which are not accounted for in the analytical formulas when calculating the natural frequencies.

A reason that it might not be possible to observe the third and fourth mode clearly in the FDD for the edgewise tests, may be that the stiffness of the beams is too high to excite the higher modes. When conducting tests with accelerometers, they easily overflow when the beam is excited. That means the beams had to be excited with light taps, and that probably does not excite the higher modes when the beam is edgewise. If the accelerometers could take a higher excitation before overflowing, then maybe there would have been a better response from the modes.

The mode shapes for the edgewise testing might produce another reason for the inadequate results. Figure 5.3 to 5.6 indicates that the mode shapes do not end at the zero point at the ends of the beams. The mode shapes should be zero at the ends of the beams because that is where the supports are and there should not be any vertical motion. The mode shapes might therefore indicate that the beam is not sufficiently connected to the supports and is in motion at the ends.

A beam situated edgewise also has a higher EI than a beam that is flatwise. This may lead to the stiffness between the support and the beam edgewise, is not sufficient enough for the

beam to recognize it as simply supported. This is a problem, because that would mean other supports conditions would have to be investigated for the beams in edgewise position. The larger beams also indicate a higher discrepancy between flatwise and edgewise, because the ratio between the EI for the edgewise and flatwise is higher for the larger beams.

It seems it is hard to obtain adequate results when testing simply supported beams with small and slender cross-sections. Considering everything that have been discussed in this section it was decided for this thesis to evaluate and compare the flatwise test results and not the edgewise, even though all beams have been tested on both directions.

### 5.5 Effects of accelerometer mass

The dynamic modulus of elasticity obtained from the Operational Modal method was lower than the expected modulus of elasticity for many of the beams, especially the spruce beams. The expected static modulus is around 11 000 N/mm<sup>2</sup> for a C24 beam (as seen in Appendix-A4). When calculating the dynamic modulus of elasticity from the fundamental frequency with equation 1, the line mass of the beam is a parameter. The dynamic modulus of elasticity given in table 5.27 is calculated using only the line mass of the timber beams. The authors soon realized that since the accelerometers are attached and resting at the top of the beams when testing, they may be working together as one unit when the beams are excited. This means the frequencies obtained from testing are affected by the mass of the accelerometers. Thus, using only the line mass of the timber beams when calculating the DMOE will result in a lower DMOE. The reason for this comes from equation 7. When a higher mass, as accelerometers, is applied to a beam the natural frequencies will be reduced. If then only the line mass of the timber is used for calculating the DMOE, it will result in a lower DMOE. To account for the weight of the accelerometer reducing the natural frequencies, the mass of the accelerometers should be added to the line mass when calculating the DMOE of the beams.

This phenomenon would only have significant effects on systems were the weight ratio between the accelerometer and the beam is large. The accelerometers were therefore weighed. The weight of all ten accelerometers was 2,75 kg. Table 5.31 indicates the ratio between the weight of the accelerometers and the beams.

*Table 5.31 - Table of accelerometer mass to beam mass*

Beam	Mass of beam (kg)	Ratio of accelerometer mass to beam mass
1	13,75	20,0 %
2	14,95	18,4 %
3	14,7	18,7 %
4	12,85	21,4 %
5	13,7	20,1 %
6	11,55	23,8 %
7	17,6	15,6 %
8	19,35	14,2 %
9	24,15	11,4 %
10	14,35	19,2 %
11	17,5	15,7 %
12	14,15	19,4 %

As table 5.31 indicates, the weight of the accelerometers is significant compared to the weight of the beams. This will in turn affect the natural frequencies and the calculated DMOE.

At this point it was decided to add the mass of the accelerometers to the line mass when calculating the DMOE for the beams. Table 5.32 shows the DMOE with and without the mass of the accelerometers and the difference the mass makes.



Table 5.32 - Discrepancy between dynamic modulus of elasticity for beam with and without accelerometer mass

Beam	Dynamic modulus of elasticity (N/mm <sup>2</sup> )		Discrepancy
	Only mass of timber beam	Mass of timber beam and accelerometers	
1	7 975	9 570	17 %
2	7 730	9 152	16 %
3	8 025	9 527	16 %
4	8 660	10 513	18 %
5	9 868	11 849	17 %
6	10 259	12 702	19 %
7	9 387	10 854	14 %
8	11 699	13 362	12 %
9	15 545	17 316	10 %
10	10 201	12 167	16 %
11	13 961	16 155	14 %
12	9 422	11 253	16 %

As indicated in table 5.32 the mass of the accelerometers yielded significant differences for most of the beams. The DMOE for the beams are more satisfactory when the mass of the accelerometers is added because the values are considerably closer to the expected static modulus of elasticity of 11 000 N/mm<sup>2</sup> for a C24 beam. There are some exceptions when it comes to beams 8, 9 and 11, they give higher DMOE than expected. These beams will be discussed further in section "5.9 Evaluation of the modulus of elasticity". As seen in section "5.6 Modulus of elasticity for all methods" the DMOE with the mass of the accelerometers also provides results closer to the Timber Grader MTG and the Smartphone method. It is of the authors opinion that the mass of the accelerometers should be added to the line mass when calculating DMOE with the Operational Modal method.

5.6 Modulus of elasticity for all methods

Table 5.33 indicates the MOE obtained from all three methods: Timber Grader MTG, Operational Modal method and Smartphone method.

Table 5.33 - Modulus of elasticity for all test methods

Beam	Modulus of elasticity (N/mm <sup>2</sup> )		
	Timber Grader MTG	Operational Modal	Smartphone
1	9 219	9 570	9 642
2	8 791	9 152	8 434
3	8 825	9 527	8 659
4	9 597	10 513	9 908
5	11 690	11 849	11 679
6	12 418	12 702	12 115
7	10 574	10 854	10 583
8	12 884	13 362	13 200
9	16 144	17 316	17 229
10	11 550	12 167	11 806
11	16 478	16 155	16 104
12	10 539	11 253	11 341

As table 5.33 indicates, the modulus of elasticity is similar for all three methods. Figure 5.13, 5.14, and 5.15 indicates the regression between the different methods to see if there are a correlation between them.

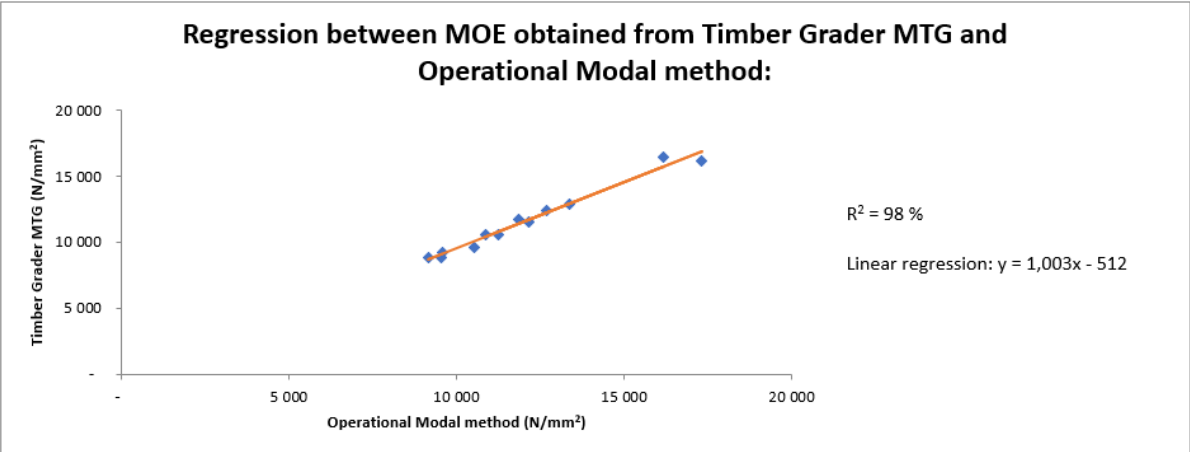


Figure 5.13 - Regression for MOE between Timber Grader MTG and Operational Modal method

The R<sup>2</sup> for the MOE between the Timber Grader MTG and Operational Modal method is 97 %. As can be observed in figure 5.13 the regression line between the two methods is adequate. This implies there is a decent correlation between the two methods.

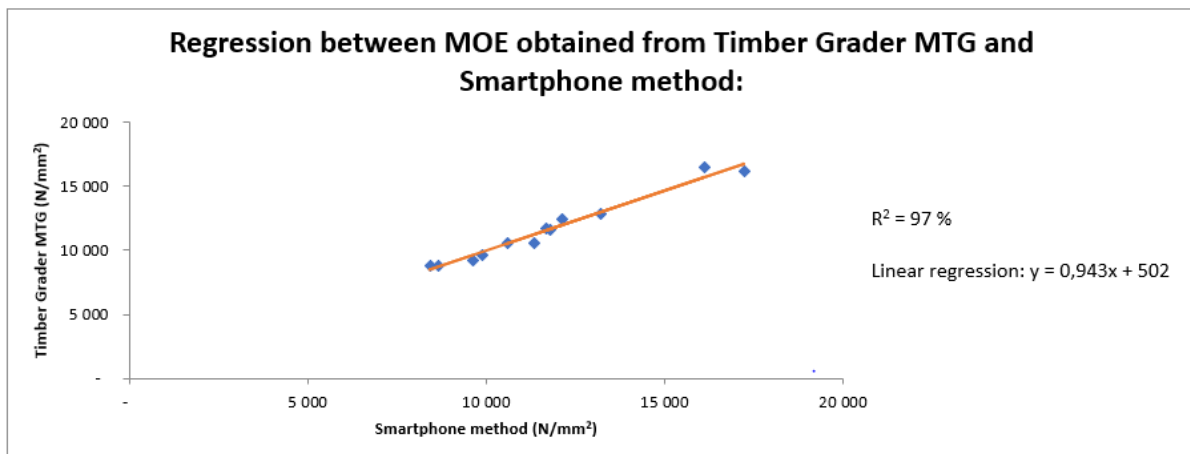


Figure 5.14 - Regression for MOE between Timber Grader MTG and Smartphone method

The  $R^2$  for the MOE between the Timber Grader MTG and the Smartphone method is 97 %. As observed in figure 5.14 the regression line is decent, so the correlation between these two methods is also adequate.

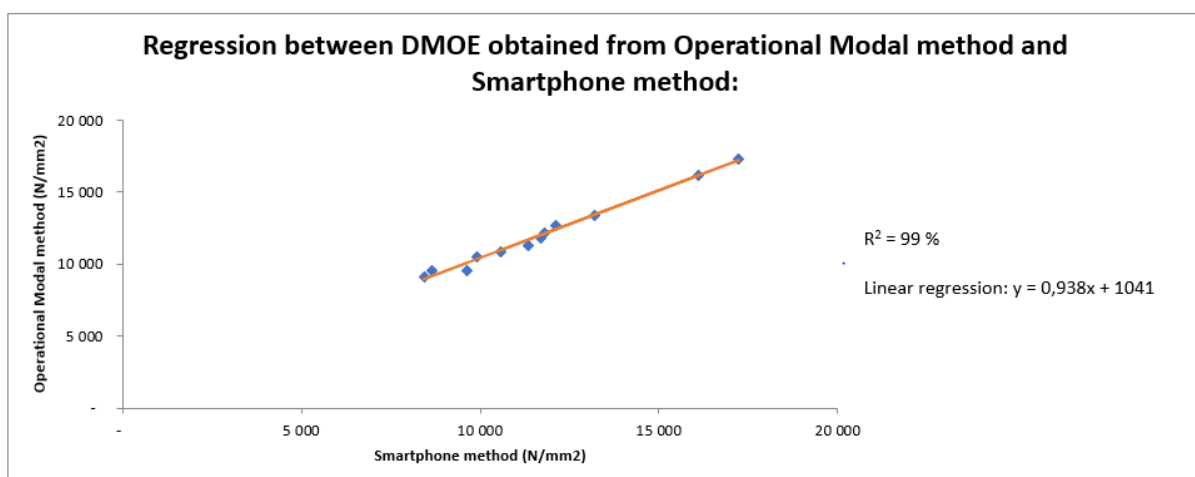


Figure 5.15 - Regression for DMOE between Smartphone method and Operational Modal method

The  $R^2$  for the DMOE between the Operational Modal method and the Smartphone method is 99 %. As observed in figure 5.15 the regression line is decent, so the correlation between these two methods is also adequate.

The regressions between the different methods are a positive sign for the reliability of all the methods. When one method provides a higher or lower MOE, the other methods also provide a higher or lower MOE.

Tests to obtain the static modulus of elasticity were not performed. That means the authors have no basis to claim that the MOE obtained from these three methods can be used to

evaluate the mechanical properties of timber beams. If static tests were conducted, it would be possible to do a regression between modulus of elasticity obtained from static testing and the MOE obtained from the different non-destructive methods.

According to the earlier work, as presented in the state-of-the-art, different researchers found that the values of the obtained DMOE and SMOE are not always 1:1. For some Operational Modal tests, the DMOE was usually higher than the SMOE, and with other tests, the DMOE was usually lower than the SMOE. Other researchers have also found that the DMOE mostly matches the SMOE. What most of the researchers found, is that there is good regression between static modulus of elasticity and dynamic modulus of elasticity for each of the different Operational Modal test conducted. That means it could be possible, with enough repetitive testing and a good regression model, to derive a mathematical equation to calculate the SMOE of a beam using the obtained DMOE from non-destructive testing.

## 5.7 Effect of moisture on the modulus of elasticity

An interesting aspect to investigate is if the moisture contents of the beams have any correlations with the MOE obtained from the different methods. As explained in chapter "4. Method", the beams moisture contents were measured before every test. The Timber Grader MTG tests were the first tests conducted, so the moisture contents were measured by drying timber specimens completely and comparing the wet and dry weight. This is the best method to determine moisture content in timber. Table 5.34 shows the static modulus of elasticity for the Timber Grader MTG and the corresponding moisture contents.

Table 5.34 - Table of moisture content and MOE for Timber Grader MTG

Beam	Timber Grader MTG	
	Static modulus of elasticity (N/mm <sup>2</sup> )	Moisture content (%)
1	9 219	15,7 %
2	8 791	16,2 %
3	8 825	15,1 %
4	9 597	12,3 %
5	11 690	16,3 %
6	12 418	14,7 %
7	10 574	18,0 %
8	12 884	19,9 %
9	16 144	20,0 %
10	11 550	24,9 %
11	16 478	64,7 %
12	10 539	19,1 %

As can be observed in table 5.34 the moisture content for beam 11 was significant. This was also easily observable when the beams were bought. The beam was both heavy and noticeably moist on the surface and at the cut ends. It was envisaged by the authors that the high moisture content might lead to some conflicting results.

Figure 5.16 indicates a regression between the moisture content in the beams and the static modulus of elasticity obtained from the Timber Grader MTG.

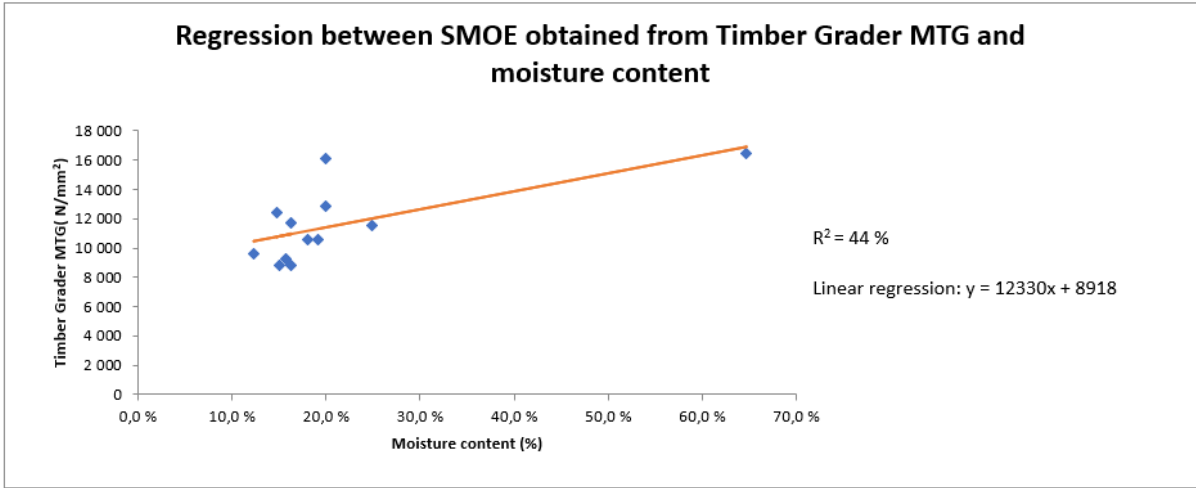


Figure 5.16 - Regression between SMOE and moisture content for Timber Grader MTG

The  $R^2$  for the regression was 44 %. This regression seems to indicate that there are little to no correlation between the moisture content and the SMOE obtained from the Timber Grader MTG.

The Operational Modal tests were conducted sometime later then the Timber Grader MTG. This allowed the timber beams to dry out in an environment designed to balance the moisture content in the beams to 12 % and a temperature of 20 degrees Celsius. The beams moisture contents were measured with a moisture meter as stated in section "4.3 Moisture content". This instrument is less accurate than drying and weighing the specimens. Table 5.35 indicates the DMOE and moisture content for the beams tested with the Operational Modal test.

Table 5.35 - Table of moisture content and DMOE for Operational Modal method

Beam	Operational Modal method	
	Dynamic modulus of elasticity (N/mm <sup>2</sup> )	Moisture content (%)
1	9 570	13,9 %
2	9 152	14,4 %
3	9 527	11,7 %
4	10 513	15,5 %
5	11 849	15,8 %
6	12 702	12,6 %
7	10 854	16,1 %
8	13 362	15,8 %
9	17 316	14,0 %
10	12 167	14,4 %
11	16 155	21,7 %
12	11 253	11,5 %

As can be observed in table 5.35 the moisture content for beam 11 has been drastically reduced. Figure 5.17 shows the regression between the DMOE obtained from Operational Modal method and the moisture content in the beams.

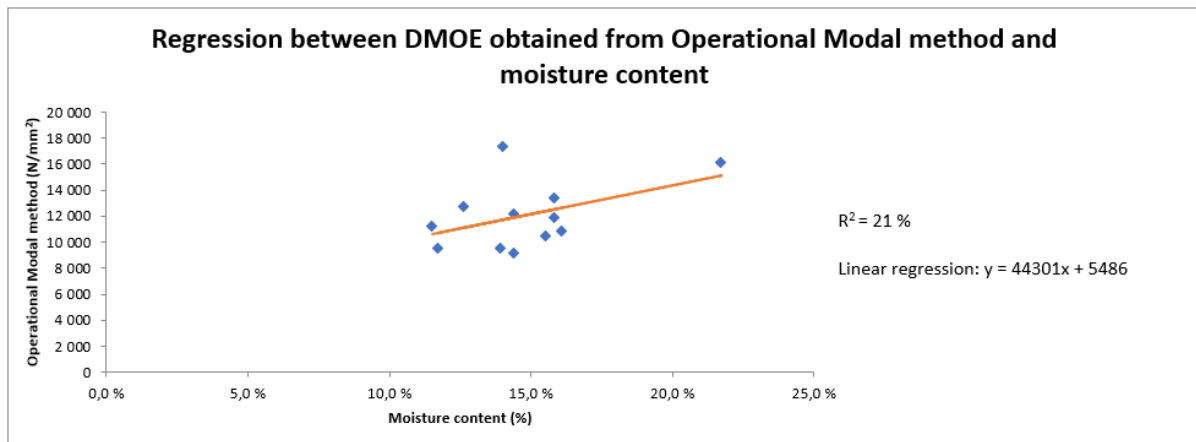


Figure 5.17 - Regression between DMOE and moisture content for Operational Modal method

The R<sup>2</sup> for the regression is 21 %. This regression indicates that there is even less correlation between the moisture content and the obtained DMOE, when testing with the Operational Modal method.

Table 5.36 indicates the DMOE and moisture content for the beams tested with the Smartphone method.

Table 5.36 - Table of moisture content and DMOE for Smartphone method

Beam	Smartphone method	
	Dynamic modulus of elasticity (N/mm <sup>2</sup> )	Moisture content (%)
1	9 642	13,9 %
2	8 434	14,4 %
3	8 659	11,7 %
4	9 908	15,6 %
5	11 679	15,8 %
6	12 115	12,6 %
7	10 583	16,1 %
8	13 200	15,8 %
9	17 229	14,0 %
10	11 806	14,4 %
11	16 104	21,7 %
12	11 341	11,5 %

Figure 5.18 indicates the regression between Smartphone method and the moisture content of the beams.

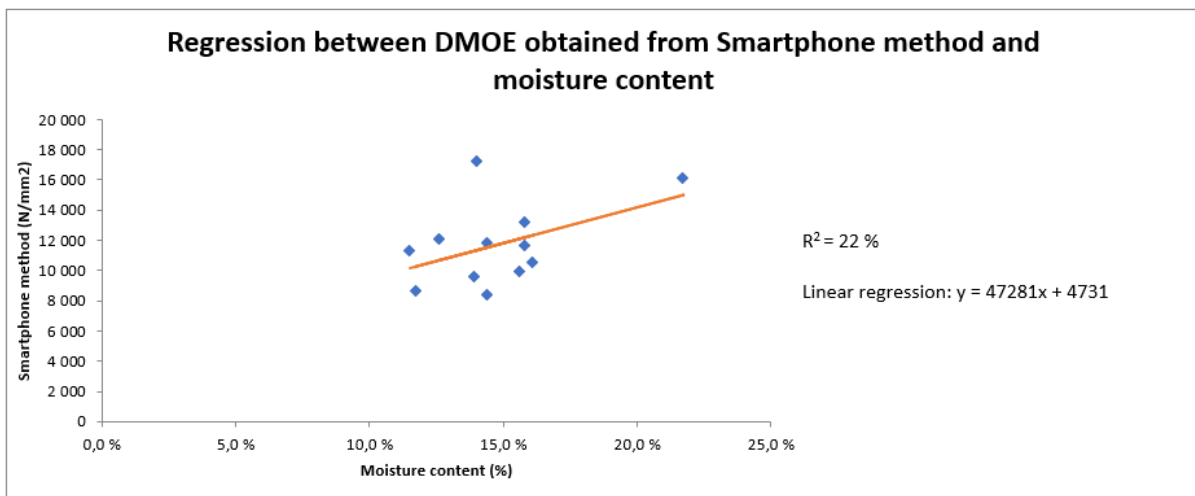


Figure 5.18 - Regression between DMOE and moisture content for Smartphone method

The R<sup>2</sup> for the regression is 22 %. This regression also indicates little correlation between the moisture content and the obtained DMOE from Smartphone method.



### 5.8 Effect of density on the modulus of elasticity

The correlation between the density of the beams and the obtained modulus of elasticity is interesting to investigate. Table 5.37 indicates the SMOE obtained from the Timber Grader MTG and the beams density at the time of testing.

Table 5.37 - Table of SMOE and density for Timber Grader MTG

Beam	Timber Grader MTG	
	Static modulus of elasticity (N/mm <sup>2</sup> )	Density (kg/m <sup>3</sup> )
1	9 219	371
2	8 791	401
3	8 825	406
4	9 597	456
5	11 690	494
6	12 418	421
7	10 574	480
8	12 884	547
9	16 144	679
10	11 550	524
11	16 478	801
12	10 539	523

It seems from table 5.37 that the higher density a beam has, the higher the SMOE is, which is expected. Figure 5.19 shows the regression between the SMOE obtained from the Timber Grader MTG and the beams density.

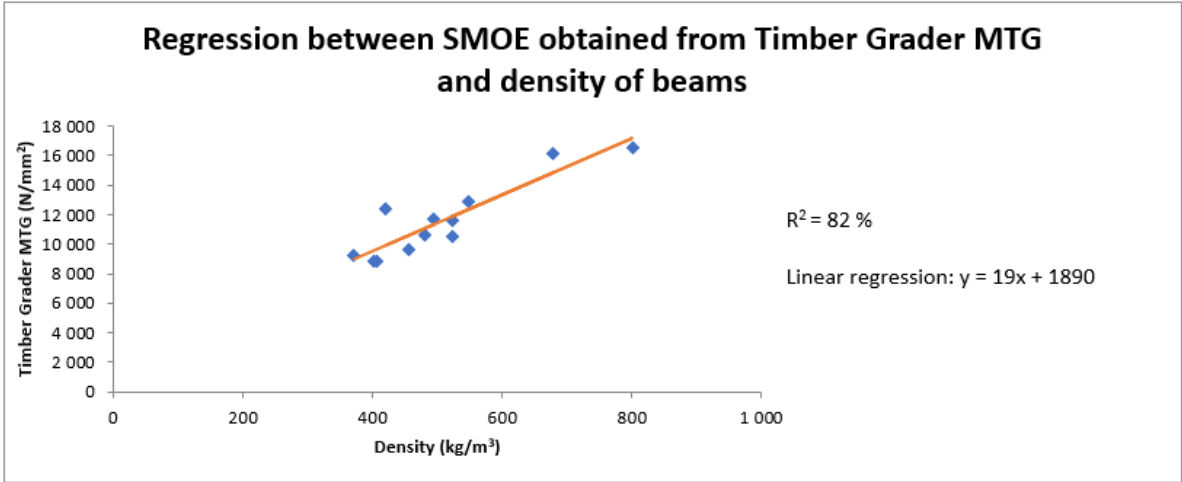


Figure 5.19 - Regression between SMOE and density for Timber Grader MTG

The R<sup>2</sup> is 82 %. This means there is somewhat a correlation between the SMOE obtained from the Timber Grader MTG and the density of the beams.

Table 5.38 indicates the DMOE obtained from the Operational Modal method and the beams density at the time of testing.

Table 5.38 - Table of DMOE and density for Operational Modal method

Beam	Operational Modal method	
	Dynamic modulus of elasticity (N/mm <sup>2</sup> )	Density (kg/m <sup>3</sup> )
1	9 570	375
2	9 152	406
3	9 527	401
4	10 513	462
5	11 849	496
6	12 702	421
7	10 854	478
8	13 362	528
9	17 316	680
10	12 167	508
11	16 155	616
12	11 253	512

Figure 5.20 indicates the regression between the DMOE obtained from the Operational Modal method and the beams density.

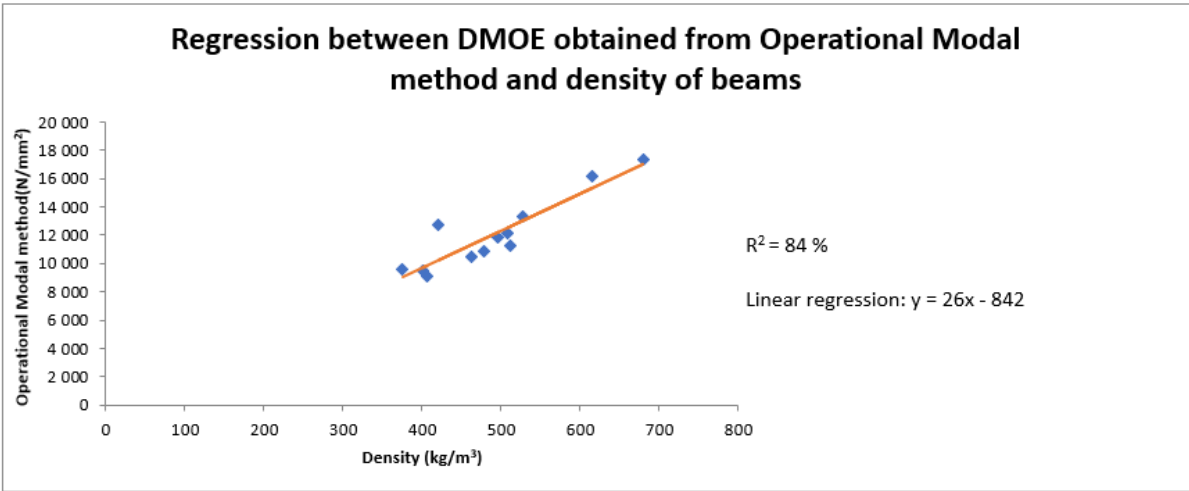


Figure 5.20 - Regression between DMOE and density for Operational Modal method

The R<sup>2</sup> is 84 %. This indicates that there is also a correlation between the DMOE obtained from the Operational Modal method and the density of the beams.

Table 5.39 indicates the DMOE obtained from the Smartphone method and the beams density at the time of testing. The density of the beams at the time of testing with the smartphone, were the same as when the testing occurred with the Operational Modal method.

Table 5.39 - Table of DMOE and density for Smartphone method

Beam	Smartphone method	
	Dynamic modulus of elasticity (N/mm <sup>2</sup> )	Density (kg/m <sup>3</sup> )
1	9 642	375
2	8 434	406
3	8 659	401
4	9 908	462
5	11 679	496
6	12 115	421
7	10 583	478
8	13 200	528
9	17 229	680
10	11 806	508
11	16 104	616
12	11 341	512

Figure 5.21 indicates the regression between the DMOE obtained from the Smartphone method and the beams density.

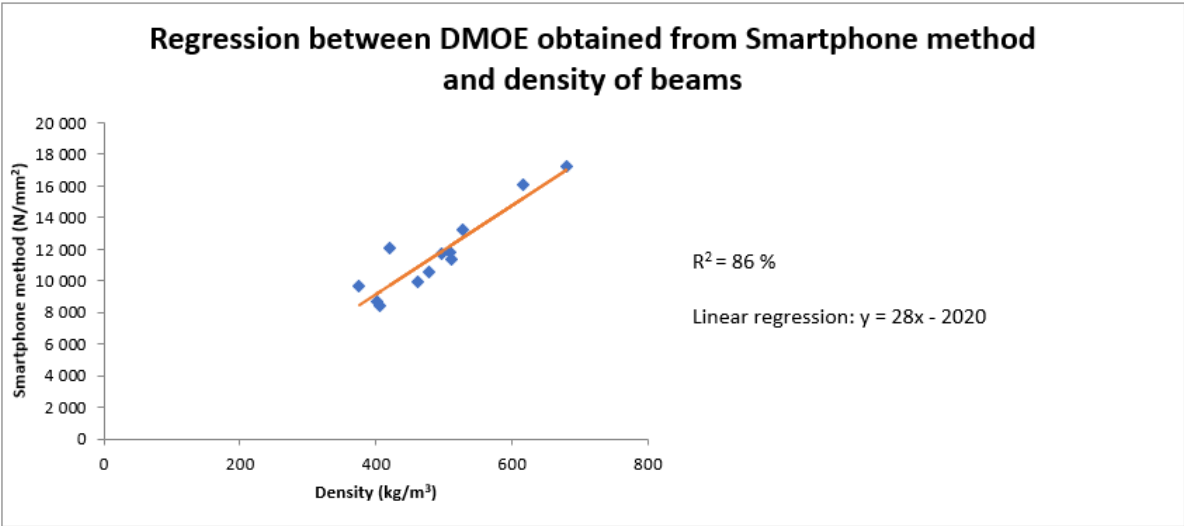


Figure 5.21 - Regression between DMOE and density for Smartphone method

The R<sup>2</sup> is 85,5 %. This regression also seems to confirm the fact that the density of the beams and the obtained DMOE have a correlation.

## 5.9 Evaluation of the modulus of elasticity

The MOE of all the 12 beams vary. It is observed that the spruce beams averagely have a lower MOE than the pine beams. Since it appears the MOE and the density of the beams have a decent correlation, it could explain why the pine has a higher MOE than the spruce. Most of the pine beams have larger masses than the spruce beams. The dimensions of the spruce and pine are identical, and the MOE appears to be independent of the moisture content. The explanation for the higher density in the pine may therefore be attributed to the impregnation however, further tests may have to be conducted to confirm this.

According to the manual of the Timber Grader MTG the device has never been tested on impregnated timber before. This could mean that the Timber Grader MTG is providing incorrect results. But how could that be when the Timber Grader MTG correlates very well with the other test methods? Perhaps the Operational Modal method, and the Smartphone method are also not compatible with impregnated timber? The impregnation in the timber might influence the natural frequencies in the beam. If this is the case, the impregnation might lead to increase in the fundamental frequency, which in turn increases the MOE. This will not be in accordance with the real MOE, since the impregnation does not increase the stiffness of timber. The authors have not acquired any research on this topic, so this is only a possible assumption for the higher MOEs in the pine beams. The only way to discover if the results for the different methods are reliable is to conduct static testing.

Beams 9 and 11 have a significantly higher MOE than the other beams. Again, this might be because these beams have a higher density. For beam 9 it might seem that it has more impregnation than the other beams, because it has high mass, but an average moisture content. The high density of beam 11 might stem from its moisture content, that gives it a higher mass. The high mass might also be a combination of both high levels of impregnation and moisture.

## 5.10 Damages and defects

### 5.10.1 Operational Modal method

It can be observed in table 5.40 that changes in the fundamental frequency, due to damages, are not significantly higher than the changes from repetitive testing, in terms of percentage. The repetitive tests indicated that the maximum percentage change for the fundamental frequency was 1,54 % and for the DMOE it was 3,11 %.

*Table 5.40 - Change of the fundamental frequency between undamaged and damaged flatwise beams using Operational Modal method*

Flatwise change of the fundamental frequency in percentage				
		Fundamental frequency (Hz)		Change in percentage (%)
		Frequency of undamaged beam from Operational Modal method	Frequency of damaged beam from Operational Modal method	
Small beams with hole in the middle	Beam 4	5,768	5,699	-1,20 %
	Beam 11	6,477	6,287	-2,93 %
Small beams with hole in the quarter points	Beam 5	5,943	5,844	-1,67 %
	Beam 10	6,096	6,035	-1,00 %
Big beams with hole in the quarter points	Beam 2	5,814	5,73	-1,44 %
	Beam 8	6,271	6,18	-1,45 %
Big beams with hole in the middle	Beam 1	6,142	6,142	0,00 %
	Beam 9	6,233	5,974	-4,16 %

Earlier literature has stated that changes in the natural frequency due to damages are low. The bending strain for the fundamental frequency is at the maximum in the mid-span of a beam and it gradually decrease towards the supports. It is therefore assumed that the changes in the fundamental frequency will be more significant when a hole/damage is in the mid-span of a beam.

It is also important to keep in mind that holes in the larger beams (198 mm) make up a smaller part of the cross section than for the smaller beams (148 mm). The smaller beams may therefore be more affected by the holes than the larger beams in terms of bending strain.

If stiffness in the beams is reduced by making holes, it is expected to alter the modal properties of the beams in terms of lowering the natural frequencies.

Creating holes in the beams will reduce the mass of the beam, and if the stiffness is upholding, it is assumed that the natural frequency will increase, as seen in equation 6. A significant change in the natural frequencies may not be observed due to the reduction of mass increasing the natural frequencies while the removal of material in the beam reduces the stiffness and in turn the natural frequencies. If the fundamental frequency is in reality almost identical in an undamaged and damaged beam, and mass is removed when calculating the DMOE, lower values will be obtained.

Furthermore, the holes that are created are centred along the neutral axis of the beams where the bending stress is at the minimum. In that case, a hole centred along the neutral axis might not affect the bending stiffness significantly and the removal of mass will only lead to the natural frequencies of the beam increasing. If a cut in the beam was induced instead of a hole, almost no mass would have been removed from the beam. Changes in the natural frequencies would then only be related to the change of stiffness in the beam, and uncertainties surrounding removal of mass would be eliminated.

The significance of holes is expected to be greater on smaller than bigger beams where the ratio between the diameter of the hole and the height of the beam are more significant.

In table 5.41 it is seen that for some of the beams, the changes in percent of the DMOE due to damages are higher than the change in percentage from repetitive testing. The most significant change in percentage for the DMOE in the repetitive testing was 3,11 %. In table 5.41 it is seen that all the beams except beam 1 have a higher change in the DMOE than the repetitive tests.

Table 5.41 - Change of the dynamic modulus of elasticity between undamaged and damaged flatwise beams using Operational Modal method

Flatwise change of the DMOE in percentage				
		Dynamic modulus of elasticity (N/mm <sup>2</sup> )		
		DMOE of undamaged beam from Operational Modal method	DMOE of damaged beam from Operational Modal method	Change in percentage
Small beams with hole in the middle	Beam 4	10513	10 165	-3,31 %
	Beam 11	16155	14 845	-8,11 %
Small beams with hole in the quarter points	Beam 5	11849	11 318	-4,48 %
	Beam 10	12167	11 750	-3,43 %
Big beam with hole in the quarter points	Beam 2	9152	8 738	-4,52 %
	Beam 8	13362	12 800	-4,21 %
Big beams with hole in the middle	Beam 1	9570	9 483	-0,91 %
	Beam 9	17316	15788	-8,82 %

The changes in the DMOE due to damages are observable in table 5.41 and may only be due to the DMOE being calculated with a lower mass and lower natural frequencies due to variabilities in testing. Since changes are not observable in the natural frequencies it is hard to determine the effect, the damages have on the stiffness of the beams.

When evaluating the second mode it is expected that the bending strain is zero in the mid-span and maximum in the quarter points of the beam. This is because there is a node at the mid-span and anti-nodes at the quarter points of mode 2. Hence, it is expected that a damage in the mid-span does not affect the second mode too much. Furthermore, it is expected that a damage at the quarter points can affect the second mode significantly. The location of damages in relation to the neutral axis of the beam are also important since the bending strain is highest at the bottom and the top of the cross-section. A damage close to the neutral axis will have less significance.

Table 5.42 indicates the change of the second natural frequency in the damaged beams. It is observable that beams with holes at the quarter-points tend to be more affected than the beams with holes in the mid-span when it comes to the second natural frequency. This correlates to the authors expectations. It is also important to mention that in the repetitive tests the highest value of change in terms of percentage for the second mode was 1,08 %. All the discrepancy for the beams with holes in the quarter points in table 5.42 indicates a reduction higher than this. That means it might be possible to see that there is a damage in the beam.

Table 5.42 - Change of the second natural frequency between undamaged and damaged flatwise beams

Flatwise Change of the second natural frequency in percentage				
		Second natural frequency		
		Frequency of undamaged beam from Operational Modal method	Frequency of damaged beam from Operational Modal method	Change in percentage
Small beams with hole in the middle	Beam 4	22,6	22,3	-1,33 %
	Beam 11	24,52	24,96	1,79 %
Small beams with hole in the quarter points	Beam 5	23,01	22,18	-3,61 %
	Beam 10	22,99	22,51	-2,09 %
Big beams with hole in the quarter points	Beam 2	23,03	22,19	-3,65 %
	Beam 8	24,24	23,23	-4,17 %
Big beams with hole in the middle	Beam 1	24,11	24,32	0,87 %
	Beam 9	23,7	23,64	-0,25 %

For the third mode the maximum bending strain along the span will be in the mid-span and at L/6 from each support. The location of the holes at the quarter points are between an anti-node and node of the third mode. The hole in the middle of the beam is at an anti-node of the third mode. It is therefore expected to see a change in the natural frequency for the third mode when the hole is in the mid-span of a beam. Since the holes at the quarter points are not located where the anti-nodes of the third mode are, it is possible the natural frequencies will not be significantly affected. Furthermore, there are two holes for the beams damaged at the quarter-points and only one hole for the beams damaged in the mid-span. It might therefore be difficult to decide the effect of two holes in the quarter-points versus one point in the mid-span for the third mode. Table 5.43 indicates the changes in the natural frequencies for the third mode. As seen in table 5.43 there is not a clear difference between having a hole in the mid-span versus having two holes at the quarter-points.



For the repetitive tests, the highest difference in percentage for the third mode was 0,87 %. This might give us an indication that damages in the beams have been detected.

Table 5.43 - Change of the third natural frequency between undamaged and damaged flatwise beams

Flatwise change of the third natural frequency in percentage				
		Third natural frequency (Hz)		
		Frequency of undamaged beam from Operational Modal method	Frequency of damaged beam from Operational Modal method	Change in percentage
Small beams with hole in the middle	Beam 4	51,22	50,51	-1,39 %
	Beam 11	57,29	55,56	-3,02 %
Small beams with hole in the quarter points	Beam 5	53,38	52,02	-2,55 %
	Beam 10	53,68	52,96	-1,34 %
Big beams with hole in the quarter points	Beam 2	53,11	51,77	-2,52 %
	Beam 8	56,69	55,06	-2,88 %
Big beams with hole in the middle	Beam 1	54,85	54,86	0,02 %
	Beam 9	56,37	55,17	-2,13 %

The fourth mode has zero bending strain at the mid-span and quarter-points of the beam due to these areas being nodes for the fourth mode. The holes on all the beams are located close to the nodes of the fourth mode. It is therefore expected that the change in percentage, due to damages, for the fourth mode is not significant. For the repetitive testing, the maximum change in percentage was 2,42 %. Table 5.44 indicates the change of natural frequencies for the fourth mode. In table 5.44, all the beams except beam 8 have a smaller change in percentage than the repetitive test.

Table 5.44 - Change of the fourth natural frequency between undamaged and damaged flatwise beams

Flatwise Change of the fourth natural frequency in percentage				
		Fourth natural frequency		
		Frequency of undamaged beam from Operational Modal method	Frequency of damaged beam from Operational Modal method	Change in percentage
Small beams with hole in the middle	Beam 4	90,21	88,74	-1,63 %
	Beam 11	99,72	99,64	-0,08 %
Small beams with hole in the quarter points	Beam 5	94,02	93,08	-1,00 %
	Beam 10	93,03	93,79	0,82 %
Big beams with hole in the quarter points	Beam 2	91,96	90,27	-1,84 %
	Beam 8	99,36	95,15	-4,24 %
Big beams with hole in the middle	Beam 1	97,08	97,01	-0,07 %
	Beam 9	96,74	96,83	0,09 %

### 5.10.2 Timber Grader MTG

In table 5.45 the changes in the SMOE before and after damages have been inflicted can be observed. The Timber Grader MTG measures the longitudinal SMOE. The changes appear to be highest in the smaller beams. It was expected that the holes in the small beams would be more significant than the holes in the bigger beams, since the ratio between the diameter and height are higher in the small beams. The authors speculate that it would be harder for the sonic wave emitted from the Timber Grader MTG to travel around the holes in the smaller beams and the travel-time would be longer, which would result in a lower SMOE.

Table 5.45 - Change of the static modulus of elasticity between undamaged and damaged flatwise beams using the Timber Grader MTG

Flatwise change of SMOE				
		Timber Grader MTG SMOE (N/mm <sup>2</sup> )		
		SMOE of undamaged beam from Timber Grader MTG	SMOE of damaged beam from Timber Grader MTG	Change in percentage
Small beams with hole in the middle	Beam 4	9597	8848	-7,80 %
	Beam 11	16478	15240	-7,51 %
Small beams with hole in the quarter points	Beam 5	11690	10496	-10,21 %
	Beam 10	11550	10797	-6,52 %
Big beams with hole in the quarter points	Beam 2	8791	8450	-3,88 %
	Beam 8	12884	12530	-2,75 %
Big beams with hole in the middle	Beam 1	9219	8802	-4,52 %
	Beam 9	16144	15507	-3,95 %

The SMOE is affected by the bending strain in a beam. The bending strain is highest in the top and the bottom of the cross-section of a beam under load and zero in the neutral axis. A hole in the centre of a beam might therefore not affect the bending strain if the hole is small enough. The authors speculate that the Timber Grader MTG does not consider the location of a damage in the cross-section of a beam because it is measuring the longitudinal SMOE. This could mean that the Timber Grader MTG does not consider the significance bending strain has on the stiffness.

If the Timber Grader MTG is held in line with a hole it might provide a higher reduction of the SMOE than if it was not held in line of the hole. The assumption for this is that if the wave has a free passage the wave will travel back faster and hence provide a higher SMOE. It would be wise to investigate how the location of holes affect the Timber Grader MTG by creating holes at the top or bottom of a beams cross-section.

### 5.10.3 Smartphone Method

The fundamental mode has highest bending strain in the mid-span of a beam. It is therefore expected that holes in the mid-span will provide a higher change in the fundamental frequency than holes at the quarter-points. It is also important to keep in mind that holes in the larger beams make up a smaller part of the cross section than for the smaller beams. The

smaller beams may therefore be more affected by the holes than the larger beams in terms of bending strain. Repetitive testing was conducted for the Smartphone method, and the maximum change in percentage for DMOE was 0,07 % and for the fundamental frequency it was 0,03%. Table 5.46 indicates the change in fundamental frequency between undamaged and damaged beams using the Smartphone method. Table 5.46 indicates that the smaller beams tend to be more affected by the holes in the beams than the larger ones.

Table 5.46 - Change of the fundamental frequency between undamaged and damaged flatwise beams using Smartphone method

Flatwise change of the fundamental frequency in percentage				
		Fundamental frequency (Hz)		
		Frequency of undamaged beam from the Smartphone method	Frequency of damaged beam from the Smartphone method	Change in percentage
Small beams with hole in the middle	Beam 4	6,168	6,074	-1,52 %
	Beam 11	6,956	6,562	-5,66 %
Small beams with hole in the quarter points	Beam 5	6,464	6,268	-3,03 %
	Beam 10	6,558	6,364	-2,96 %
Big beams with hole in the quarter points	Beam 2	6,071	6,069	-0,03 %
	Beam 8	6,66	6,461	-2,99 %
Big beams with hole in the middle	Beam 1	6,754	6,657	-1,44 %
	Beam 9	6,562	6,464	-1,49 %

Table 5.47 indicates the change in DMOE between undamaged and damaged beams using the Smartphone method. In table 5.47 it is seen that it also tends to be the smallest beams that have the biggest reduction in DMOE. This is expected since the fundamental frequency for the smaller beams also tended to be most reduced. With the Smartphone method it is not possible to investigate the mode shapes, which is used as a parameter to reinforce the results and identify the support conditions. This might make it difficult to check if the assumed support condition is correct. When calculating the DMOE it is important to know the systems support conditions or else the DMOE calculated may be incorrect.

Table 5.47 - Change of the dynamic modulus of elasticity between undamaged and damaged flatwise beams using Smartphone method

Flatwise change of DMOE				
		Smartphone DMOE (N/mm <sup>2</sup> )		
		DMOE of undamaged beam from the Smartphone method	DMOE of damaged beam from the Smartphone method	Change in percentage
Small beams with hole in the middle	Beam 4	9908	9481	-4,31 %
	Beam 11	16104	13915	-13,59 %
Small beams with hole in the quarter points	Beam 5	11679	10805	-7,48 %
	Beam 10	11806	10942	-7,32 %
Big beams with hole in the quarter points	Beam 2	8434	8262	-2,04 %
	Beam 8	13200	12422	-5,89 %
Big beams with hole in the middle	Beam 1	9642	9267	-3,89 %
	Beam 9	17229	16717	-2,97 %

#### 5.10.4 Knots in beams

The effect that knots may have on the modulus of elasticity of beams were examined by counting all knots larger than 5 mm in diameter. Table 5.48 indicates the modulus of elasticity obtained from the different methods and number of knots in the beams. In table 5.48 it is seen that the beams with the lowest number of knots have the highest MOE. Otherwise, as seen from the regression in figures 5.22 to 5.24 there are little correlation. Regression between SMOE from Timber Grader MTG and number of knots shows a regression  $R^2$  of 61 %. Regression between the DMOE from the Smartphone method and the number of knots have a regression  $R^2$  of 60%. The regression between the Operational Modal method and number of knots shows a regression  $R^2$  of 61%. This indicates that the number of knots is not a crucial part for the MOE obtained from the three different methods.

Table 5.48 - Number of knots vs modulus of elasticity

Beam	Knots > 5 mm	Timber Grader MTG (N/mm <sup>2</sup> )	Operational Modal method (N/mm <sup>2</sup> )	Smartphone (N/mm <sup>2</sup> )
4	42	9 597	10 513	9 908
5	41	11 690	11 849	11 679
7	33	10 574	10 854	10 583
3	29	8 825	9 527	8 659
1	28	9 219	9 570	9 642
2	28	8 791	9 152	8 434
12	27	10 539	11 253	11 341
10	21	11 550	12 167	11 806
6	20	12 418	12 702	12 115
8	6	12 884	13 362	13 200
9	6	16 144	17 316	17 229
11	3	16 478	16 155	16 104

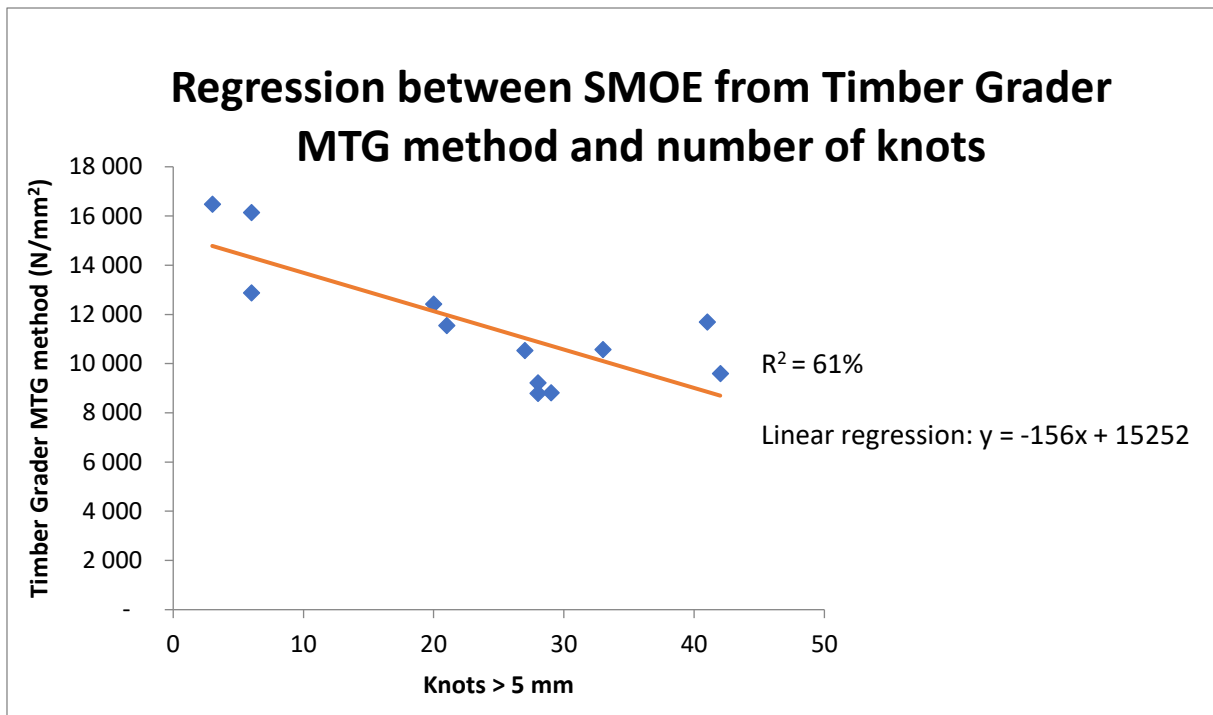


Figure 5.22 - Regression between modulus of elasticity from Timber Grader MTG and knots

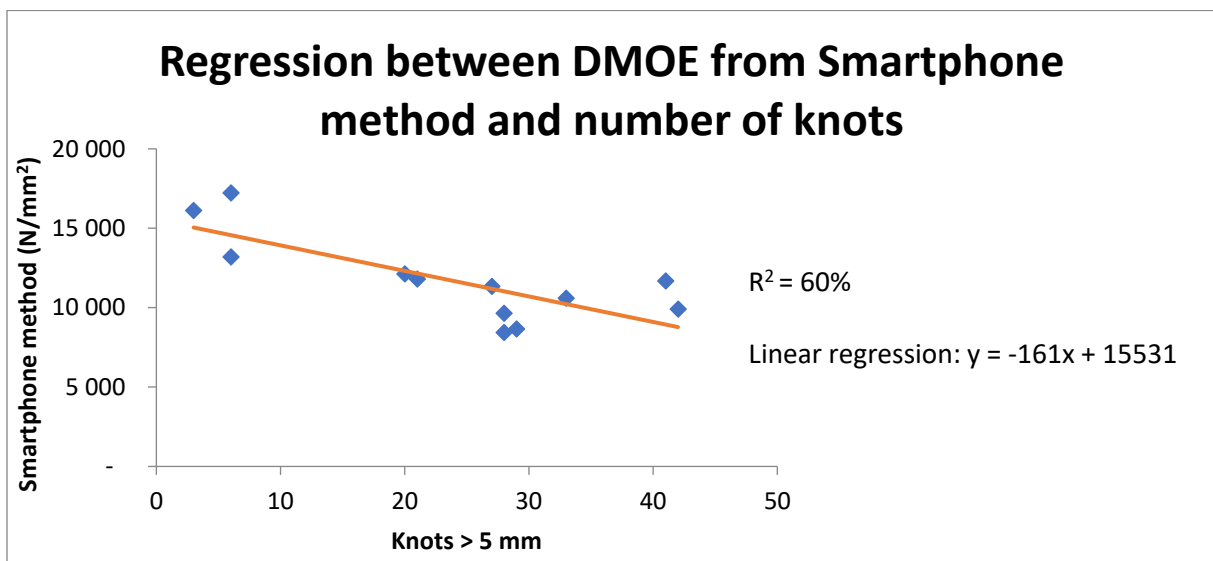


Figure 5.23 - Regression between dynamic modulus of elasticity from Smartphone method and knots

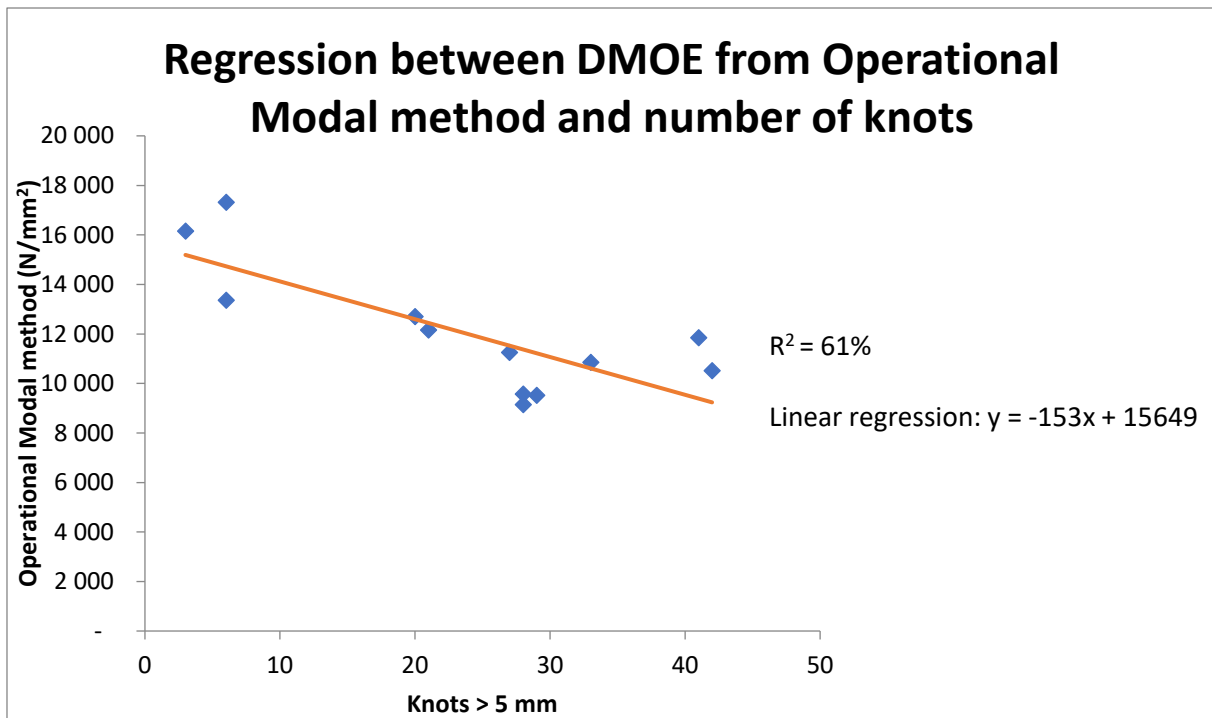


Figure 5.24 - Regression between dynamic modulus of elasticity from Operational Modal method and knots

## 5.11 Summary discussions

### 5.11.1 Undamaged beams

As discussed, the Timber Grader MTG is consequent in its results no matter the support condition or if the beams are edgewise and flatwise. When it comes to the Operational Modal method and the Smartphone method, it seems that the methods are extremely sensitive with regards to both the support conditions and if the beams are edgewise and flatwise.

Operational Modal tests makes it hard to obtain precisely the same results between repetitive tests.

It seems like the weight of the accelerometers needs to be added to the calculations of DMOE to get satisfactory results when conducting tests with the Operational Modal method.

All three test methods have a decent regression and correlation which is positive for the reliability of the methods. It is hard to know how the resulting MOEs correlates to static testing.

Moisture content and the MOE of the different methods does not seem to have much of a correlation, but the density seems to do so.



The authors find the values for MOE for some of the pine beams to be irregular. The values might be irregular because of moisture and impregnation but should be confirmed with further testing.

5.11.2 Damages and defects on beams

In figures 5.25 to 5.27, three regressions are done to check the correlation between the MOE obtained from the three methods on damaged beams. In the regression between the Operational Modal method and the Smartphone method a regression  $R^2$  of 96% was obtained. The regression between the Timber Grader MTG method and the Smartphone method indicates a regression  $R^2$  of 93%. The regression  $R^2$  between the Timber Grader MTG method and the Operational Modal method was 98%. The strongest relation was obtained between the Timber Grader MTG and the Operational Modal method, but all the regression indicates decent relation to each other.

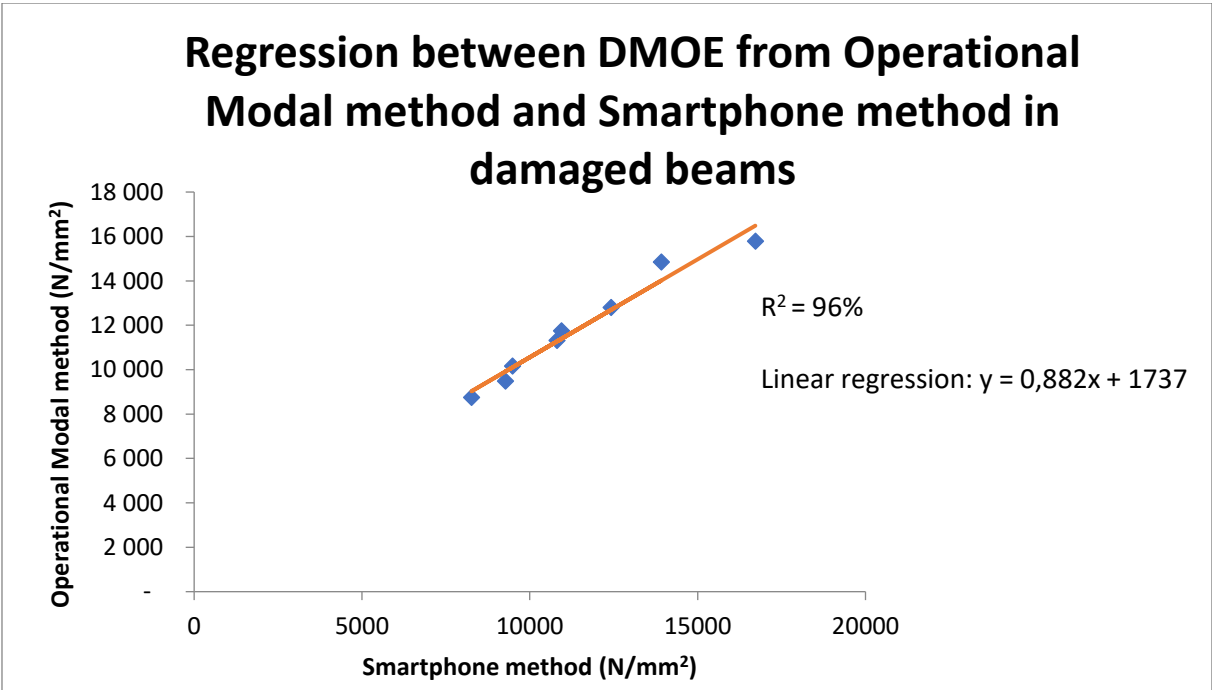


Figure 5.25 - Regression for damaged beams between Operational Modal method and Smartphone method

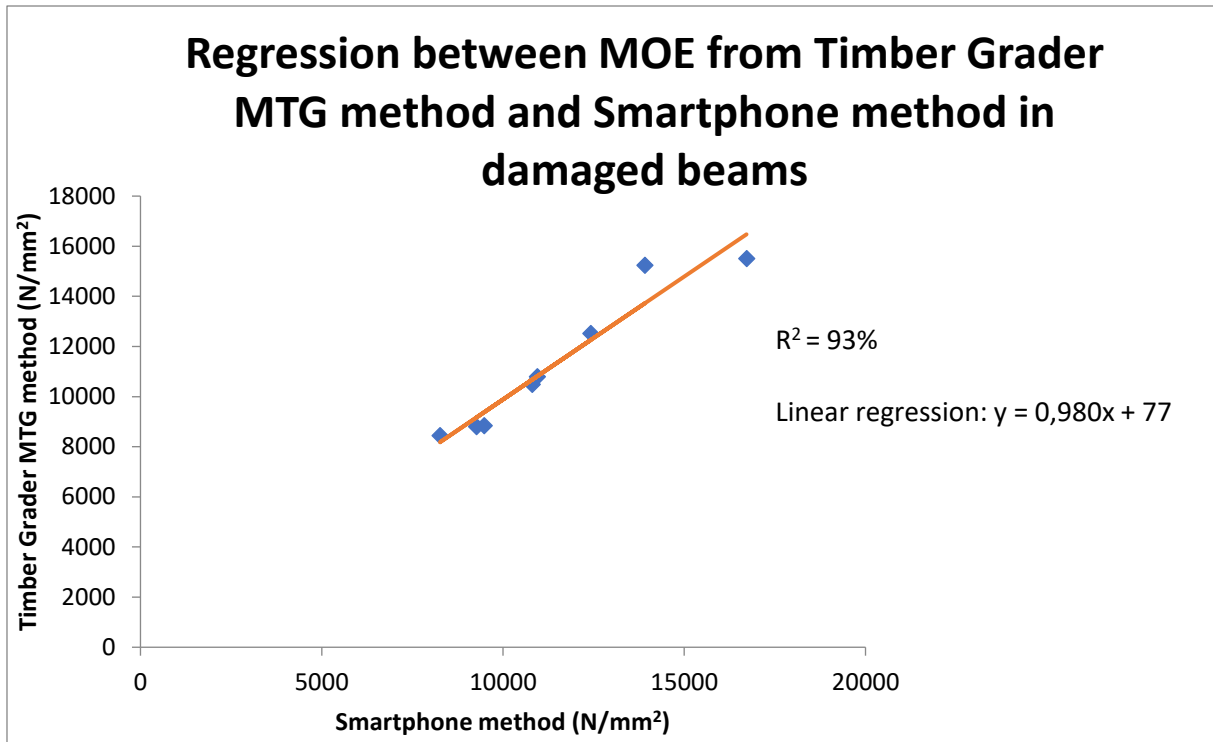


Figure 5.26 -Regression for damaged beams between Timber Grader MTG and Smartphone method

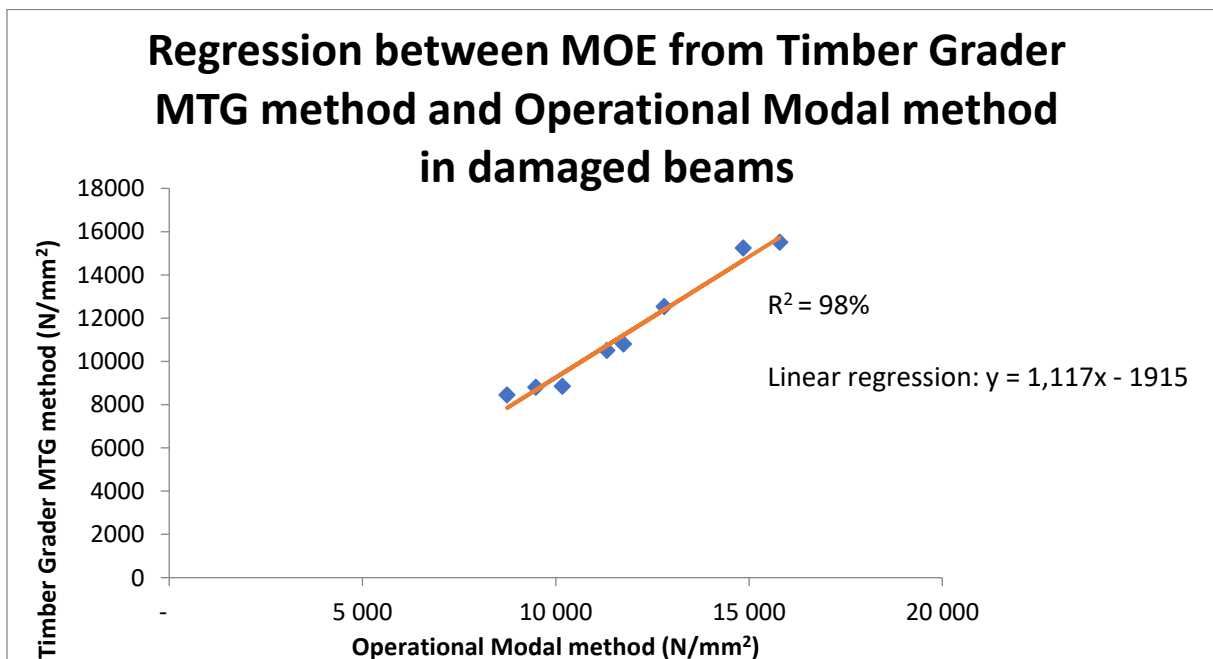


Figure 5.27 - Regression for damaged beams between Operational Modal method and Timber Grader MTG

The Timber Grader MTG appears to indicate damages in beams, but the magnitude of the damages is hard to evaluate, since the longitudinal SMOE is obtained.

There is no significant difference in the fundamental natural frequency for the Operational Modal method between undamaged and damaged beams. It is possible that the change in the fundamental frequency from the Operational Modal method is due to variabilities in the repetitive testing.

Changes in the higher-order natural frequencies may provide a more reliable indication of damages than the fundamental frequency, when conducting tests with the Operational Modal method. The effect of damages could not be observed on the mode shapes of the beams (details are provided in the digital Appendix-A6.)

The Smartphone method appears to indicate the reduction of DMOE in damaged beams, but other modal properties as mode shapes and higher-order natural frequencies cannot be evaluated.

It is assumed that the smaller beams will be more affected by holes than bigger beams. This was especially seen for the Timber Grader MTG method but also for the Smartphone method.

#### 5.11.3 Non-destructive methods on structures in their operating state

Considering the excellent correlation between the three methods in evaluating MOE of undamaged beams, though they need verification from static testing, they may be useful to evaluate timber structures in their operating state. Tests are easy to conduct and portable for all three methods, though the Operational Modal method requires some more equipment.

The way the different methods detect damages in beams, may limit their area of use. Since the Smartphone method only detects a beams fundamental frequency but is a very simple method, it may be useful for a preliminary evaluation of the structures DMOE. The next step could then be to conduct tests with the Operational Modal method to determine the other modal properties of the structure, such as mode shapes and the higher-order natural frequencies. The reason the Smartphone method cannot be used solely is because the mode shapes and higher-order natural frequencies might give an indication of the support conditions and consequently the mathematical formulas for calculating the DMOE. As discussed earlier the Timber Grader MTG indicates the existence of damages in timber beams, however the results must be verified with static testing because of the nature of the

method. The problem of accessibility may arise when trying to conduct tests with the Timber Grader MTG. In structures the ends of beams are usually hidden inside walls or other structural elements. The method requires that at least one of the beams ends are accessible, or tests cannot be conducted. In addition, there are limitations for use of the Timber Grader MTG when it comes to the dimensions of the beams.

## 6. Conclusion

The primary objective of this thesis was to compare and evaluate the mechanical properties of timber beams predicted from various non-destructive methods. The modulus of elasticity was chosen as the main parameter for the investigations. The secondary objective was to assess the effects of damages and defects on the modulus of elasticity of timber beams based on the methods chosen for this study. Three methods were evaluated: The Timber Grader MTG by Brookhuis, Operational Modal method with accelerometers, and a Smartphone method by Timbertech. Both spruce and impregnated pine of different sizes were tested.

The three non-destructive methods appear to be effective and correlate well when it comes to the modulus of elasticity of undamaged beams, however the conclusiveness would have been buttressed with results from static testing.

Operational Modal tests are sensitive to the support conditions. As has been demonstrated, minor variations in the support conditions significantly influence the natural frequencies thereby affecting the obtained dynamic modulus of elasticity.

The results obtained from the edgewise test setups appears to be poor when conducting tests with the Operational Modal method and Smartphone method based on the authors chosen support conditions.

The weight of equipment on systems are likely to influence the modal properties when conducting Operational Modal tests if the ratio of equipment to system mass is high.

The three non-destructive methods appear to correlate well when it comes to the modulus of elasticity of damaged beams, however the reliability of the different methods varies.

The Operational Modal method does not appear to give any indication of damages when observing the fundamental frequency, however damages were indicated in the higher modes. The change in the higher modes only indicates the existence of damages, not the reduction of dynamic modulus of elasticity.

The Timber Grader MTG appears to indicate the existence of damages in beams but due to the nature of the test method the authors suggest that the results be verified with static testing.

Out of the three methods the Smartphone method appears to provide better indication of the effect of damages on beams, in consideration to the dynamic modulus of elasticity.

The authors propose that the Smartphone tests may be adopted for preliminary evaluation of the dynamic modulus of elasticity of timber structures in their operating state. This is based on the fact that it measures only the fundamental natural frequency which may be a limitation of the robustness of the method. Operational Modal tests may be conducted to calibrate the smartphone and evaluate the other modal properties of the structure.

Practically the application of the Timber Grader MTG may be limited in terms of accessibility to the ends of beams which have been installed as part of a structural system.

### 6.1 Further work

A list of ideas for further work are presented below:

- More extensive repetitive testing should be conducted on a larger number of beams to check the consistency of the Operational Modal method and the Smartphone method.
- Evaluating a larger number of specimens would improve the reliability of the different non-destructive methods and make it easier to identify trends.
- Static test should be conducted on beams to reinforce the results obtained from the non-destructive methods.
- Operational Modal tests should be conducted with the free-free support condition presented at the start of chapter "4.6.6 Deciding on support conditions", considering that in hindsight the testing provided good results for edgewise beams in the first three modes.
- Cuts or cracks should be induced on beams instead of holes to evaluate damages in beams. That way no mass is removed, and only the change in the beam's stiffness will influence the natural frequencies. The authors expect this will make it easier to interpret the changes in the natural frequencies due to damages.

## References

- [1] Tekna. 2019. *7 gode grunner til å bruke tre som byggemateriale* [Online article]. Cited from: <https://www.tekna.no/kurs/innhold/7-gode-grunner-til-a-bruke-tre-som-byggemateriale/>. Downloaded: 09.05.21.
- [2] A. Harte, "Introduction to timber as an engineering material," National University of Ireland Galway 2009, [Manual of Construction Materials] Cited from: 10.1680/mocm.00000.0001.
- [3] U. B. Halabe, G. M. Bidigalu, H. V.S. GangaRao og R. J. Ross, "Nondestructive evaluation of green wood using stress wave and transverse vibration techniques," *Materials Evaluation*, vol. 55, nr. 9, s. 1013-1018, April 1995 1995.
- [4] S.-K. Au, *Operational modal analysis: Modeling, bayesian inference, uncertainty laws*, 1. Edition. Liverpool: Springer Nature, 2017.
- [5] D. Pasquale Pasca, A. Aloisio, R. Tomasi og M. Fragiaco, "Assessment of the vibrational performance of light timber floors from experimental tests," World conference on timber engineering 24-27.08, 2020.
- [6] S. Chauhan og A. Sethy, "Differences in dynamic modulus of elasticity determined by three vibration methods and their relationship with static modulus of elasticity," *Maderas. Ciencia y tecnología*, vol. 18, s. 373-382, 03.03.2016. Cited from doi: 10.4067/S0718-221X2016005000034.
- [7] N. Stubbs, C. Farrar og K. Jeong-Tae, "Field verification of a nondestructive damage localization and severity estimation algorithm," *Proceedings of SPIE - The International Society for Optical Engineering*, s. 210-218, March 1995 1995.
- [8] S. Stoykov og E. Manoach, "Damage localization of beams based on measured forced responses," *Mechanical Systems and Signal Processing*, vol. 151, s. 1-18, April 2021 2021.
- [9] G.-R. Gillich og Z.-I. Praisach, "Modal identification and damage detection in beam-like structures using the power spectrum and time–frequency analysis," *Signal Processing*, vol. 96, s. 29-44, March 2014 2014.
- [10] G. Sha, M. Radzienski, M. Cao og W. Ostachowicz, "A novel method for single and multiple damage detection in beams using relative natural frequency changes," *Mechanical Systems and Signal Processing*, vol. 132, s. 335-352, October 2019 2019.

- [11] P. Crawley og R. D. Adams, "The location of defects in structures from measurements of natural frequencies," *The Journal of Strain Analysis for Engineering Design*, vol. 14, nr. 49, s. 49-57, April 1979 1979.
- [12] B. Pedersen. 2020. *Anisotropi* [Online, encyclopedia]. Cited from: <https://snl.no/anisotropi>. Downloaded: 09.05.21.
- [13] M. I. Hamakareem. 2021. *21 types of beams in construction* [Online]. Cited from: <https://theconstructor.org/structural-engg/types-beams-construction/24684/>. Downloaded: 29.05.2021.
- [14] Ø. Vollen, *Mekanikk for ingeniører: Statikk og fasthetslære*, 2. Edition. Universitetsgaten 10, 0164 Oslo: NKI Forlaget AS, 2016.
- [15] Instron. 2021. *Modulus of elasticity: What is modulus of elasticity?* [Online]. Cited from: <https://www.instron.us/en-us/our-company/library/glossary/m/modulus-of-elasticity>. Downloaded: 09.05.21.
- [16] Wikipedia. 2021. *Young's modulus* [Online encyclopedia]. Cited from: [https://en.wikipedia.org/wiki/Young%27s\\_modulus](https://en.wikipedia.org/wiki/Young%27s_modulus). Downloaded: 09.05.21.
- [17] Y. Khan. 2019. *3-point and 4-point bending* [Online]. Cited from: <https://www.sciencedirect.com/topics/engineering/bending-tests>. Downloaded: 10.05.21.
- [18] M. Keynes, *T838 design and manufacture with polymers: Solid properties and design*. UK: The Open University 2000.
- [19] L. Meirovitch, *Fundamentals of vibration*, 1. Edition. New York: McGraw-Hill, 2001.
- [20] T. Kruglowa, "In-situ assessment of density and material properties in timber structures by non-destructive and semi-destructive testing," 2012:03, Department of Civil and Environmental Engineering, Chalmers University of Technology, Göteborg, 2012.
- [21] P. K. Hana Hasníková, "Various non-destructive methods for investigation of timber members from a historical structure," i "WOOD RESEARCH," Czech Technical University, Faculty of Civil Engineering Department of Steel and Timber Structures, Prague, Czech Republic 2014, vol. 59 (3).
- [22] Brookhuis, "Timber grader mtg: Operation instructions,"
- [23] Brookhuis, "Timber grader mtg,"



- [24] G. Felice Giaccu, D. Meloni, M. Valdes og M. Fragiaco, "Dynamic determination of the modulus of elasticity of maritime pine cross-laminated panels using vibration methods," *WIT Transactions on Ecology and The Environment*, vol. 226, 2017 2017.
- [25] L. Meirovitch, *Analytical methods in vibrations*, 1. Edition. New York: The MacMillan Company, 1967.
- [26] Ø. Grøn. 2020. *Frekvens* [Online encyclopedia]. Cited from: <https://snl.no/frekvens>. Downloaded: 10.05.21.
- [27] J. A. Støvneng. 2020. *Egenfrekvens* [Online encyclopedia ]. Cited from: <https://snl.no/egenfrekvens>. Downloaded: 10.05.21.
- [28] B. I. Facility. *Capturing images*. Cited from: <https://microscopy.berkeley.edu/courses/dib/sections/02Images/sampling.html>. Downloaded: 11.05.21.
- [29] A. K. Chopra, *Dynamics of structures: Theory and applications to earthquake engineering*, 4. Edition. Prentice Hall, One Lake Street, Upper Saddle River, NJ 07458: Pearson Education, Inc, 2012.
- [30] R. Brincker, L. Zhang og P. Andersen, "Modal identification from ambient responses using frequency domain decomposition," *IMAC 18 : Proceedings of the International Modal Analysis Conference (IMAC)*, s. 625-630, February 7-10, 2020 2000.
- [31] Brookhuis. 2021. *Handheld moisture meter fmd6* [Online]. Cited from: <https://www.brookhuis.com/wood-testing/moisture-content/moisture-content-handhelds/handheld-fmd6/>. Downloaded: 13.05.21.
- [32] PCE. 2021. *Mechanical timber grader mtg* [Online]. Cited from: <https://www.industrial-needs.com/technical-data/mechanical-timber-grader-mtg.htm>. Downloaded: 14.05.21.
- [33] S. Sargeant. 2021. *Brookhuis mtg timber grader 'ready to go 1'* [Online]. Cited from: <https://www.scosarg.com/brookhuis-mtg-timber-grader-ready-to-go-1>. Downloaded: 14.05.21.
- [34] HBM, "Quantum x operating manual," 2019.
- [35] P. Piezotronics, "Model 393b12: Seismic, high sensitivity, ceramic shear icp® accel., 10 v/g, 0.15 to 1k hz, installation and operating manual,"

- [36] P. Piezotronics. 2021. *Model : 482c05 | four-channel, icp<sup>®</sup> sensor signal conditioner* [Online]. Cited from: <https://www.pcb.com/products?model=482C05>. Downloaded: 15.05.21.
- [37] HBM. 2021. *High-end measurement quality at an attractive price per channel* [Online]. Cited from: <https://www.hbm.com/en/2255/quantumx-mx1601b-universal-amplifier-for-standard-signals/>. Downloaded: 15.05.21.
- [38] P. Piezotronics. 2021. *Model : 393b12 | accelerometer, icp<sup>®</sup>, seismic* [Online]. Cited from: <https://www.pcb.com/products?m=393B12>. Downloaded: 15.05.21.
- [39] P. piezotronics. 2021. *Model : 024r50 | cables* [Online]. Cited from: <https://www.pcb.com/products?m=024R50>. Downloaded: 15.05.21.
- [40] K. Company. 2021. *Luxorparts utp-nettverkskabel cat. 6 hvit 20 m* [Online]. Cited from: [https://www.kjell.com//no/produkter/nettverk/nettverkskabler/nettverkskabler-i-ferdig-lengde/luxorparts-utp-nettverkskabel-cat.-6-hvit-20-m-p68086?gclid=Cj0KCQjw78yFBhCZARIsAOxgSx2Yh-B0slh7F\\_gc3Vs3svmWnwkr4eEIR4tImXfK2o3ObgckgHy\\_B34aAtxCEALw\\_wcB&gclsrc=aw.ds](https://www.kjell.com//no/produkter/nettverk/nettverkskabler/nettverkskabler-i-ferdig-lengde/luxorparts-utp-nettverkskabel-cat.-6-hvit-20-m-p68086?gclid=Cj0KCQjw78yFBhCZARIsAOxgSx2Yh-B0slh7F_gc3Vs3svmWnwkr4eEIR4tImXfK2o3ObgckgHy_B34aAtxCEALw_wcB&gclsrc=aw.ds). Downloaded: 30.05.21.
- [41] P. piezotronics, "Model 482c05 four-channel, icp<sup>®</sup> sensor signal conditioner installation and operating manual,"
- [42] HBM. 2021. *Measurement challenges?* [Online]. Cited from: <https://www.hbm.com/en/2290/catman-data-acquisition-software/>. Downloaded: 14.05.21.
- [43] M. Farshchin. 2015. *Frequency domain decomposition (fdd)* [Online]. Cited from: <https://se.mathworks.com/matlabcentral/fileexchange/50988-frequency-domain-decomposition-fdd>. Downloaded: 14.05.21.
- [44] M. Farshchin. 2015. *Convert a complex mode shape to a real mode shape* [Online]. Cited from: [https://se.mathworks.com/matlabcentral/fileexchange/52641-convert-a-complex-mode-shape-to-a-real-mode-shape?s\\_tid=prof\\_contriblnk&fbclid=IwAR1Q9XDSmcqowJKxvt9XEiH-kQyz8Uvn-8RIn6glyVYW-qcK4xFHphBAXjY](https://se.mathworks.com/matlabcentral/fileexchange/52641-convert-a-complex-mode-shape-to-a-real-mode-shape?s_tid=prof_contriblnk&fbclid=IwAR1Q9XDSmcqowJKxvt9XEiH-kQyz8Uvn-8RIn6glyVYW-qcK4xFHphBAXjY). Downloaded: 14.05.21.
- [45] *Nordic visual strength grading rules for timber*, NS-INSTA 142, 1997.
- [46] N. Trelastkontroll, "Produktdatablad for konstruksjonsvirke,"

## Appendix

### A1. Sensitivity of accelerometers

Accelerometer	Serial number	Sensitivity v/g	Sensitivity V/m/s <sup>2</sup>	Bias Level VDC
1	53811	10,48	1,068	11,4
2	53604	10,33	1,053	11,8
3	53809	10,37	1,058	11,4
4	53618	10,35	1,055	11,1
5	53810	10,35	1,055	11,4
6	53605	10,13	1,033	11,4
7	53608	10,15	1,035	11,2
8	53606	10,17	1,037	11,4
9	53607	10,21	1,041	11,1
10	53499	10,31	1,051	11,3

## A2. FDD script for Matlab

```
function [Frq,phi]=FDD(Input,Fs)

% Frequency Domain Decomposition (FDD) algorithm for modal analysis
% This code allows you to manually select the peaks by simply drawing a
% rectangle around the peaks.
% Programmer: Mohammad Farshchin, Ph.D candidate at The UofM
% Email: Mohammad.Farshchin@gmail.com
% Last modified: 4/6/2015

% Input: the name of input file that contains time history data
% Fs: sampling frequency
% Frq: identified frequencies
% phi: identified mode shapes
% Example: [Frq,phi]=FDD('Accelerations.xlsx',500);

% For detailed information about this method see: Brincker R, Zhang LM,
% Andersen P. Modal identification from ambient responses using Frequency
% Domain Decomposition. In: Proceedings of the 18th International Modal
% Analysis Conf., USA: San Antonio, 2000.

% -----
% Initialization
close all
% -----
% Import time history data: Processed acceleration data must be
% arranged in a columnwise format (one column for each measurement channel)
% Note that the acceleration data must be preprocessed (detrend, filtered
% etc.).
% Read acceleration data from the excel file
Acc=xlsread(Input);
display('FDD is in progress, please wait ...')
% -----
% Compute Power Spectral Density (PSD) matrix.
% CPSD function, with default settings, is used to compute the cross power
% spectral density matrix. More sophisticated methods can also be
% applied for more accuracy.
for I=1:size(Acc,2)
    for J=1:size(Acc,2)
        [PSD(I,J,:),F(I,J,.)]=cpsd(Acc(:,I),Acc(:,J),[],[],[],Fs);
    end
end
Frequencies(:,1)=F(1,1,:);
% -----
% Perform Modal Analysis (Use the Identifier function, below)
[Frq,phi,Fp,s1] = Identifier(PSD,Frequencies);
% Save results
save('IdResults.mat','phi','Fp','s1','Frequencies')
% -----
% Print results
display('-----')
display('                Identification Results                ')
display('-----')
% Print frequencies
display('Identified frequencies')
for I=1:size(Frq,1)
    fprintf('Mode: %d; Modal Frequency: %6.4g (Hz)\n',I,Frq(I))
end
% Print Mode shapes
```

```

display('Related mode shapes')
for I=1:size(Frq,1)
    fprintf('Mode shape # %d:\n\n',I)
    disp(phi(:,I))
end

end

%% ----- subfunctions -----
function [Frq,phi,Fp,s1] = Identifier(PSD,F)

% Compute SVD of the PSD at each frequency
for I=1:size(PSD,3)
    [u,s,~] = svd(PSD(:, :, I));
    s1(I) = s(1);
% First eigen values
    s2(I) = s(2,2);
% Second eigen values
    ms(:,I)=u(:,1);
% Mode shape
end

% Plot first singular values of the PSD matrix
figure
hold on
plot(F,mag2db(s1))
xlabel('Frequency (Hz)')
ylabel('1st Singular values of the PSD matrix (db)')

% -----
% Peak selection
% a: Draw rectangles around peaks while holding left click
% b: Press "Space" key to continue peak selection
% c: Press "any other key" if you have selected a peak by mistake and want
% to ignore it
% -----

Fp=[];% Frequencies related to selected peaks
NumPeaks=input('Enter the number of desired peaks:');
display('-----')
display('Peak selection procedure')
display('a: Draw rectangles around peaks while holding left click')
display('b: Press "Space" key to continue the peak selection')
display('c: Press "any other key" if you have selected a peak by mistake
and want to ignore it')
k=0;
while k~=NumPeaks
    A=getrect;
% Draw a rectangle around the peak
    [~,P1]=min(abs(F-A(1)));
    [~,P2]=min(abs(F-(A(1)+A(3))));
    [~,B]=max(s1(P1:P2));
    Max=B+P1-1;
% Frequency at the selected peak

scatter(F(Max),mag2db(s1(Max)),'MarkerEdgeColor','b','MarkerFaceColor','b')
% Mark this peak
    pause;key=get(gcf,'CurrentKey');
    Fp(end+1,:)= [Max,F(Max)];
    if strcmp(key,'space')

```

```

        % Press space to continue peak selection
        k=k+1;

scatter(F(Max),mag2db(s1(Max)),'MarkerEdgeColor','g','MarkerFaceColor','g')
% Mark this peak as green
    else
        % Press any other key to ignore this peak
        Fp(end,:)=[];

scatter(F(Max),mag2db(s1(Max)),'MarkerEdgeColor','r','MarkerFaceColor','r')
% Mark this peak as red
    end
end
% Number selected peaks, respectively
[~,Sr]=sort(Fp(:,2));
Fp=Fp(Sr,:);
clf
plot(F,mag2db(s1))
hold on
xlabel('Frequency (Hz)')
ylabel('1st Singular values of the PSD matrix (db)')
for I=1:size(Fp,1)

scatter(Fp(I,2),mag2db(s1(Fp(I,1))),'MarkerEdgeColor','g','MarkerFaceColor'
,'g')
    text(Fp(I,2), mag2db(s1(Fp(I,1)))*1.05, mat2str(I))
end
% Identified modal frequencies
Fpq=Fp(:,2);
% Compute mode shapes for each selected peak
for J=1:size(Fp,1)
    [ug, ~, ~] = svd(PSD(:, :, Fp(J,1)));
    phi(:,J) = ug(:,1);
end

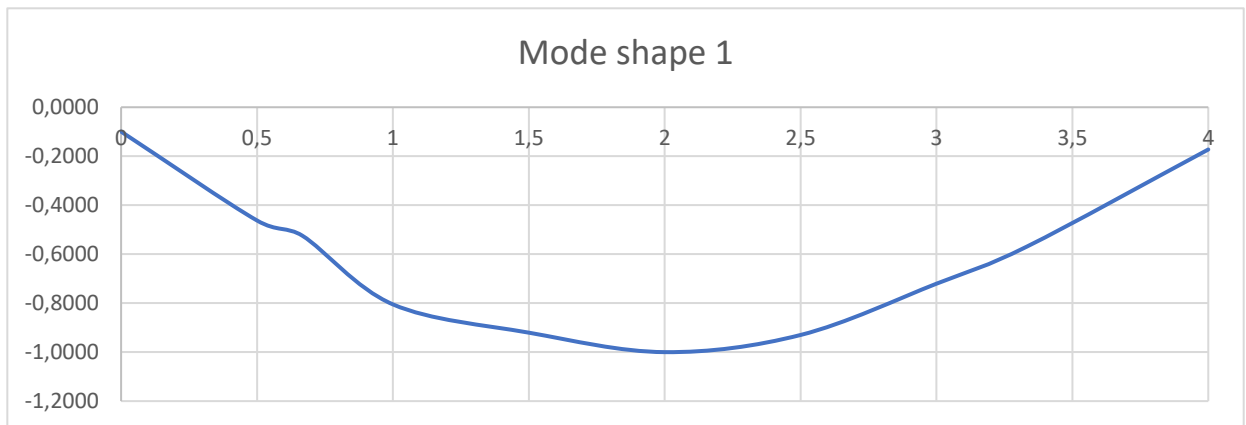
end

```

### A3. Excel-script for drawing mode shapes

	A	B	C	D	E	F	G
1							
2	Kompleks Matlab	Kompleks	Modulus	Real numbers	Imaginary	Normalized modulus	Phase Angle
3	-0.0457 + 0.0000i	=SUBSTITUTE(A3;" ";"")	=IMABS(B3)	=IMREAL(B3)	=IMAGINARY(B3)	=C3/MAXA(\$C\$3:\$C\$12)	=ATAN2(D3;E3)
4	-0.2118 + 0.0184i	=SUBSTITUTE(A4;" ";"")	=IMABS(B4)	=IMREAL(B4)	=IMAGINARY(B4)	=C4/MAXA(\$C\$3:\$C\$12)	=ATAN2(D4;E4)
5	-0.2409 + 0.0098i	=SUBSTITUTE(A5;" ";"")	=IMABS(B5)	=IMREAL(B5)	=IMAGINARY(B5)	=C5/MAXA(\$C\$3:\$C\$12)	=ATAN2(D5;E5)
6	-0.3701 - 0.0010i	=SUBSTITUTE(A6;" ";"")	=IMABS(B6)	=IMREAL(B6)	=IMAGINARY(B6)	=C6/MAXA(\$C\$3:\$C\$12)	=ATAN2(D6;E6)
7	-0.4226 + 0.0220i	=SUBSTITUTE(A7;" ";"")	=IMABS(B7)	=IMREAL(B7)	=IMAGINARY(B7)	=C7/MAXA(\$C\$3:\$C\$12)	=ATAN2(D7;E7)
8	-0.4587 + 0.0310i	=SUBSTITUTE(A8;" ";"")	=IMABS(B8)	=IMREAL(B8)	=IMAGINARY(B8)	=C8/MAXA(\$C\$3:\$C\$12)	=ATAN2(D8;E8)
9	-0.4270 + 0.0212i	=SUBSTITUTE(A9;" ";"")	=IMABS(B9)	=IMREAL(B9)	=IMAGINARY(B9)	=C9/MAXA(\$C\$3:\$C\$12)	=ATAN2(D9;E9)
10	-0.3310 + 0.0129i	=SUBSTITUTE(A10;" ";"")	=IMABS(B10)	=IMREAL(B10)	=IMAGINARY(B10)	=C10/MAXA(\$C\$3:\$C\$12)	=ATAN2(D10;E10)
11	-0.2583 + 0.0402i	=SUBSTITUTE(A11;" ";"")	=IMABS(B11)	=IMREAL(B11)	=IMAGINARY(B11)	=C11/MAXA(\$C\$3:\$C\$12)	=ATAN2(D11;E11)
12	-0.0771 + 0.0186i	=SUBSTITUTE(A12;" ";"")	=IMABS(B12)	=IMREAL(B12)	=IMAGINARY(B12)	=C12/MAXA(\$C\$3:\$C\$12)	=ATAN2(D12;E12)

	H	I	J
<b>Mode shape 1</b>			
Sign		Distance (m)	Mode shape
=IFS(AND(G3>=0;G3<PI()/2);1;AND(G3>=PI()/2;G3<=PI());-1;AND(G3>=PI();G3<=3*PI()/2);-1;AND(G3>=3*PI()/2;G3<=2*PI());1)		0	=F3*H3
=IFS(AND(G4>=0;G4<PI()/2);1;AND(G4>=PI()/2;G4<=PI());-1;AND(G4>=PI();G4<=3*PI()/2);-1;AND(G4>=3*PI()/2;G4<=2*PI());1)		0,5	=F4*H4
=IFS(AND(G5>=0;G5<PI()/2);1;AND(G5>=PI()/2;G5<=PI());-1;AND(G5>=PI();G5<=3*PI()/2);-1;AND(G5>=3*PI()/2;G5<=2*PI());1)		0,6666	=F5*H5
=IFS(AND(G6>=0;G6<PI()/2);1;AND(G6>=PI()/2;G6<=PI());-1;AND(G6>=PI();G6<=3*PI()/2);-1;AND(G6>=3*PI()/2;G6<=2*PI());1)		1	=F6*H6
=IFS(AND(G7>=0;G7<PI()/2);1;AND(G7>=PI()/2;G7<=PI());-1;AND(G7>=PI();G7<=3*PI()/2);-1;AND(G7>=3*PI()/2;G7<=2*PI());1)		1,5	=F7*H7
=IFS(AND(G8>=0;G8<PI()/2);1;AND(G8>=PI()/2;G8<=PI());-1;AND(G8>=PI();G8<=3*PI()/2);-1;AND(G8>=3*PI()/2;G8<=2*PI());1)		2	=F8*H8
=IFS(AND(G9>=0;G9<PI()/2);1;AND(G9>=PI()/2;G9<=PI());-1;AND(G9>=PI();G9<=3*PI()/2);-1;AND(G9>=3*PI()/2;G9<=2*PI());1)		2,5	=F9*H9
=IFS(AND(G10>=0;G10<PI()/2);1;AND(G10>=PI()/2;G10<=PI());-1;AND(G10>=PI();G10<=3*PI()/2);-1;AND(G10>=3*PI()/2;G10<=2*PI());1)		3	=F10*H10
=IFS(AND(G11>=0;G11<PI()/2);1;AND(G11>=PI()/2;G11<=PI());-1;AND(G11>=PI();G11<=3*PI()/2);-1;AND(G11>=3*PI()/2;G11<=2*PI());1)		3,3333	=F11*H11
=IFS(AND(G12>=0;G12<PI()/2);1;AND(G12>=PI()/2;G12<=PI());-1;AND(G12>=PI();G12<=3*PI()/2);-1;AND(G12>=3*PI()/2;G12<=2*PI());1)		4	=F12*H12



#### A4. Strength properties of timber [46]

### Fasthetsegenskaper

*(karakteristiske verdier etter NS-EN 338)*

Styrke klasse (NS-EN 338)	Bøyefasthet ( $f_{m,k}$ ) [N/mm <sup>2</sup> ]	Elastisitetsmodul ( $E_{0,mean}$ ) [kN/mm <sup>2</sup> ]	Densitet ( $\rho_k$ ) [kg/m <sup>3</sup> ]
C14	14	7	290
C18	18	9	320
C24	24	11	350
C30	30	12	380



## A5. Mode shape script for Matlab

```
function Real=ComplexModeToRealMode(Complex)
% This function converts the complex mode shape to the real valued one
% Reference: Operationa modal analysis of civil engineering structures page
% 182 and 183
% Rotate the complex mode shapes (see the RotationMaxCor function, below)
Complex=RotationMaxCor(Complex);
% 1: find the modulus of the mode shape
Modul=abs(Complex);

% 2: normalize the modulus
if nargin < 2
    Modul=Modul/max(Modul);
end

% 3: Find the phase of each component
Phase=angle(Complex);

% 4: find the sign of each component
for I=1:size(Complex,1)
    if Modul(I,1)~=0
        Sign(I,1)=SignFinder(Phase(I));
    else
        Sign(I,1)=0;
    end
end

% 5: compute the real valued mode shape
Real=Modul.*Sign;

end
function Sign=SignFinder(In)
if In>=0 && In<pi/2
    % First quarter
    Sign=+1;
elseif In>=pi/2 && In<=pi
    % Second quarter
    Sign=-1;
elseif In>=-pi && In<-pi/2
    % Third quarter
    Sign=-1;
elseif In>=-pi/2 && In<0
    % Forth quarter
    Sign=+1;
end
end
function out=RotationMaxCor(In)
% This function computes the maximum correlation line and then rotate the
% data with respect to this correlation
X=real(In);
Y=imag(In);
p=polyfit(X,Y,1);% Fit a first order line to the data
Teta=-atan(p(1)); % angle of maximum correlation line
Rot=[cos(Teta) -sin(Teta) ; sin(Teta) cos(Teta)]; % Rotation matrix
for I=1:size(In,1);
    N=Rot*[X(I);Y(I)];
    out(I,1)=N(1)+N(2)*1i;
end
end
```

## A6. Digital Appendix

Appendix-A6 is a digital folder where all the results for this thesis is saved and located. The content of this folder is listed here:

- FDD for all damaged and undamaged beams, edgewise and flatwise
- Mode shapes for all damaged and undamaged beams, edgewise and flatwise
- Regressions and tables for all damaged and undamaged beams
- Test-results for tested support conditions in Operational Modal method
- Test-results in terms of natural frequencies and related MOE for all damaged and undamaged beams, both edgewise and flatwise, with all three non-destructive methods.



**Norges miljø- og biovitenskapelige universitet**  
Noregs miljø- og biovitenskapelige universitet  
Norwegian University of Life Sciences

Postboks 5003  
NO-1432 Ås  
Norway